UNIVERSITY OF NAPOLI FEDERICO II

Doctorate School in Molecular Medicine

Doctorate Program in Genetics and Molecular Medicine
Coordinator: Prof. Lucio Nitsch
XXVIII Cycle

"Role of non-integrin laminin receptor and prion-like protein Shadoo in the trafficking and folding of cellular prion protein"

***PhD*: Anna Pepe**

***Tutor*: Dr.ssa Daniela Sarnataro**

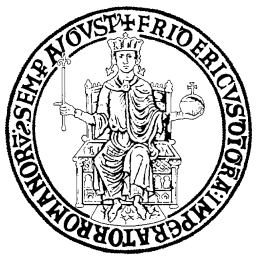

Napoli 2016

Table of contents

List of Abbreviations

AD: Alzheimer disease
BMDC: Bone Marrow Dendritic cell
BSE: Bovine spongiform encephalopathy
CJD: Creutzfeldt-Jakob disease
CLR: Calreticulin
CMA: chaperon-mediated autophagy
CNS: Central nervous system
CNX: Calnexin
DC: Dendritic cell
DRM: detergent resistant membrane
EE: Early Endosome
ER: endoplasmic reticulum
ERC: Endosomal Recycling Compartment
ERAD: ER-associated degradation system
LYS: Lysosomes
fCJD: familial Creutzfeldt-Jakob disease
FDC: follicular dendritic cell
FFI: Fatal familial insomnia
FSE: feline spongiform encephalopathy
Gnd-HCl: Guanidine hydrochloride
GSS: Gerstmann-Sträussler-Scheinker syndrome
GPI: glycosylphophatidylinositol
HD: Huntington disease
HS: heparan sulfate
iCJD: iatrogenic Creutzfeldt-Jakob disease
kDa: kilo Dalton
KO: Knock down
M: molar
mRNA: messenger RNA
µ: micron
NaOH: sodium hydroxide
NH4Cl: ammonium chloride
nm: nanometer
NSC47924: 1-((4-methoxyanilino)methyl)-2-naphthol
PK: proteinase K
PMCA: protein misfolding cyclic amplification
Prion: proteinaceous infectious particles
PrP^{C}: cellular (i.e. wild type) prion protein

PrP^{Sc}: scrapie (i.e. infectious) prion protein

PrPres: protease-resistant prion protein

ROS: reactive oxygen species

SDS: sodium dodecyl sulfate

sCJD: sporadic Creutzfeldt-Jakob disease

TGN: trans-Golgi-network

TME: transmissible mink encephalopathy

TSE: transmissible spongiform encephalopathy

TX-100: Triton X-100

UK: United Kingdom

USA: United States of America

vCJD: variant Creutzfeldt-Jakob disease

W: tryptophan

WB: Western Blot

37/67kDa LR : 37/67kDa Laminin Receptor

37LRP: 37 Laminin Receptor Precursor

67LR: 67 Laminin Receptor

ABSTRACT

Abstract

Transmissible spongiform encephalopathies (TSE), also known as prion diseases, are fatal neurodegenerative disorders which can affect both in humans and animals. They occur as sporadic, infectious or genetic disorders (Prusiner *et al.;* 1998). A major feature of these diseases is the conversion of the non-pathogenic cellular prion protein (PrP^{C}) into the pathogenic scrapie isoform (PrP^{Sc}). This isoform has a strong tendency to polymerize, forming amyloid aggregates and accumulating in the cells, thus resulting in neurodegeneration. The possible mechanisms of the prion conversion reaction into the PrP^{Sc} are still unknow; and could be involved other cellular factors which could trigger, enhance, or accelerate scrapie prion formation. An important role has been proposed for the 37/67 kDa laminin receptor in prion infections, since it has been shown to act as the receptor for both PrP^{C} and PrP^{Sc} (Reiger *et al.;* 1999, Gauczynski *et al*.; 2001). Moreover, the 37/67 kDa laminin receptor is required for PrP^{Sc} propagation in cultured cells, thus suggesting that 37/67kDa LR-PrP^{C} interaction is related to the pathogenesis of prion diseases. As a result, the inhibition of this receptor may be a strategic therapy against prion diseases.

In the first part of my thesis we have investigated the relationship between 37/67kDa LR and PrP^{C} in the presence of specific LR inhibitor compound. We have characterized the trafficking of 37/67kDa LR in both neuronal and non-neuronal cells, finding the receptor on the cell surface and nuclei, and identified the 67kDa LR as the almost exclusive isoform interacting with PrP^{C}.

Here, we show that the treatment with the 37/67kDa LR inhibitor, NSC47924, affects both the direct 37/67kDa LR-PrP^{C} interaction *in vitro* and the formation of the immunocomplex in live cells, inducing a progressive internalization of

37/67kDa LR and then its degradation *via*-lysosomes. On the other hand, PrP^C is stabilized on the cell surface.

These data reveal NSC47924 as a useful tool to regulate PrP^C and 37/67kDa LR trafficking and degradation, representing a novel small molecule to be tested against prion diseases.

Another important issue in prion diseases is the search for a cofactor involved in the conversion process of PrP^C into PrP^{Sc}. Thus, it is important to evaluate the role of other genes and proteins in TSE pathogenesis and susceptibility. A very promising candidate is Shadoo, a glycosylated GPI-anchored protein like PrP^C. It is a natively unstructured protein (Watts *et al.* 2007) that resembles aspects of the PrP^C N-terminal and central region (Daude *et al*. 2010). Physiologically, Shadoo shows neuroprotective properties similar to those of PrP^C (Watts et al. 2007): therefore, it is possible that Shadoo and PrP^C may be functionally related. Shadoo is expressed in the mouse brain less widespread than PrP^C and is prominent in two regions in which PrP^C is notably absent, suggesting that it could provide a PrP^C-like function into areas of the brain in which PrP^C is deficient. The downregulation of Shadoo expression in the brain of prion-infected animals and the direct *in vitro* interaction between prion protein and Shadoo (Jiayu *et al*. 2010) suggest a relationship between Shadoo and prion replication. However, the contribution of this interaction to the evolution of prion pathologies or to the PrP^C folding pathway remains uncertain (Ciric *et al*. 2015). Similar to PrP^C, Shadoo recombinant protein is able to form amyloid assemblies in *vitro* (Watts *et al*. 2010): this feature, however, hasn't been verified *in vivo* yet. Our laboratory has demonstrated that a perturbation of the lipid rafts induces PrP^C misfolding (Sarnataro *et al*. 2004), suggesting that they have a protective role in pathological conversion of PrP^C. Therefore, in the second part of my thesis we have characterized Shadoo subcellular localization and folding properties in neuronal

cells because we reasoned that, if Shadoo possesses the natural tendency to convert to amyloid-like forms *in vitro*, it should also be able to acquire scrapie-like characteristics in live cells also.

We have found that Shadoo, under native conditions, is partially misfolded in neuronal cells. Moreover, lipid rafts perturbation and proteasomal block increased misfolding of the protein.

INTRODUCTION

1. An Overview on the nature of prions

1.1) Prion diseases and the prion hypothesis

Prion diseases or also Transmissible Spongiform Encephalopathies (TSEs) are fatal neurodegenerative disorders which can occur in both humans and animals. A major feature of these diseases is the conversion of the non-pathogenic, cellular prion protein (PrP^{c}) into the pathogenic scrapie isoform (PrP^{Sc}), (Stahl and Prusiner, 1991). This isoform has a strong tendency to polymerize, forming amyloid aggregates which accumulate in the brain. The accretion of this abnormal protein takes place mainly in the brain and in the lymphoreticular system, accompanied with neuronal vacuolation (spongiosis) and neuronal death. After an extremely long incubation time, affected individuals show progressive neurological symptoms (such as rapid neurological decline involving neuronal loss, dementia, loss of movement coordination, and a spongiform degeneration of the brain), all terminating with death (Prusiner *et al*., 1994).

The Creutzfeldt-Jakob disease (CJD) is the most common type within the human prion diseases (Creutzfeldt *et al.*, 1920), which can be classified into four categories: sporadic (sCJD), (Jakob *et al*., 1921), inherited/familial (fCJD), (Kirschbaum *et al.*, 1924), iatrogenic (iCJD), (Duffy *et al*., 1974), and variant (vCJD), (Will *et al*., 1996). It has been suggested that the variant type (vCJD) is due to ingestion of BSE-contaminated food; familial disorders (fCJD) are the inheritance of autosomal-dominant mutations within the *Prnp* locus gene. Transplantation of tissues or injection of hormones originating from individuals suffering from CJD, as well as the use of contaminated surgical instruments, result in the iatrogenic form of CJD. Gerstmann-Straussler–Scheinker syndrome (GSS),

(Gerstmann et al., 1936), fatal familial insomnia (FFI), (Lugaresi et al., 1986), its sporadic form (sFI), (Mastrianni *et al*., 1999; Parchi *et al.*, 1999), and kuru (Gajdusek and Zigas, 1957) are other human prion diseases. Animal TSEs have been observed in different species: bovine spongiform encephalopathy (BSE) in cattle (Wells *et al*., 1987), scrapie in sheep, chronic wasting disease (CWD) in deer and elk, feline spongiform encephalopathy (FSE) in cats (Wyatt *et al*., 1990), transmissible mink encephalopathy (TME) (Burger and Hartsough, 1965), chronic wasting disease in wild ruminants (CWD) (Williams and Young, 1980), (Wells *et al*., 1987), and encephalopathies of a number of zoo animals (exotic ungulate encephalopathy, EUE), and transmission of BSE to pigs.

The different modes of transmission still haven't been understood. Several hypotheses about the nature of the infectious agent have been proposed. Initially, this agent was thought to be a slow virus (Sigurdsson *et al*., 1954; Thormar *et al*., 1971). However, further research has indicated that the infectious particle was substantially different from viruses and other conventional agents. In particular, its uncommon resistance to UV radiation and nucleases has led to the proposal that the infectious agent was devoid of nucleic acid (Alper *et al*., 1967; Prusiner *et al*., 1982, 1998). In 1967, J. S. Griffith postulated the hypothesis that the causative agent might be a protein (Griffith *et al*., 1967). The theory of a self-propagating proteinaceous agent (Bolton *et al*., 1982) was proposed after the isolation of a protease-resistant sialoglycoprotein specifically associated with infectivity, which was called the prion protein (PrP) (Bolton *et al*., 1982).

The term prion, due to Stanley Prusiner, is the abbreviation for *"Proteinaceous Infectious Particle"* and was defined as a "small proteinaceous infectious particle that resists inactivation by procedures which modify nucleic acids" (Bolton *et al*., 1982; Prusiner *et al*., 1982). This newly discovered pathogen (protease-resistant prion protein - PrPres - also called PrP^{Sc} from scrapie) was isolated from the brain

of infected animals (Bolton *et al*., 1982). Interestingly, infectivity was substantially reduced by agents capable of destroying protein structures and by anti-PrP antibodies (Gabizon *et al*., 1988).

1.2) Cell biology of PrP^C: expression and functions

PrP^C is a normal cellular protein that is expressed in the neurons and glia of brain and spinal cord, but also in several peripheral tissues and leukocytes. In the adult central nervous system, PrP^C is widely distributed in neocortical and hippocampal neurons, cerebellar Purkinje cells and spinal motor neurons (Caughey *et al*.,1988; Bendheim *et al.,* 1992; Hartle *et al*., 1996). The normal function of PrP^C remains unknown, although its localization on the cell surface would reflect with roles in cell adhesion, ligand uptake or transmembrane signaling. Some PrP^C possible functions may include: a neuroprotective role due to antiapoptotic activity, memory formation and neurogenesis, and a functional role in copper metabolism due to its copper binding capacity (Bounhar *et al*., 2001; Diarra-Mehrpour *et al*., 2004). Different proteins including laminin, which is an extracellular protein, N-CAM, Aa cell surface component with an important role in neuronal aggregation, and tyrosine kinase Fyn implicating a role of PrP^C in cell signaling (Mouillet-Richard *et al*., 2000). PrP^C may reduce copper, inducing a protection against oxidative stress (Brown *et al*., 1997). It has been demonstrated that PrP^C knockout mice exhibit 50% lower copper concentration in synaptosomal fractions than wild-type mice. Thus, PrP^C might regulate the copper concentration in the synaptic region and may play a role in the reuptake of copper into the presynapse (Kretzschmar *et al*., 2000). *In vivo* experiments revealed that protein and lipid oxidation is increased in skeletal muscles, heart, and liver of $Prnp^{0/0}$ mice,

suggesting a PrP^C function related to cellular antioxidant defenses (Klamt *et al.*, 2001).

PrP^C may fail to play its normal function when it is converted to PrP^{Sc} isoform. Mice lacking PrP^C ($Prnp^{0/0}$) show no obvious phenotype; they display no gross developmental or anatomical defects, but are reported in some studies to have elctrophysiological and structural abnormalities in the hippocampus, loss of cerebellar Purkinje cells alterations in circadian rhythm and sleep pattern, and changes in learning and memory (Bueler *et al*., 1992).

Prnp $^{0/0}$ mice and cells derived from these mice are resistant to infection with prion agents; primary culture neurons are not killed by the toxicity of prion agents; prions cannot proliferate in the brain of Prnp $^{0/0}$ (Bueler et al., 1993). Therefore, it is clear that PrP^C plays an important role in the mechanism of infection and contributes to the pathogenesis of prion diseases.

1.3) Structure and biosynthesis of PrP^C

PrP^C is a cell surface protein, most of which is found on the plasma membrane and does not remain on the cell surface after its delivery there but, rather, constitutively cycles between the plasma membrane and endocytic compartment via clatrin coated pits-dependent pathway (Harris *et al.,* 1999). Moreover, in our laboratory it has been demonstrated that lipid rafts-dependent pathway plays a key role in the endocytosis of PrP^C in epithelial cells (Sarnataro *et al*., 2009). PrP^C undergoes a number of post-traslational modification in the ER and Golgi. After cleavage of a 23 amino acid signal peptide in the endoplasmic reticulum (ER), a glycosylphosphatidil inositol (GPI) anchor, which mediates its anchoring to the membrane, is attached to the C-terminus of the protein (Stahl et al.; 1987). The two Cys residues 179 and 214 are engaged in the formation of a disulphide bond

essential for the stability of the protein (Haraguchi et al.; 1989; Turk et al., 1988; Vana et al., 2006)

PrP^C in the ER is subject to addition of N-linked oligosaccharide chains at two asparagine (N) (residues 181 and 197 humans) in the C-terminal part. These chains are of high mannose type and are sensitive to the digestion by endoglycosidase-H. In the Golgi they are subsequently modified to more complex oligosaccharides that contain sialic acid and are resistant to endoglycosidase-H (Caughey et al., 1989).

PrP^C undergoes two post-traslational cleavages as part of its normal metabolism; the first cleavage is proteolytic and occurs within the N-terminal fragment that could serve as a biologically active ligand. The second occurs within the GPI anchor and releases the polipeptide chain into the cytosol and is specifically degraded by the proteasome (Figure 1).

Like other GPI-anchored proteins (Zurzolo et al., 1994; Lipardi et al., 2000) both PrP^C and PrP^{SC} have been found enriched in rafts and are typically resistant to extraction in Triton X-100 (Taraboulos et al., 1992; Naslavsky et al., 1997; Harris, 1999) and are able to float in the lighter fractions of sucrose density gradients (Sarnataro et al., 2002). Lipid rafts are dynamic lipid assemblies enriched in cholesterol and sphingolipids. The raft association of PrP^C is mediated by both its GPI-anchor and the N-terminal region of its ectodomain. Lipid rafts do not have a role in PrP^C exocytic trafficking, as is typical for other GPI-anchored proteins (Sarnataro et al., 2002), but as shown by us PrP^C association with lipid rafts in the ER stabilizes its conformation (Sarnataro et al., 2004). An impairment of rafts-association by cholesterol depletion during the early stage of PrP^C biosynthesis leads to protein misfolding in ER, suggesting a functional role for rafts in the protection of PrP^C folding (Sarnataro et al., 2004).

1.4) The pathogenic isoform PrP^{Sc} and replication mechanisms

The molecular basis of the conversion of PrP^{C} into a pathogenic isoform PrP^{Sc} is still unknown. Current evidence suggests that the fundamental difference between the two forms of PrP lies in their conformation. PrP^{C} is monomeric and digested by proteinase K, whereas PrP^{Sc} forms highly insoluble aggregates and shows higher resistant to proteolytic digestion.

The spectroscopic studies demonstrated a conformational difference between PrP^{C} and PrP^{Sc}, PrP^{C} has a high α-helical content of approx. 42%, with little or no β-sheets (approx. 3%), whereas PrPSc contains approx. 30% α-helices and approx. 45% β-sheets (Pan et al., 1993). Because of the lack of antibodies specific to PrP^{Sc}, the subcellular distribution of has been PrP^{Sc} extremely difficult to assess and a range of discordant studies indicate that it has a wide distribution, in particular at the plasma membrane and in endolysosomal compartment (McKinley *et al*., 1991; Arnold *et al*., 1995); (Figure 1). Characterizing the exact intracellular localization of PrP^{C} and PrP^{Sc} is important for identifying the intracellular compartment and the mechanisms that underlie prion formation.

Formation of PrP^{Sc} could take place either at the plasma membrane, where the first contact between endogenous PrP^{C} and exogenous PrP^{Sc} is likely to occur, or immediately after its internalization in the endolysosomal or recycling compartment (Jaffry *et al.*, 2001; Marjanovic *et al.*, 2009); (Figure 1). Another possibility is that after its internalization PrP^{Sc} undergoes retrograde transport to the Golgi apparatus and/or to the ER, thereby perturbing the biosynthesis of newly synthesized prion protein and triggering the formation of the PrP^{Sc} isoform from the PrP^{C} precursor. Some studies suggest that the ER might have a significant role in the conversion of PrP^{C}.

Thus, through this compartment a high amount of substrate for the conversion reaction travels and it is conceivable that it is easier to transconform the nascent polypeptide than to convert mature, correctly folded forms of the protein.

Involvement of the ER in pathological conversion is also supported by studies in which Harris e al., 2003 demonstrated that acquisition of the initial scrapie-related features of mutant PrP occurred in the ER (Harris *et al*., 2003). Furthermore, several studies have shown that the ER-associated degradation pathway is both involved in the degradation of pathogenic PrP mutants that are linked with familial prion diseases and responsible for the normal degradation pathway of misfolded PrP isoforms that is, incorrectly folded isoforms of PrP^{C} (Zanusso et al., 19). By different studies it has been demonstrated that the ER, plasma membrane and endocytic compartments are important in prion formation, but they might be differentially involved. The ER could function in amplifying the PrP^{Sc} form after retrograde transport to the ER. In genetic prion diseases, by contrast, the ER could represent the compartment in which mutant PrP molecules are spontaneously transformed to PrP^{Sc} or PrP^{Sc}-like conformers.

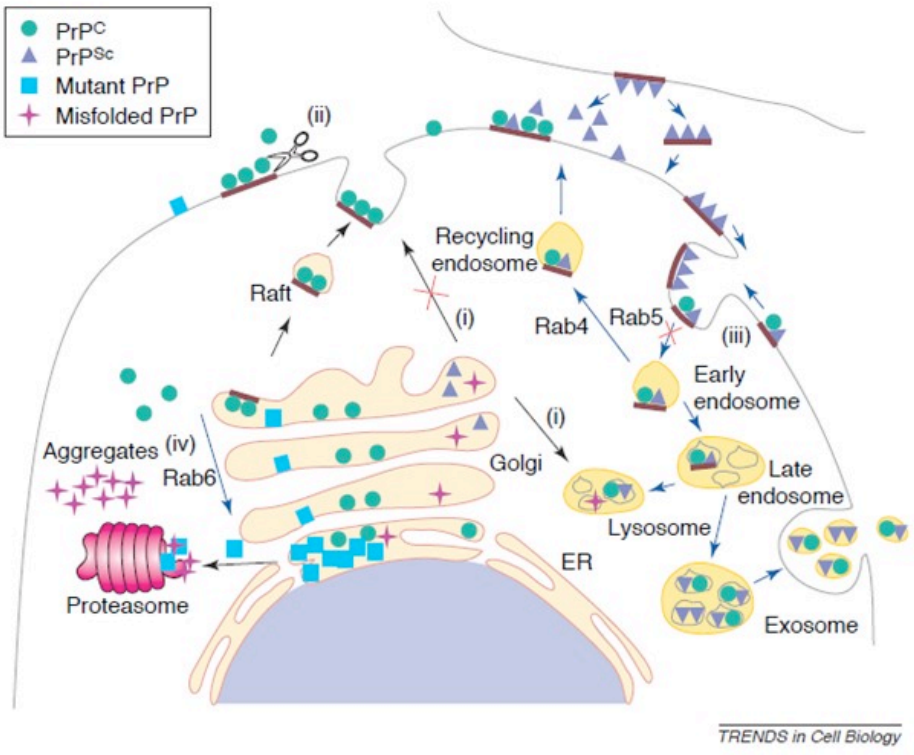

Figure 1. Intracellular trafficking of PrP^{C} and PrP^{SC}, and possible pathways of PrP^{SC} formation. PrP^{C} is synthesized in the ER, in which it acquires post-translational modifications and in which misfolded PrP and hereditary pathological mutants (mutant PrP) are partially degraded by the proteasome after retro-translocation through the cytosol. PrP^{C} has also been found in the neuronal cytosol and, under some experimental conditions, misfolded PrP aggregates are also present in the cytosol. After ER quality control, PrP^{C} is transported through the Golgi apparatus to the cell surface, at which it associates with rafts and is internalized by clathrin- and/or caveolin-dependent mechanisms. Blocking transport of PrP^{C} to the plasma membrane and rerouting it to lysosomes for degradation (i), and releasing nascent PrP^{C} from the cell surface (ii) prevent the formation of PrP^{Sc}. A reduction in PrP^{C} internalization (iii) also decreases PrP^{Sc} formation. Both PrP isoforms are found in Rab5-positive early endosomes, pass through late endosomes and are totally (PrP^{C}) or partially (PrP^{Sc}) degraded in acidic lysosomes. Moreover, part of the PrP^{C} pool is recycled back to the plasma membrane in a Rab4-dependent pathway, and both PrP^{C} and PrP^{Sc} are found associated with exosomal membranes in the extracellular medium of infected cells. Finally, the ER has been postulated to have a role in prion conversion by amplifying PrP^{Sc} formation after the Rab6a dependent retrograde transport of PrP^{C} (iv) (Campana *et al.,* 2005).

Lipid rafts have been proposed as possible sites for the conversion of PrP^{C} to PrP^{Sc}. Its role in the formation of PrP^{Sc} is inferred from the finding that both PrP^{C} and PrP^{Sc} are present in rafts extracted from infected cells and from mouse brain (Taraboulos et al., 1992; 1995; Botto et al., 2004). The type of rafts associated with each isoform has different characteristics (Naslavsky et al., 1997). However, lipid rafts have been further implicated in PrP^{C}-PrP^{Sc} trans-conformation because removing PrP^{C} from rafts by exchanging its GPI-anchor for a transmembrane domain prevents the formation of PrP^{Sc} (Taraboulos et al., 1995; Kaneko et al., 1998).

Conversely, impairing of PrP^{C} rafts association by cholesterol depletion during the early stage of its biosynthesis leads to protein misfolded (Sarnataro *et al*., 2004), suggesting that rafts have a protective role in the trans-conformational process.

A chief issue is how lipid rafts control the formation of PrP^{Sc}. Three models have been proposed: i) rafts could be involved in the targeting of PrP^{C} to the specific compartment in which PrP^{Sc} transconformation occurs; ii) rafts could contain machinery that is indispensable for PrP^{Sc} formation, such as proteins that facilitate its conversion; iii) rafts could provide a favorable environment for transconformation by facilitating close encounters between PrP^{C} and PrP^{Sc} (Campana *et al*., 2005), (Figure 2).

Moreover, Marijanovic *et al.* (2009) characterized the subcellular compartmentalization of PrP^{C} and PrP^{Sc} in the neuronal infected cell line and showed that while PrP^{C} was enriched at the plasma membrane (PM) and in the Golgi, PrP^{Sc} was found predominantly in the endocytic pathway, in early endosomes and late endosomes/lysosomes and specifically enriched in recycling endosomes (ERC).

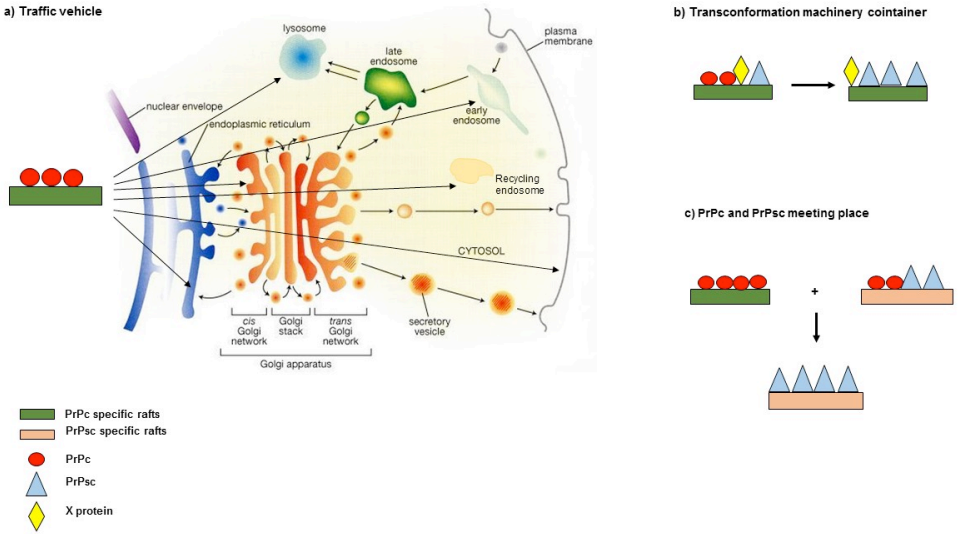

Figure 2. Potential roles of raft association in prion formation. Rafts could be implicated in different aspects of prion conversion as indicated by the models shown. (a) Rafts could be the vehicle of prion transport to an intracellular compartment, such as the plasma membrane (PM), endolysosomes, caveolae or ER, in which the transconformation occurs. (b) Rafts could contain the factors (protein X or lipid chaperones) comprising the transconformation machinery. (c) Rafts could be a platform on which PrP^{C} accumulation occurs, functioning to promote the encounter between PrP^{C} and PrP^{Sc} and to enhance the prion conversion reaction (modified by Campana *et al.,* 2005)

1.5) Prion hypothesis and replication models of prions

In prion diseases, the possible mechanisms of the prion conversion reaction into the PrP^{Sc} abnormal isoform is unknown. Following the intuition of Griffith (1967), that an abnormal infectious protein can propagate by interacting with its normal counterpart, *"the protein-only hypothesis*" proposed that PrP^{Sc} amplifies itself by converting PrP^{C} to the PrP^{Sc} in a reaction that, once started in different cell types of the central nervous system (CNS), causes fatal neurodegeneration. The fact that administration of a small quantity of PrP^{Sc} can induce conversion of the host PrP^{C}

and that the ablation of the PrP-encoding gene renders animals resistant to prion diseases (Bueler et al., 1993; Brandner et al., 1996), represents the strongest evidence in favor of the prion hypothesis.

However, the infectious agent, PrP^{Sc}, alone or its interactor PrP^{C}, are not able to reproduce the infection process in vitro. An alternative model, the *"unified theory"* was proposed to incorporate both the protein-only and the protein plus nucleic acid hypotheses (Weissmann,1991). According to this model, PrP^{C}- PrP^{Sc} conversion is the principal pathogenic event, but a co-prion agent such as a small host-specified nucleic acid associated with PrP^{Sc} a small interfering (si)RNAs and microRNAs represent a crucial component required to modulate pathogenic conversion (Weissmann, 1991).

Then, it was proposed the "*refolding*" model in which PrP^{C} unfolds and refolds under the influence of PrP^{Sc} (Prusiner, 1991); the *nucleation model*, or "*seeding*" that describes how PrP^{C} can spontaneously assume different conformations (such as PrP^{C} and PrP^{Sc}), which are in equilibrium (Come et al., 1993; Harper and Lansbury, 1997). In physiological conditions the equilibrium of the reaction strongly favors PrP^{C}, because PrP^{Sc} conformation acquires high activation energy (Come et al., 1993; Harper and Lansbury, 1997). The presence of a PrP^{Sc} crystal-like seed abolishes this energy barrier by stabilizing the PrP^{Sc} conformation and by promoting the rapid monomer addition of PrP^{Sc} to the seed (Jarrettand Lansbury, 1993). Moreover, the overexpression of PrP^{C} in cell cultures is not sufficient to initiate and maintain prion replication (Montrasio et al., 2001), indicating the requirement of an auxiliary host factor(s) a "Protein X or Co-Factor for Protein" (Enari et al., 2001; Peretz et al., 2001). Weissmann (2004) proposed a *dynamic susceptibility model*, where the capacity of cells to propagate prions would depend on a synthesis-degradation equilibrium. If the rate of prion synthesis would not be equal or exceed twice the rate of its degradation, prions would be eliminated from

cells after infection. Instead, when the rate of scrapie formation is more than twice that of its degradation, the high prion accumulation could trigger cell death. Thus, the ability of the cell to efficiently sustain prion replication would depend on this delicate equilibrium (Weissmann et al.; 2004, Fasano et al.; 2006).

2. 37 /67 kDa LR non-integrin laminin receptor

2.1) Looking into 37/67 kDa laminin receptor

The 37/67 kDa human laminin receptor (LamR) is a non-integrin cell surface receptor for laminin-1, a variety of viruses (Mercurio et al., 1990) and prion protein (Rieger *et al.,* 1997). Because of its wide range of ligands, 37/67kDa LR plays a role in numerous pathologies; its over expression correlates with a highly invasive cell phenotype and increased metastatic ability, mediated by its interactions with laminin-1. In 1983, this receptor for ECM (extracellular matrix) glycoprotein laminin was isolated and identified by three different laboratories from murine melanome cells (Rao *et al*., 1983), human breast carcinoma cells and normal muscle cells (Lesot *et al*., 1983). The isolated receptor had an apparent molecular mass (as estimated by SDS/PAGE) of approx 67kDa. The receptor bound laminin with high affinity and specificity (Montuori, N., & Sobel, M.E, 1996); consequently, this receptor was named 67LR (67 kDa Laminin Receptor) and more recently, LAMR1(laminin receptor 1), (Lesot et al., 1983; Malinoff & Wicha, 1983; Rao *et al.,* 1983). Then, cDNA clones encoding for human and murine 67 LR were isolated. Unexpectedly, none of the isolated human and murine cDNA encoded for a 67kDa protein but for a peptide only 295 amino acid long, with a calculated molecular weight of 32 kDa and an apparent electrophoretic mobility in SDS-polyacrilamide gel of about 37 kDa. This peptide was considered to be the precursor of 67LR and named according to its molecular

mass, 37 kDa laminin receptor precursor (37 LRP) (Wewer *et al.,* 1986; Rao *et al.,* 1989; Castronovo et al., 1991). The mechanism by which 37LRP converts into the mature 67LR is incompletely understood. Recent evidences demonstrate that 67 LR is acylated by fatty acids, suggesting that 37LRP can dimerize with itself or with another peptide by strong hydrophobic bonds mediated by fatty acids. However, the amino-acid compositions of 67LR and 37LRP are identical, suggesting homodimer formation (Buto et al., 1998). Although, the 37LRP reveals some interesting and unusual features such as: there are no N-linked carbohydrate-attachment sites or typical transmembrane domains; there is no recognized signal sequence at the N-terminus for entry and translation in the endoplasmic reticulum. However, the N-terminal region contains a hydrophobic segment (aminoacids 86–101) that has been hypothesized to act as a transmembrane domain. Finally, there is an unusual C-terminal 70-amino-acid segment, which is trypsin-resistant and highly negatively charged which contains five repeats with the sequence (D/E)W(S/T), (Rao et al., 1989; Castronovo et al., 1991; DiGiacomo, V., & Meruelo 2015). The most intriguing observation is that the homologues to 37LRP/67LR can be found in all five kingdoms (archeabacteria, eubacteria, fungi, plants animals) and are likely to be present in all organisms (Nelson *et al*., 2008). Phylogenetic analysis of the 37/67 LR sequence suggested that the acquisition of the laminin-binding capability by the 37LRP gene product is linked to the evolution of the C-terminus, particularly the appearance of the palindromic sequence LMWWML. Interestingly, phylogenetic analysis carried out on 37LRP gene from different species indicated that all of these proteic sequences are derived from orthologous gene, and that 67LR was originally a ribosomal protein "37LRP/p40", an acidic ribosomal protein of molecular mass approx. 40 kDa wich acquired the additional novel function of a laminin receptor through evolution (Deminova *et al*., 1996; Ford *et al*., 1999). In 1992, Auth and Brawerman

demonstrated that the 37LRP/p40 protein is the murine equivalent of human 37LRP. More evidences suggest that the 37LRP/p40 protein is a component of the translational machinery (Auth and Brawerman 1992). They show that 37LRP/p40 is part of a cytoplasmic structure that is involved in the translation process.

The identified binding epitopes for laminin-1 are residues 161–180, referred to as Peptide G, (Castronovo et al., 1991), residues 205 and 220, called as the direct binding region, and the TEDWS-containing C-terminal repeats (Landowski et al., 1995). The palindromic sequence LMWWML (a.a. 173-178) within Peptide G has been suggested to be the minimal sequence responsible for laminin binding, the two consecutive tryptophan (W) residues are impotant for protein to protein interaction. Other laminin binding sites have mapped on laminin receptor, and are the residues Phe32, Glu35, and Arg155 (Jamieson et al., 2011). Laminin receptor are seemingly capaple of binding heparan sulfate (HS) and laminin-1 simultaneously (Guo et al., 1999; Kazmin et al., 2000; Zidane 2013). HS binding may act as a laminin binding stabilization. Moreover, 37LRP/67LR is a high affinity receptor not only for laminin-1 but also for the cellular and infectious prion proteins (PrP^{C} and PrP^{Sc}, respectively) and plays an important role in prion diseases.

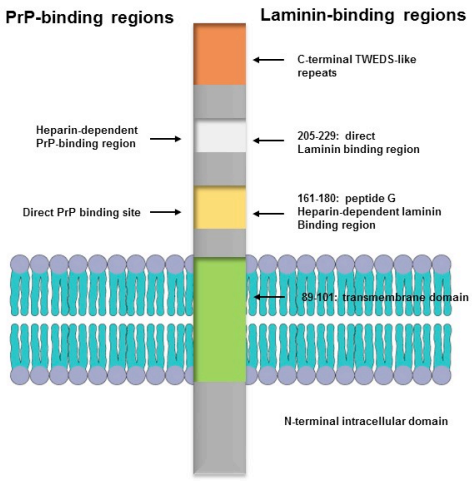

Figure 3. Main functional regions and binding sites of 37/67 kDaLR. Laminin receptor interacts directly with laminin, and at least three regions of the C-terminal domain of the receptor are thought to be involved: (i) the most C-terminal 53 amino acids containing four acidic TEDWS repeats; (ii) a putative helical stretch between amino acids 205–229; and (iii) a heparan-sulfate-dependent laminin-binding region from 161–180. PrP binds the direct binding site, making contact with residues 161–179 of 37/67 kDa LR. It is of interest to note that the same region (161–180) of 37LRP corresponds to one (of three) laminin-binding sites, which is known as the peptide G region. The second PrP site is an indirect interaction site and is mediated by the presence of HSPGs. This indirect binding site maps to amino acids 53–93 on PrP, and either 101–160 or 180–295 of laminin receptor (modified by Nelson *et al*., 2008).

2.2) 37LRP/67LR cancer and neurodegenerative disease

As a transmembrane receptor, 37/67 kDa LR serves several functions such as cell migration, cell-matrix adhesion, cell viability proliferation and angiogenesis (Montuori *et al*., 1996; Ardini *et al*., 2002; Berno *et al*., 2005). However, 37/67 kDa LR has been shown to be involved in the mobilization of HSCs (haemopoietic stem cells) by granulocyte-colony-stimulating factor, and the expression levels of 37/67 kDa LR positively correlate with mobilization efficiency of HSCs. HSC cells stimulate angiogenesis and are thought to give rise to new endothelial cells. Interestingly, 37LRP/67LR is involved in the regulation of cell proliferation and

survival. Indeed, reduction of its expression results in apoptosis; on the contrary, the 37/67 kDa LR dependent cell signaling pathways are important for cell survival (Selleri *et al*., 2006). The receptor is identified as an interacting partner of PED/PEA-15 (phosphoprotein enriched in diabetes/phosphoprotein enriched in astrocytes), an anti-apoptotic protein whose expression is increased in several human cancers, enabling cell proliferation and resistance to apoptosis (Montuori *et al*. 2011; Formisano *et al*., 2012; Khumalo *et al*., 2015). A strong correlation has also been established between 37/67 kDa LR and cancer angiogenesis; indeed, the high expression of this protein correlates with the increase of tumor angiogenesis (Stitt *et al*., 1998; Khusal *et al*., 2013). Recently, it has been described that the 37/67 kDa LR specific antibody, W3, blocked cancer angiogenesis (Zuber *et al*., 2012). The role of the laminin receptor in cancer progression has been a topic of great interest for many years and has therefore been extensively investigated. Given that 37/67 kDa LR is involved in a number of cellular processes and is found in numerous cellular locations (the cell surface, the cytoplasm, the perinuclear compartment and the nucleus), additional roles of this receptor in cancer progression have been suggested. Many results show that a number of cancer types, such as gastric, colon, colorectal, cervical, breast, lung, ovarian, pancreatic and prostate cancers, reveal an overexpression of the 37/67 kDa LR on their cell surface; the use of anti-LRP/LR specific antibodies significantly hampers the two key steps of metastasis, adhesion and invasion (Menard *et al*., 1998; Montuori *et al*., 1999; Zuber *et al*., 2008). Taken together, many results strongly suggest that the 37/67 kDa LR laminin-1 interaction in tumor cells enhances the proteolytic cleavage of the basement membrane, thus facilitating invasion and migration.

Laminin receptor could be implicated in neurodegenerative disease also, such as Alzheimer's disease (AD). AD is the most prevalent form of dementia; the accumulation of the amyloid beta (Aβ) peptide is largely considered the primary disease causing agent in Alzheimer's disease, it is generated through the sequential proteolytic cleavage of the Amyloid Precursor Protein (APP) by β and γ secretases. The amyloid beta (Aβ) shares the same binding partners and a common cellular location of 37/67 kDa LR, thus it has been proposed an involvement of the 37/67 kDa LR receptor in the pathogenesis of Alzheimer's disease (AD). show that 37/67 Jovanovic et al., 2013 kDa LR can bind and can co-localize with the AD relevant proteins APP, β and γ-secretase, respectively, revealing a role for 37/67 kDa LR in the regulation of APP processing. Moreover, its modulation could affect Aβ cytotoxicity and its release from cells (Javanovic *et al*., 2013; Pinnock *et al*., 2015).

2.3) The 37/67 kDa LR as the receptor for PrP^{c} and Prp^{Sc}

In a yeast two-hybrid screen technology in Saccharomyces cerevisiae, the 37 kDa laminin receptor precursor (LRP) was identified as an interactor for the prion protein (Rieger *et al.,* 1997). Further in vitro studies on neuronal and non-neuronal cells proved that both the 37 kDa LRP and the 67 kDa high affinity laminin receptor act as the receptor for the cellular prion protein (Gauczynski *et al.,* 2001; Sarnataro et al., 2016). Mapping analysis of the LRP-PrP interaction site in S. cerevisiae revealed that PrP and laminin share the same binding domain (amino acids 161 to 180) on LRP. The PrP^{C} binds to 37LRP/67LR kDa via two domains, termed PrPLRPd1(aa 144-179) and PrPLRPd2(aa 53-93).

The frist one binds directly to LRP/LR whereas the second one depends on the presence of heparan sulphate proteoglycanes (HSPGs) on the cell surface. Moreover, the aa 161-179 of LRP/LR directly bind PrP^C (PrPLRPd1). The indirect HSPG-dependent binding domain might be located between aa 101-160 or between aa 180-259 of laminin receptor (Hundt *et al.;* 2001).

How prions are introduced into the cells is still debated. Although an important role has been proposed for the 37 kDa/67 kDa laminin receptor in prions internalization.

Indeed, we have recently demonstrated (Sarnataro et al., 2016) that37/67kDa LR and PrP^C co-immunoprecipited in neuronal cells also. Moreover, 37/67 kDa LR are involved in the internalization, accumulation and propagation of abnormal PrP^{Sc} in scrapie-infected neuronal cells in vitro (Gauczynski *et al.,* 2001; Leucht *et al.,* 2003) and, 37/67 kDa LR expression levels are greatly increased in the brain, spleen and pancreas of scrapie infected rodents (Rieger *et al.,* 1997).

As accumulation of bovine PrP^{Sc} in Peyer's patches after oral infection in animal models has been found this implies that prions cross the intestinal epithelial barrier. However, the mechanisms that lead to the internalization of prion particles in human intestinal cells after the oral ingestion of bovine prion-infected tissues, it is still under investigation. The M cells, present in the covering epithelium of Peyer's patches, has a high phagocytosic activity and are involved in the uptake of prions (Da Costa Dias *et al.;* 2011). Previous results obtained in neonatal mice and in primates have described the presence of PrP^{Sc} in enterocytes after oral exposure to prion strains (Morel *et al.,* 2005). Enterocytes are the major cell population of the intestinal epithelium, even at the level of Peyer's patches, and are known to actively participate in endocytosis of nutrients, macromolecules, or pathogens through their polarized traffic equipment. Human enterocytes express both PrP^C and the 37 /67 kDa LR in their apical brush border.

Morel *et.al;* 2005 demonstrated the specificity of bovine prion uptake in human enterocytes using the human Caco-2/TC7 cells, which have most of the morphological and functional characteristics of normal human enterocytes. Bovine prion is rapidly endocytosed through the 37 /67 kDa laminin receptor and trafficked toward early endosomes (Morel *et al*.; 2005).

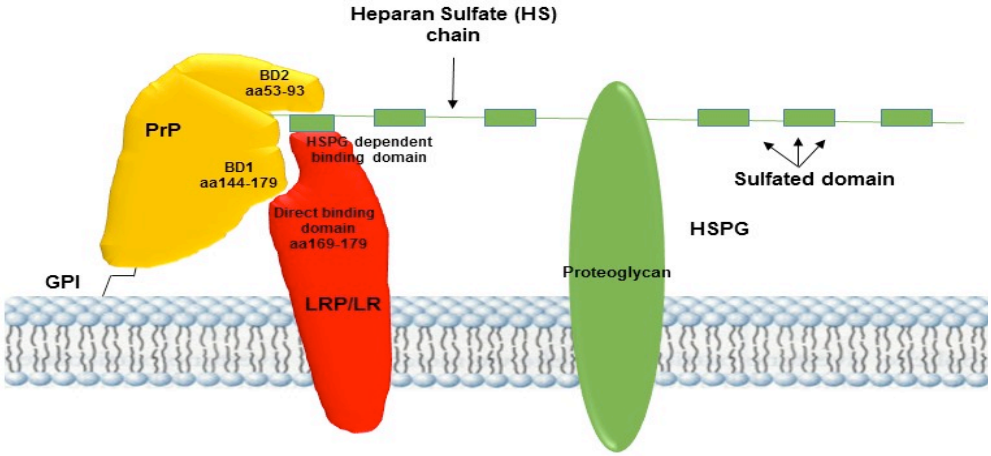

Figure 4. Model for the function of 37/67 kDa LR (LRP/LR) as the receptor for PrP. The PrP molecule binds to LRP/LR via PrPLRPbd1 and PrPLRPbd2. PrPLRPbd2 (aa53-93) is dependent on the presence of the heparan sulfate arm of a HSPG molecule whereas PrPLRPbd1 (aa 144-179) interact directly with LRP/LR. The simultaneous presence of both PrPLRPbd1 and PrPLRPbd2 would stabilize the binding of PrP and laminin receptor. Direct binding of 37/67kDa LR to PrP occurs via the direct binding site located between aa 169-179 of LRP/LR. The indirect HSPG dependent binding domain might locate between aa 205-229 (modified by Gauczynski *et al.,* 2001).

2.4) Molecular strategy to inhibit 37/67 kDa lamini receptor

The importance of the receptor in the PrP^{Sc} propagation is confirmed by several studies in which laminin receptor downregulation is able to reduce the PrP^{Sc} formation in scrapie-infected neuronal cells (Vana and Weiss, 2006). Thereupon several approaches regarding prion diseases targeting 37/67 kDa LR have been developed (Castronovo *et al.,*1991; Gauczynski *et al*., 2001; Khumalo *et al*., 2015) including *i)* anti-37/67 kDa LR antibodies (Chiesa *et al*., 2009), *ii)* polysulfate glycans (Prusiner *et al*., 1998) and *iii)* small interfering RNAs directed against the LRP m RNA (McKinley *et al*., 1991). As anti-37/67 kDa LR antibody, it has been used the polyclonal antibody (W3). It has shown curative effect on scrapie infected N2a cells (Leucht et al., 2003). This antibody a) prevents the binding of infectious prions to mammalian cells (Gauczynski *et al*., 2006) and b) blocks endocytosis of PrP BSE by enterocytes (Morel et al., 2005). Since a polyclonal antibody format is not suitable for a therapy in animals or humans, single-chain antibodies directed against 37/67 kDa have been developed. Different studies characterized two single chain antibodies (scFvs) N3 and S18 that are directed against 37/67 kDa LR. The single chain antibody S18 shows inhibitory effects on prion replication in vivo, indeed, peripheral prion propagation levels are reduced. However, the S18 mediated reduction of the peripheral PrP^{Sc} propagation was not concomitant with a significant prolongation of the incubation and survival times in scrapie infected mice treated with scFv S18. One reason for that might be the short half-life of the antibody, approx. 12 h in the blood of animals (Zuber *et al.;* 2008).

As polysulfated Glycanes can be a molecular target to inhibit infections prions, Gauczynski *et al*; 2006 have shown that Heparan sulfate mimetics (HMs), which represent dextran-based molecules (chemically substituted with defined amounts

of carboxymethyl, hydrophobic benzylamide, and sulfated groups) inhibit PrP^{Sc} synthesis in infected neuronal cells and impair the endocytosis of prion rods. It was suggested that the HM molecules might act by directly interfering with the PrP^{C}/PrP^{Sc} conversion process. One of the mechanisms suggested claims that the Heparan sulfate mimetics block PrP^{Sc} binding to the cells by competing with the binding to heparan sulfate and to LRP/LR (Gauczynski *et al*.; 2006).

However, anti-TSE strategies targeting PrP and laminin receptor have been contested, since the molecules injected into the brain of mice led to rapid neuronal apoptosis (Solforosi *et al*., 2004). Other compounds are highly toxic and lacks of the permeability across the blood-brain barrier. This prompted us to test the effect of a specific 37/67 kDa LR small organic inhibitor NSC47924 on prion protein biology of prions.

3. Biological properties of the PrP-like protein Shadoo

3.1) Looking into *Prnp* and *Sprn* genes: Structural homology and diversity

The SPRN gene, located on chromosome 7 in mice and 10 in humans, encodes Shadoo (Sho), a N-glycosylated glycophosphatidylinositol-anchored (GPI) protein that shows neuroprotective properties. Shadoo is the third member of mammalian prion protein family, which includes prion protein (PrP), encoded from *Prnp* gene, and Doppel, a testis-specific protein involved in the male reproductive system, encoded from *Prnd*. The *Prnp* gene is located on chromosome 2 in mice and 20 humans. It consists of three exons with the entire open reading frame located in exon 3. Like *Prnp*, the entire open reading frame of *Sprn* is contained within a single exon. *Sprn* gene was discovered in a public domain database for nucleotide sequences, showing some similarities to the *Prnp* sequence.

Thus, it was revealed that *Sprn* could encode a short protein resembling the flexibly disordered N-terminal part of the PrP: in particular, the alanine- and valine-rich central hydrophobic region. The protein was named Shadoo (Shadow of Prion Protein) and was discovered in *silico* by Premzl *et al*. in 2003. After an NMR study and circular dichroism analyses (Premzl et al., 2003; Watts *et al*., 2007), they defined Shadoo as a natively unstructured protein. *Sprn* gene seems to be present in the genomes of lower organisms, such as zebrafish, all the way up to rodents and primates (Premzl *et al*., 2003).

3.2) Proteic structure of Prion and prion-like protein Shadoo

PrP^C is synthesized with N- and C- terminal signal sequences; the N-signal peptide targets it to the endoplasmic reticulum (ER), but not very efficiently, because small amounts of cytoplasmic PrP are generated. In the ER, first PrP N-signal peptide and C-terminal signal peptide are removed, followed by the addition of a GPI anchor, which tethers PrP^C to the outer leaflet of the plasma membrane (Harris *et al*., 1999). As a GPI-anchored protein, PrP^C is found in cholesterol-rich lipid raft domains within the membrane. The overall architecture of Shadoo recalls the N-terminal half of PrP^C, although Shadoo lacks the octarepeat sequences found in PrP^C. In particular, there are several features which are present in both Shadoo's and PrP's natively unstructured N-terminus: *i)* tandem positively charged RRG boxes (rich in glycine, serine, alanine and arginine; aa.26 to 48 aa), predicted to bind RNA (Lau *et al*., 2012); *ii)* HD (hydrophobic tract, from aa63 to aa 82); *iii)* N-linked glycosylation, but in Shadoo it is predicted to occur at a single site; *iv)* C-terminal attachment signal for the GPI anchor. Shadoo appears to lack any discernible elements of secondary structure, in concordance with its homology to the unstructured N-terminus of PrP^C (Watts *et al*., 2007; Daude and Westaway *et al*., 2011); (see Figure 5). This could be explained by the fact that: *i)* the Shadoo region analogous to the α-helical domain present in PrP^C is not long enough to accommodate three α-helices; *ii)* Shadoo misses cysteine residues, preventing the formation of stabilizing disulfide bridges (Daude *et al*., 2010).

More recently, it has been demonstrated that ER signal peptide of Shadoo has the property to mediate an alternative targeting to mitochondria. The targeting direction of this signal peptide is determined by intrinsically disorder elements within the nascent chain. (Pfeiffer *et al*., 2013) Loss of the pro-α-helical domains

and/or deletion of the C-terminal GPI signal sequence promote Shadoo translocation into mitochondria. In addition, the finding that a C-terminal GPI-anchor signal sequence is sufficient to promote efficient ER import of Shadoo indicates that the nascent chain remains translocation competent until the complete protein is synthesized. On the other hand, proteins containing structured domains are efficiently imported into ER

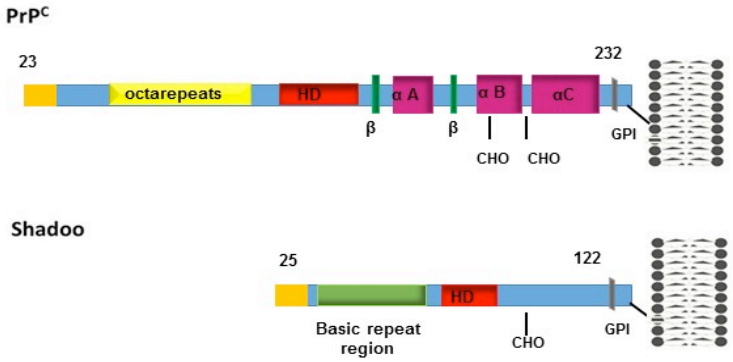

Figure. 5 Domain structures of PrP^C and Shadoo Proteins. The schematic in PrP^C includes octarepeats, hydrophobic region ('HD'); a, alpha helices; b strands ('b') and N-glycosylation sites (CHO). For Shadoo the basic repeats, HD and single N-glycosylation site are shown. Diagonal slashes adjacent to GPI attachments sites of PrP^C and Shadoo indicate the existence of an endoproteolysis site(s) that result(s) in secreted forms of the respective proteins (modified by Watts *et al.,* 2010).

3.3) Endoproteolitic processing of prion protein family

A feature of the prion glycoprotein family is their endoproteolitic processing. Endoproteolysis of prion protein probably plays a fundamental role in PrP^{Sc} propagation, because the predominant C-terminal fragment switches from C1 to C2 fragments during disease progression. Under healthy conditions, a-cleavage of PrP^C is abundant, and generates a 17- kDa C-terminal fragment, named 'C1'.

This fragments are generated by a cleavage that disrupts the neurotoxic and amyloidogenic region of PrP^C, immediately preceding the hydrophobic domain, whose residues are 106-126. During disease, α-cleavage occurs less frequently than β-cleavage after the octarepeat region, thus making the 'C2' fragment dominant. The 106-126 residues remain intact in C2, suggesting a role for C2 in prion diseases.

Incomplete descriptions of cleavage products for Shadoo have been reported but their characterization could be promising for knowledge of the biological significance of PrP^C. In fact, some studies have indicated that the N-terminal domain of PrP^C can be replaced by that of Shadoo and maintains its ability to protect cells from stress-induced toxicity, thus indicating that Shadoo and PrP^C are involved in similar signalling pathways. Cleavage of Shadoo generates fragments that possess overlapping functions with those of PrP^C and involves the generation of the C2 fragment, that is generated together with the C1 Shadoo fragments by a common mechanism (for example a hypothetically C1 protease that may cut inefficiently at the adjacent C2 site); (Mays *et al*., 2014). However, Shadoo fragments biological function remain largely unknown.

3.4) Shadoo expression and its relationship with PrP^C

Expression of Shadoo in the mouse brain is less widespread than PrP^C. Shadoo is most readily apparent in the hippocampus and it is found in the cell body in some neurons of the lateral hypothalamus. Then it is prominent in two regions in which PrP^C is notably absent: the Purkinje cells in the cerebellum and the dendritic processes of hippocampal pyramidal cells. Moreover, the physiological function of Shadoo in CNS is unknown and evaluating *Sprn* knockout mice may help to clarify its role.

Recent studies report that $Sprn^{0/0}$ animals don't have malformation at birth or in adult life. On the other hand, *Prnp* $^{0/0}$ mice is not lethal and lack a strong phenotype in the mammals (Beuler et al., 1992; Manson et al., 1994), despite its early embryonic expression; moreover, *Prnp* lack induced embryonic lethality in Zebrafish, arguing for the involvement of the Prion protein family in embryonic development. Whereby, in the mammals, another protein takes over PrP^{C} function in knockout mice; Shadoo, which shares some spatial regulation and properties with PrP^{C}, appears to be a good candidate for being this hypothetical, host-encoded PrP-like protein. Interestingly, a lethal embrionic phenotype was described in *Prnp* $^{0/0}$ mice and *Sprn* knockdown. The $Prnp^{KO}Sprn^{KD}$ embryos suffer from a neural defect with a failure of closure of the cranial tube. However, it is commonly accepted that such a default could not explain the observed lethality, but a developmental defects of trophoblastic lineage was sufficient to explain the observed lethal phenotype (Young *et al*., 2009; Passet *et al*., 2012). Other studies have reported that *Prnp* and *Sprn* KO mice did not produce embryonic lethality (Daude *et al*., 2012). Three hypotheses were proposed that could conciliate this discrepancy in phenotype: *i)* the use of similar but not identical genetic backgrounds, *ii)* an adaptation of the Sprn-knockout embryos to the lack of this protein and *iii)* an alteration of the Sprn-overlapping Mtg1 transcript expression level by the shRNA.

Similar to PrP, recombinant mouse and sheep Shadoo proteins are able to form amyloid assemblies under native condition (Daude *et al*., 2010). Shadoo HD region seem to have self-assembly properties (Rambold *et al*. 2008) and the ability to form amyloid. The conformational and assembly properties of this HD region seems to dictate important biological activities.

An intriguing aspect of Shadoo biology is its prion-disease specific downregulation (Westaway *et al*., 2011).

However, the mechanism governing the loss of Shadoo protein during disease remains to be determined.

Recently, it has been shown that Shadoo levels are reduced in the brains of mice infected with the RML strain of prions, in the brains of prion-infected rodents and sheeps (Watts *et al*., 2007). Furthermore, nonsense mutations in the SPRN gene were found in two patients with variant CJD, but not in control patients. On the other hand, Shadoo overexpression did not influence the kinetics of prion replication in mice. The quantitative inverse relationship between Shadoo and protease-resistant PrP^{Sc} levels in the brain, suggests that the relative levels of these two proteins are mechanistically linked. Thus, Shadoo may be an indicator of an early response to PrP^{Sc} accumulation in the central nervous system (CNS) hundreds of days prior to the onset of neurological symptoms (Watts *et al*., 2007).

Recently it was demonstrated PrP^{C}-Shadoo interaction in a yeast two-hybrid system. To examine the regions of PrP^{C} and Shadoo responsible for their interaction to each other, a series of deletion mutants were constructed and the interactions were assayed. Thus, the interaction site of PrP^{C} is 108–126 and of Shadoo, 61–77 (Jiayu *et al*., 2010). However, the contribution of this interaction to the evolution of prion pathology or to the folding pathway of PrP^{C} remains uncertain.

More recently, Ciric el al, (2015) have described for the first time that Shadoo can interfere with the PrP-folding pathway and prion replication process. Using cross-linking experiments, they showed that full-length PrP^{C} and Shadoo are able to form a more stable 1:1 heterocomplex exhibiting quaternary structure different from the one formed in the absence of Shadoo. However, Shadoo also cooperatively interacts with C-terminal C1 fragment of PrP^{C}, derived from physiological PrP^{C} proteolytic processing.

Indeed, C1 fragment has been reported to act as a dominant–negative inhibitor of PrP^{Sc} formation (Westergard *et al*., 2011). The cooperative binding of Shadoo to the C1 fragment traps the fragment and thus interferes with its dominant negative inhibitor property, which could enhance the PrP^{Sc} replication process. The dual binding behaviour of Shadoo may thus confer regulatory properties on the prion conversion process (Figure 6).

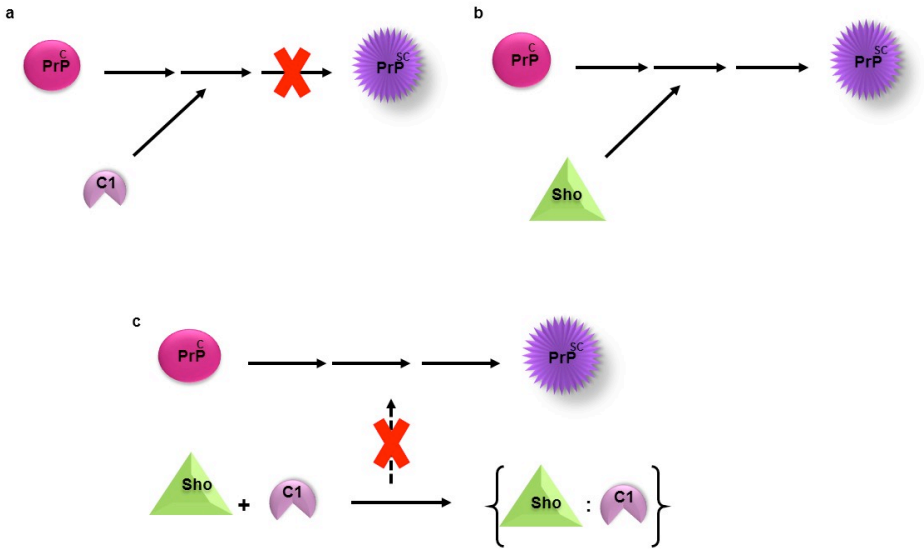

Figure 6. Proposed modes of Shadoo (Sho) action on the conversion of PrP^{C} to PrP^{Sc}. (a) PrP truncated form C1 has been reported to act as dominant-negative inhibitor of PrP conversion. (b) By directly interacting with full-length PrP, Sho modifies the PrP-folding pathway and thereby enhances the conversion rate (c) An allosteric interaction between Sho and PrP truncated form C1 traps C1in a multimeric complex, switching off the dominant-negative inhibition of C1 and thus enhancing the conversion process (modified by Ciric *et al*., 2015).

AIMS

Aims of the study

Prion diseases lack effective therapeutic treatment to date; they are caused by the conversion of the cellular prion protein (PrP^{C}) into the disease-associated form PrP^{SC}, which is the aggregated, misfolded isoform of PrP^{C}, which accumulates in the central nervous system. However, it is not yet understood how the misfolding of prion protein induces neurodegeneretion. It has been demonstrated by *in vitro* and *ex-vivo* experiments that prion propagation requires the presence of the non-integrin laminin receptor (Leucht et al., 2003), implicating that the approaches which downregulate 37/67kDa LR are promising alternative strategies for the treatment of prion diseases.

Since PrP^{C} shows a number of binding partners, it is important to evaluate the role of the other genes and proteins in prion diseases, as well.

Recently, it has been observed that the infected scrapie brain presented a reduction of Shadoo protein levels (Daude *et al.,* 2010). Moreover, intriguing aspect of Shadoo biology is its natural tendency to convert to amyloid-like forms *in vitro* (Daude *et al.,* 2010) and its capability to act as an holdase on PrP^{C} folding .This feature could represent a functional link between PrP^{C} and Shadoo in the conversion of PrP^{C} to its misfolded isoform (PrP^{Sc}).

My PhD work has been focused on two major projects:

- PROJECT 1: The effects of 37/67 laminin receptor (LR) inhibitor, NSC47924, on LR cellular localization and on its interaction with the cellular prion protein
- PROJECT 2: Role of lipid rafts and proteasome in the acquisition of "scrapie-like" properties of PrP-like protein Shadoo in neuronal cells

MATERIALS AND METHODS

Reagents and antibodies

Cell culture reagents were purchased from Sigma-Aldrich Laboratories (St Louis, MO) . The SAF32 and SAF61 antibodies (directed, respectively, against the N- and C-terminal domain of PrP^{C}) were from Bertin Pharma-Bioreagent Department (France). The anti- KDEL, anti-CNX, anti-CLR, anti-Golgin, anti-EEA1 and anti-ERp57 antibodies were from StressGen Biotechnologies Corp (Victoria, BC, Canada). Anti-Lamp1 antibody was from BD Pharmigen and anti-b-tubulin antibody was from Abcam. SPRN (R-12) sc-136909 Shadoo-Antibody, TRAP1 sc-13557, Bip/Grp78 (sc-1051), F1atpase, ATP5B subunit, sc-58619, anti-GAPDH (sc-69778) from Santa Cruz Biotechnology. Anti-Transferrin Alexa-488-conjugated (Tfr488), Alexa-488-, Alexa-546-conjugated secondary Abs and Lysotracker Red DND-99 were from Invitrogen (Molecular Probes). DRAQ5 and DAPI dyes were purchased from Cell Signal Technology. Protein-A-Sepharose was from Sigma. Biotin-LC was from Pierce and all other reagents were obtained from Sigma Chemical Co. (St Louis, MO. Production of recombinant and anti-67LR antibodies: a recombinant His-tagged 37LRP polypeptide (r37LRP) was made in bacteria and Nickel affinity purified, as described (Pesapane *et al*., 2015; Jovanovic *at al*., 2015). (Human) Recombinant PrP (PO2) was from Abnova (Taipei, Taiwan). The polyclonal 5004 Ab able to recognize both the 37 kDa and the 67 kDa forms of LR is used in the immunofluorescence, Western blot analysis and immunoprecipitation was performed using the polyclonal 4290 Ab was made against a C-terminal peptide derived from LR and was a kind gift from Dr. Mark E. Sobel (Bethesda, MD); the NSC47924 inhibitor has been already described (Pesapane *et al*., 2015). ALLN was from Calbiochem (La Jolla, CA), Methyl-β-cyclodestrin (βCD) from Sigma Chemical Co. (St Louis, MO).

Cell culture and drug treatment

GT1 (hypothalamic neuronal mouse cell line) and HEK-293-LR (HEK-293 stable expressing T7/His-tagged 37LRP; Pesapane, *et al*., 2015) were grown in Dulbecco's modified Eagle's medium (DMEM), with 4500 mg/glucose/L, 110 mg sodium pyruvate and L-glutamine (SIGMA D6429), supplemented with 10% fetal bovine serum. SHSY5Y (derived from human neuroblastoma), were grown in RPMI-1640 (Euroclone), with 4500 mg/glucose/L, 110 mg sodium pyruvate and L-glutamine (SIGMA D6429), supplemented with 10% fetal bovine serum. Cells were cultured at 37°C under 5% CO2. For inhibitor NSC47924 treatment, the cells were washed in serum free medium, incubated for 30 min at room temperature (RT) in Areal medium (13.5 g/l of Dulbecco's modified eagle's medium with glutamine without NaHCO3 (SIGMA-D-7777), 0.2% BSA and 20mM HEPES, final pH 7.5) and for further indicated times at 37 °C under 5% CO2 in the presence of 20 μM inhibitor in DMEM supplemented with 1% serum. NH4Cl (20 mM in culture medium) was used to inhibit endo/lysosomal protein degradation for 2 days. Proteasomal block was performed with 150 μM ALLN for 7 hours in complete medium**.** Methyl-β-cyclodextrin (βCD) treatment was carried out as described elsewhere (Keller and Simons, 1998). Briefly, GT1 cells were plated on dishes and βCD (10 mM) was added to the Areal-medium containing 1 h at 37°C to cells.

Indirect immunofluorescence and confocal microscopy

To analyze protein steady-state localization, GT1 cells were cultured to 50–70% confluence in growth medium for three days on coverslips, washed in PBS, fixed in 4% paraformaldehyde (PFA), permeabilized or not with 0.2% TX-100 for 5 min (where indicated) and processed for indirect immunofluorescence using specific

antibodies 1 hours in PBS/BSA 0.2%. The cells were incubated with anti-PrP SAF32 (IgG2) monoclonal antibody (2 mg/ml, 1:100) and anti-37/67kDa LR rabbit 5004 policlonal antibody (1 mg/ml, 1:50) to label PrP^C and 37kDa/67kDa LR, followed by incubation with fluorophore-conjugated secondary antibodies. For lysosome and mitochondria staining, cells were incubated for 1 hr with Lysotracker (1:1000) and 1 hr with Mitochondria (1:1000) respectively in complete medium before fixing. Where indicated, anti-Lamp1 antibody was used as marker of endo-lysosmal compartment. For Tfr-Alexa 488 staining, the cells were incubated 45 min in complete medium before proceeding with immunofluorescence. Nuclei were stained by using DRAQ5 dye (1:5000) or DAPI (1:1000) in PBS.

To analyze cell surface localization of 37/67kDa LR and PrP^C, the cells were first incubated (or not, control) with the inhibitor for the indicated times and then fixed in PFA 4% and processed for immunofluorescence under non permeabilized conditions by labelling laminin receptor and PrP^C with the specific antibodies.

Internalization assay. In order to exclusively label the cell surface 37/67kDa LR and PrP^C protein pools and to follow their fate from the cell surface, GT1 cells grown on coverslips were first incubated (pulse) with 5004 and SAF32 primary antibodies for 30 min at 4 °C (which blocks membrane trafficking events; Arancibia-Cárcamo *et al.,* 2006). Primary antibodies were diluted in Areal Medium. The cells were then washed to eliminate excess of unbound antibodies and then shifted at 37 °C under 5% CO2, to allow endocytic processes, for indicated times (chase) in the presence or not of 20 mM NSC47924 in the culture medium. GT1 cells were fixed and permeabilized before incubation with fluorescently-conjugated secondary antibodies and laser scanning confocal analyses (Sarnataro *et al*., 2009).

Pearson's correlation coefficient (PCC) was employed to quantify colocalization (Bolte *et al*., 2006) between 37/67kDa LR and PrP^C (as well as other intracellular markers), and was determined in at least 25 cells from four different experiments. PCC was calculated in regions of 37/67kDa LR and reference protein co-presence (Bolte *et al*., 2006). In brief, the Otsu algorithm was applied to segment laminin receptor and PrP^C (as well as other intracellular markers) images, in order to define co-localization regions of the reference proteins. The PCC was then calculated in the defined regions for the images of interest. Whereas PCC provides an effective statistic for measuring overall association of two probes in an image, it has the major shortcoming that it indirectly measures the quantity of one protein that colocalizes with a second protein (Dunn *et al*., 2011). This quantity can be measured via Manders' Colocalization Coefficient (MCC). The degree of colocalization between 37/67kDa LR and PrP^C was quantified using the colocalization finder and JaCoP plug-in of ImageJ software (http://rsb.info.nih.gov/ij/). MCCs were measured for at least 25 cells per sample. Immunofluorescences were analysed by the confocal microscope Zeiss META 510 equipped with an oil immersion 63x 1.4 NA Plan Apochromat objective, and a pinhole size of one airy unit. We collected twelve-bit confocal image stacks of 10-15 slices at 0.4µm Z-step sizes from dual- or triple-labeled cells using the following settings: green channel for detecting Alexa-488, excitation 488 nm Argon laser, emission bandpass filter 505–550 nm; red channel for detecting Alexa-546, excitation 543 nm Helium/Neon laser, emission bandpass filter 560–700 nm (by using the meta monochromator); blue channel for detecting DAPI, excitation 405 nm blue diode laser, and emission bandpass 420–480 nm; blue channel for detecting DRAQ5, excitation 633 nm Helium/Neon laser.

Measurements of fluorescence intensity were taken on a minimum of three confocal stacks per condition, from a single experiment (~84 cells), using LSM 510 Zeiss software. The background values raised by fluorescent secondary antibodies alone, were subtracted from all samples.

Shadoo indirect immunofluorescence: GT1 cells were grown for 3 days on coverslips, washed with PBS, fixed and processed for indirect immunofluorescence (the cells were permeabilized with methanol/acetone 1:1) using anti-Sho R12 pAb and anti-PrP^C SAF32 mAb. Sho and PrP^C were visualized with Alexafluor-546 or 488-conjugated secondary antibody, respectively. Images were acquired by a Leica SP5 TCS SMD confocal microscope by using a 63x oil immersion objective, a 488 nm Argon laser for AlexaFluor-488 conjugated secondary antibodies (green channel), a 561 nm laser for AlexaFluor-546 conjugated secondary antibodies (red channel); 633 nm laser for DRAQ5 (nuclei, blue channel). Pearson Correlation Coefficient (PCC) was employed to quantify colocalization (Bolte and Cordelières, 2006).

Immunoprecipitation/Co-immunoprecipitation

To immunoprecipitate PrPC or 37/67kDa LR, the cells were grown in 100 mm dishes, washed three times with cold PBS and lysed on ice for 20 min in lysis buffer 1 (25mM Tris-HCl pH 7.5, 150 mM NaCl, 5mM EDTA, 1% TX-100) with protease inhibitor mixture (leupeptin, antipain, pepstatin, and 1 mM phenylmethylsulfonyl fluoride). The samples were quantified with Bradford assay with Bio-Rad Protein Assay Dye Reagent Concentrate, diluited 1:5 in water; 1.2 mg of proteins were immunoprecipitated, while 80 mg of proteins were kept for totals. Lysates were pre-cleared with protein-A sepharose beads (5 mg/sample) for 30 min at 4°C and incubated overnight with 1μg/ml SAF32 or SAF61 anti-PrP antibodies, or with a polyclonal anti-LR 4290 antibody (2μg/sample) to

immunoprecipitate 37/67kDa LR (both coupled with Protein-A sepharose); (Campana et al., 2007). Pellets were washed three times with cold-lysis buffer 1, then boiled with SDS sample buffer 2X (Tris 1M pH 6.8, SDS 10% , glycerol 20% and bromophenole blue and 10% b-mercaptoethanol), loaded on 12% polyacrylamide gels (30% ACRYL/BIS SOL 37.5:1), and revealed by Western blotting with 4290 and/or SAF32 Abs followed by ECL detection (Pierce Euroclone). Densitometric analysis was performed using the free image-processing software ImageJ.

Immunoprecipitation of Molecular Chaperones

To immunoprecipitate Calreticulin (CLR) the cells were grown in 100 mm dishes, washed three times with cold PBS and lysed JS buffer (1% TX-100, 150m M NaCl, 1% Glycerol, 50 mM HEPES, p H 7.5, 1.5 mM MgCl2, 5 mM EGTA) with protease inhibitor coktail, for 20 min on ice, screped and microfuge tubes. The lysates were then precleared with protein A-Sepharose beads (5 mg/sample) for 30 min and incubated overnight at 4°C with CLR. The pellets were washed twice with cold lysis buffer and three times with PBS. The samples were then boiled with SDS-sample buffer (Sarnataro et al., 2004). TRAP-1 immunoprecipitation was carried out on 1,5 mg of total extracts. Cells were lysed in cold lysis buffer [20 mm Tris (pH 7.5) 60 mm KCl, 15 mm NaCl, 2 mm EDTA, 1% (vol/vol) Triton X-100, 1 mm phenylmethylsulfonyl fluoride, 2 mg/ml aprotinin, 2 mg/ml leupeptin. Protein concentration was quantified using the Bio-Rad protein assay kit (Bio-Rad Laboratories)Lysates were incubated O/N with 50 μl(1mg/ml) protein Protein A/G magnetic beads (Bio-Rad) and TRAP-1 (1μg/ml) antobody. Negative control experiments were performed by adding magnetic beads and IgM to the cleared lysate. Then, the Co-IP was washed with PBS-T (PBS + 0.1% Tween 20), beads were magnetized and supernatant were discarded. Pellets were boiled with SDS sample buffer 2X at 95°C. The samples were loaded on 14% polyacrylamide gels and revealed by Western blotting against Shadoo, CLR and TRAP-1.

Biotinylation assay

GT1 cells grown on dishes were cooled on ice and biotinylated with NHS-LC-Biotin at 4°C (Zurzolo et al., 1994). Cells were lysed for 20 min using buffer 1 (25mM Tris-HCl (pH 7.5), 150 mM NaCl, 5mM EDTA, 1% TX-100).

Biotinylated cell surface proteins were immunoprecipitated with streptavidin beads (40 ml/sample, Pierce n. 20349). 37/67kDa LR was specifically immunorevealed with the 4290 pAb and PrP^C with SAF32 mAb. In the case of NSC47924 treatment, the cells were first incubated with the inhibitor (or not, control) for indicated different times and then, biotinylated on ice, following the protocol described above.

Steady-state plasma membrane distribution: 80% confluent cell layers on plates were biotinylated and processed for immunoprecipitation with streptavidin beads (biotinylated material, cell surface), as previously described (Sarnataro et al., 2002). To recover the biotinylated immunoprecipitated Shadoo and PrP^C, the samples were boiled with Laemmli buffer for 10 min and then loaded on 14% gels. After transfer on PVDF by Western blot, total and cell surface Shadoo and PrP^C were revealed with R-12 and SAF32 antibody, respectively.

Binding of soluble r37LRP to immobilized human recombinant PrP

High binding plates with 96 flat-bottomed wells (Corning, Amsterdam, ND) were coated with 125 ng/well of human recombinant PrP diluted in PBS, or BSA as a negative control, and incubated at 4 °C overnight. After a wash in PBS, residual binding sites were blocked for 1 h at 37°C with 200 ml of blocking buffer (2% FCS, 1 mg/ml BSA, in PBS). Wells were incubated with 2 mg r37LRP (diluted in PBS, 1 mg/ml BSA), which contained a 6X-His-tag, alone or in presence of NSC47924, for 1 h at 37 °C. Each well was washed three times with wash buffer (0.5% Tween in PBS). Penta-His HRP conjugate (1:500) (Qiagen, Hilden, Germany) was added for 2 h at room temperature. After washing, substrate solution was added and absorbance was detected at 490 nm on an ELISA plate

reader (Bio-Rad). Binding was determined by subtracting background absorbance (BSA wells).

Statistical analysis

Statistical significance of samples against untreated cells was determined by One-way analysis of Variance (ANOVA), followed by the Dunnett's test. Each value represents the mean±SEM of at least three independent experiments performed in triplicate (*,§, $P< 0.05$).

QproteomeTM Mitochondria Isolation

QproteomeTM Mitochondria Isolation kit from Qiagene (37612) was used to purify mitochondria from eukaryotic cells. 6×10^6 SHSY5Y cells were processed. The cell suspension was centrifuged at 500 x g for 10 min at 4°C. Supernatant was removed and the pellet was washed using 1 ml of 0.9% NaCl solution for two times. After washing, cells were suspended with 1 ml of Lysis Buffer (protease inhibitor solution was added) which selectively disrupts the plasma membrane without solubilizing it, resulting in the isolation of cytosolic proteins. Plasma membrane and compartmentalized organelles, such as nuclei, mitochondria, and the endoplasmic reticulum (ER), remained intact and were pelleted by centrifugation at 1000 x g for 10 min at 4°C. The resulting pellet was resuspended in 500 µl of Disruption Buffer, repeatedly passed through a narrow-gauge needle (to ensure complete cell disruption), and centrifuged at 1000 x g for 10 min at 4°C.

The pellet contains nuclei, cell debris, and unbroken cells. The supernatants were centrifuged at 6000 x g for 10 min at 4°C. The pellet contains mitochondria. The supernatant represents the microsomal fraction.

The mitochondrial pellet was washed with 1 ml Mitochondria Storage Buffer and then Centrifuged at 6000 x g for 20 min at 4°C. Then the mitochondrial pellet was re-suspended with 100 ml of Mitochondria Storage Buffer.

Each isolated fraction was quantified with Breadford assay with Bio-Rad Protein Assay Dye Reagent, diluited 1:5 in water. 15mg of proteins of each fraction (cyt-ER-Mito) were boiled with SDS-sample buffer 2X, loaded on 14% polyacrylamide gel and reveled by western blotting with SPRN-R12 antibody to reveal Shadoo. PVDF membranes were probed with GAPH, F1ATPase and BiP, as cytosol, mitochondria and ER marker respectively.

TX-100 extraction

Cells grown in 60-mm dishes were washed twince with PBS containing 1mM CaCl2 and 1mM MgCl2 (PBS C/M) and then lysed for 20 min on ice in 1ml Extraction Buffer (25 mM Hepes pH 7.5, 150 Mm NaCl, 1% TX-100). Lysates were collected and centrifuged at 14000 r.p.m. for 2 min at 40C. Supernatants, representing the soluble material, were removed and 1% SDS was added; the pellets were then solubilized in 100 µl of Solubilization buffer (50 mM Tris p H 8.8, 5 mM EDTA, 1% SDS). DNA was sheared through a 22-g needle. The pellets were solved, boiled 3 min and 900 µL of Extraction buffer was added. Proteins were TCA precipitated from the soluble and insoluble materials and Shadoo was revealed by Western blotting with R-12 antibody.

Assay for DRM-association

Sucrose density gradients

Cells were grown to confluence in 150-mm dishes, washed in PBS Ca++/Mg++ and lysed for 20 min in TNE/TX-100 1% on ice (Sarnataro et al., 2002; Broquet et al., 2003). Lysates were scraped from dishes and sheared though a 22-g needle and then centrifuged at 14.000 rpm 10 min at 4°C. Supernatants were placed at the bottom of centrifuge tube, brought to 40% sucrose. A sucrose gradient (5-35% TNE) was layered on the top of the lysates and the samples were centrifuged at 39.000r.p.m. for 18h in an ultracentrifuge (model SW41 Beckman Institute, Fullerton, CA, USA). One-milliliter fractions (12 fractions in total) were harvested from the top of the gradient. Specifically, starting from the top of the gradient the fractions 4-7 (representing DRMs) and 8-12 (non-DRMs) were collected and loaded on gel. After transfer on PVDF by Western blot, Shadoo, PrP^{C} and Flotillin-2 were revealed by specific antibodies and ECL.

Assays for scrapie properties

Triton/Doc insolubility: cells were lysed in Triton/Doc buffer (0.5% Triton X-100, 0.5 Na Deoxicolate, 150 mm NaCl and 100 mm Tris, pH 7.5) for 20 min and cleared lysates were centrifuged at 265000×g for 40 min in a TLA 100.3 rotor of Beckman Optima TL ultracentrifuge. Shadoo was recovered in the supernatants and pelleted by TCA precipitation. It has been shown that in these conditions only PrP^{Sc} but not PrP^{C} from brain extracts and cell culture lysates (from CHO, NIH 3T3 or neuroblastoma cells) will sediment (Lehmann and Harris, 1997; Priola and Chesebro 1998).

Proteinase-K digestion: to measure proteinase K-resistance, lysates were digested with proteinase- K (3.3 μg/ml or 20 μg/ml, as indicated) for 2 and 10 min at 37 °C; the proteins were TCA precipitated and then analyzed for Shadoo by immunoblotting with the specific antibody. The conditions used for proteinase digestion are identical to those previously published (Lehmann and Harris, 1997; Priola and Chesebro, 1998; Sarnataro et al., 2004)

RESULTS AND DISCUSSION

PROJECT-1

Results

1.1) PrP^C and 37/67kDa LR expression and intracellular localization in both neuronal and non-neuronal cells

The endogenous laminin receptor from neuronal GT1 cell lysates migrated on SDS-PAGE as two different bands corresponding, respectively, to the laminin receptor precursor (37kDa LRP) and the mature band (presumably the acylated isoform or the homodimeric/heterodimeric one) as shown before (Montuori et Sobel, 1996). Lysates from HEK-293-LR cells stably transfected with a human 37LRP cDNA were loaded for reference (Pesapane *et al*., 2015) (Figure 1a). As already observed (Buto *et al*., 1998), the precursor molecule showed an anomalous electrophoretic mobility, which accounts for an apparent molecular mass of ~44 kDa, and as previously described by Alqahtani *et al*., 2014, in cells expressing endogenous 37kDa LRP and 67kDa LR, the latter species runs in SDS–PAGE gels with an
apparent molecular mass of ~60 kDa, which is lower than might be expected of a homodimer of 37kDa LRP. The most likely explanation for this is that LR is resistant to denaturation in SDS, and thus maintains a more compact structure than during SDS–PAGE and runs with a higher electrophoretic mobility.

PrP^C was typically glycosylated, showing different bands ranging from ~27 to ~37 kDa; the unglycosylated form which migrates at ~27 kDa, the intermediate monoglycosylated form, which migrates at 28–30 kDa; and the highly glycosylated forms which migrate as bands spanning 33–37

kDa (Zannuso *et al*.,1998; Sarnataro *et al*., 2004). We next analyzed the subcellular localization of both laminin receptor and PrP^C, by indirect immunofluorescence and confocal microscopy of neuronal GT1 cells grown on coverslips (Figure 1b).

PrP^C was found mainly on the cell surface and in the Golgi area as previously demonstrated in GT1 cells and other neuronal cell lines (Shyng *et al*.,1993; Pimpinelli *et al*., 2005), while the receptor, accordingly to previous data showing a nuclear localization of laminin receptor and its interaction with histones (Kinoshita et al., 1998; Nikles et al., 2005), showed a nuclear-like and plasma membrane staining pattern (Figure 1b). Yellow-orange spots in the merged immunofluorescence images (Merge) of non-permeabilized cells in Figure 1b (InSet), indicate a fraction of 37/67kDa LR is also found on the plasma membrane with PrP^C.

The Pearson's Correlation Coefficient PCC, produced a value of 0.78, which reflects the good degree of colocalization of the two proteins on the cell surface. We estimated, by Mander's Colocalization Coefficient, MCC, that 72% of 37/67kDa LR colocalized with PrP^C on the plasma membrane and that 45% of PrP^C colocalized with 37/67kDa LR. These data indicate that the remaining 28% of laminin receptor could be free to be engaged by other interactors, such as laminin-1.

To assess the precise nature of receptor subcellular localization, 37/67kDa LR co-immunostaining was performed also with the antibody specific for molecular markers of different intracellular organelles, such as Golgin (for Golgi apparatus), KDEL (for the ER), EEA1 (for early endosomes). Transferrin Alexa 488-conjugated (Tfr) was used to label recycling endosomes and Lysotracker red for lysosomes (Figure 2). As expected, the PCC test produced a value close to zero, which indicated the absence of laminin receptor in the Golgi apparatus, as well as in other intracellular organelles.

1.2) Interaction between 37/67kDa laminin receptor and PrP^C

In vitro identification of direct and heparan sulphate proteoglycan-dependent interaction sites mediating the binding of the cellular PrP to laminin receptor (Hundt et al., 2001) and the findings concerning the high-affinity binding curve between GST-PrP and iodinated laminin receptor (Graner et al., 2000), prompt us to characterize the interaction between 37/67kDa LR and PrP^C in mammalian neuronal and non-neuronal cells.

In order to understand whether PrP^C and 37/67kDa LR entertained physical interaction in the cells, we subjected them to co-immunoprecipitation (Co-IP) from total cell lysates. Specifically, we first immunoprecipitated PrP^C from lysates and then immuno-identified laminin receptor in the precipitate by Western blotting. As shown in the Figure 3a, the 67kDa isoform of laminin receptor could be immunoprecipitated with a greater extent (compared to immature 37kDa LRP) along with PrP^C in GT1, as well as in HEK-293 cells (Figure 3c), whereas the precursor remained in major measure in the supernatant (SN) of the immunoprecipitate.

Importantly, to confirm the occurrence of the co-immunoprecipitation, we used an anti-laminin receptor antibody in the precipitation step and one against PrP^C to visualize prion protein in the Western blotting of the immunoprecipitate (Figure 3b).

To specifically discern the cellular compartment involved in 37/67kDa LR-PrP^C interaction, we performed cell-surface co-immunoprecipitation assays in the same conditions of the previous immunoprecipitation experiment with the exception that here (Figure 4) the cells were incubated on ice with the anti-PrP antibody SAF61, before lysis. As expected from the immunofluorescence data, the two proteins were both present at the cell surface, and again almost exclusively the mature 67kDa LR co-immunoprecipitated with PrP^C on the surface of live cells. Calnexin and Calreticulin (ER chaperones markers, CNX and CLR), which were used as control of the specificity of the

immunoprecipitation step, were also detectable in the immunocomplex. The presence of Calnexin and Calreticulin in the IP against PrP^C from the cell surface was unexpected and is further discussed below (see Discussion). Moreover, we conceive that cell surface PrP^C is complexed with cell surface CRL and CNX, but that this doesn't' show up in whole cell immunoprecipitates, because during the cell surface binding of PrP^C with SAF61 antibody we selectively enrich the CNX and CLR complexed with PrP^C on the plasma membrane.

Therefore, in order to ascertain the specificity of the Co-IP between LR and PrP^C, the same membrane used for immunoblotting with anti-CNX and anti-CLR antibodies, were stripped and hybridized with anti-Golgin antibody, a marker of the Golgi apparatus and anti-KDEL and ERp57 antibodies to test the presence of other Endoplasmic Reticulum-(ER) proteins in the IP. Protein-A beads alone were carried as control of the assay (Figure 2b, lane B). Notably, as shown in the Fig. 2b, Golgin, as well as KDEL and ERp57 proteins were absent from the PrP^C-37/67kDa LR immunocomplex.

1.3) The 37/67kDa laminin receptor inhibitor NSC47924 impairs PrP^C-37/67kDa LR binding both *in vitro* and in live cells

Previous studies demonstrated the requirement of the 37/67kDa LR system for prion propagation in vitro (Rieger *et al*., 1999; Leucht *et al*., 2003). Thus, a possible anti-prion therapy approach could target the 37/67kDa LR to impair 37/67kDa LR-PrP^C interaction. To this aim, we decided to study whether NSC47924, an inhibitor of 37/67kDa LR binding to laminin-1 (Pesapane *et al*., 2015), and directed to a laminin-active site of 37/67kDa LR, which is shared with PrP^C, influenced the interaction between 37/67kDa LR and PrP^C and eventually their intracellular trafficking. NSC47924 is directed to the "peptide G" domain of 37kDa LRP (aa 161-180), which is also the domain of HSPG-independent binding of 37/67kDa LR to PrP^C (Hundt *et al*., 2001). Since 67kDa LR derives from homo or hetero-

dimerization of 37kDa LRP (Buto et al., 1998; Landowski et al., 1995), NSC47924 is likely an inhibitor of both isoforms. Therefore, the ability of NSC47924 to inhibit the binding of human recombinant soluble 37LRP (r37LRP) to human recombinant PrP was first evaluated by ELISA assays (Figure 5a). Purified His-tagged r37LRP was incubated on wells pre-coated with human recombinant PrP, and binding was detected by anti-His HRP. As a control for binding specificity, r37LRP binding to BSA-coated wells was also evaluated in parallel and the absorbance readings subtracted. r37LRP binding to recombinant PrP was specifically inhibited by NSC47924. Thus, NSC47924 is a specific inhibitor of 37/67kDa LR direct binding to PrP^C, *in vitro*.
To test the compound in live cells, we performed co-immunoprecipitation assays in both control condition and treatment of GT1 and HEK-293 cells with the inhibitor (20 μM NSC47924) (IC50=20 μM for inhibition of 37/67kDa LR binding to laminin-1 Pesapane et al., 2015). Interestingly, the presence of NSC47924 in kinetic Co-IP assays (Figure 5b), impaired the formation of the 37/67kDa LR-PrP^C immunocomplex in GT1, as well as in HEK-293 cells, in a time-dependent manner; furthermore, inhibitor incubation induced a decrease of 67kDa LR and a progressive and substantial increase of PrP^C in the immunocomplex (Figure 5b, IP lane), as shown by the protein ratios plotted in the graphs (Figure 5b, right panels).

1.4) The NSC47924 inhibitor affects the trafficking of 37/67kDa LR from the cell surface stabilizing PrP^C on the plasma membrane

To understand why NSC47924 exerts the aforementioned effects and dissect the mechanism by which it acts in the cells, we decided to investigate whether the localization and intracellular trafficking of 37/67kDa LR and PrP^C were perturbed by the inhibitor treatment. Thus, we performed kinetic biotinylation assays (Figure 6a) in which, GT1 cell surface proteins were biotinylated before and after inhibitor treatment at different times.

37/67kDa LR and PrP^C were immunoidentified with the specific primary antibodies by a Western blot analysis on both streptavidin-immunoprecipitated materials (which contains only biotinylated proteins) and total cell lysates (which contains biotinylated and non-biotinylated proteins). We found that the 37kDa LRP was the most represented isoform both on the plasma membrane and in the total cell lysates. This latter isoform together with the 67kDa LR, starting from 30 min up to 180 min of NSC47924 treatment, progressively decreased from the cell surface in a time-dependent manner (Figure 6c), possibly due to a stimulated internalization and degradation. Interestingly, the presence of NSC47924 induced stabilization of cell surface PrP^C (Figure 6b, bottom panel), thus reinforcing the results found in the Co-IP assays, where the presence of 67kDa LR in the immunocomplex decreased in favour of PrP^C (see Figure 5b).

In parallel, we employed double indirect immunofluorescence kinetic assays monitoring the presence of both 37/67kDa LR and PrP^C on the cell surface after different times of NSC47924 treatment under non-permeabilized conditions. To this aim, GT1 cells were treated or not (control) with the inhibitor for the same times of the biotinylation assays; after that, as shown in Figure 8, the cells were fixed and processed for immunofluorescence to analyse the presence of 37/67kDa LR and PrP^C on the cell surface. In agreement with biotinylation experiments, we found that while cell surface signal of 37/67kDa LR decreased on the plasma membrane in a time-dependent manner, PrP^C was stably present on the cell surface indicating an opposite effect of the compound on the trafficking of the two proteins.

In order to specifically investigate the effect of NSC47924 on the intracellular fate of the two proteins, we performed double indirect immunofluorescence assays under permeabilized conditions, following specifically the cell surface laminin receptor and PrP^C pools (Figure 7). GT1 cells, were first incubated on ice (t=0' at 4 °C, which blocks membrane trafficking, Arancibia-Carcamo et al., 2006) with the

primary antibodies against both laminin receptor and PrP^C and then treated at 37 °C (which allows membrane trafficking) with or without the inhibitor, from 30 min up to 180 min, fixed and permeabilized. Accordingly, to Co-IP assays, the two proteins colocalized on the cell surface and already after 30 min at room temperature (RT), both 37/67kDa LR and PrP^C entered the cells, as shown by the punctate staining. The presence of the inhibitor, (t=30' RT, room temperature, + NSC47924) induced internalization of 37/67kDa LR and a decrement of PrP^C colocalization, which was totally abolished with increasing times of inhibitor treatment (t=90' and 180'). The disappearance of punctate laminin receptor staining which resulted somewhat sparse into the cells and sharply less intense compared to control, supports the results from biotinylation kinetics (Figure 5a), confirming that the inhibitor stimulates 37/67kDa LR internalization and possibly its degradation, while PrP^C was stabilized on the cell surface due to its prevented internalization. This effect could be explained by assuming that PrP^C becomes not able to be internalized because of the absence of its receptor.

To characterize 37/67kDa LR internalization in GT1 cells, we performed double immunofluorescence assays by labelling laminin receptor and a marker of early endosomal pathway EEA1, followed by confocal microscopy analysis (Figure 9a). Differently from untreated GT1 cells, 37/67kDa LR colocalized with EEA1 under NSC47924 treatment. A PCC average value higher than 0.6 (N=100) was found. This partial early endosomal accumulation was clearly evident after 30 min inhibitor treatment. Interestingly, NSC47924 treatment induced a substantial re-localization of 37/67kDa LR in the endo-lysosomal compartment, as indicated by colocalization with Lamp-1 in double indirect immunofluorescence assays (Figure 9b). A PCC average value higher than 0.7 (N=100) was found after 90 min and a value of 0.8 after 180 min. We confirmed 37/67kDa LR internalization via early-endosomes (Figure 9b) and its lysosomal-

mediated degradation (Figure 9b and Figure 10a). Indeed, the effect of inhibiting lysosomal protein degradation on 37/67kDa LR fragment generation, was determined incubating GT1 cells for 2 days in culture medium containing 20 mM NH4Cl, in the presence (30', 180') or not (-) of NSC47924 inhibitor (Figure 10 panels c, d). We found that NH4Cl treatment resulted in accumulation of 37/67kDa LR and inhibition of 37/67kDa LR fragment generation (180' NSC47924 control *versus* +NH4Cl, and quantification in panel d) implying that NSC47924 also affects 37/67kDa LR lysosomal-mediated degradation. Moreover, as shown in Fig. 6c, the fragment did not reach the cell surface.

Taken together, these results indicate that the inhibitor specifically interferes with 37/67kDa LR cell surface interaction with PrP^C, stimulating internalization of both 37kDa and 67kDa LR isoforms suggesting that NSC47924 might act through sterical hindrance contrasting physiological 37/67kDa LR cell surface interaction with laminin-1 and PrP^C.

Discussion

Mapping analysis in yeast two-hybrid system and cell-binding assay identified PrPLRPbd1 (amminoacids aa 144-179) as a direct and PrPLRbd2 (amminoacids aa 53-93) as an indirect HSPG-dependent laminin receptor precursor (LRP)-binding site on PrP^C (Hundt *et al*., 2001).

Furthermore, cell-binding and internalization studies proved that 37/67kDa LR acts as the receptor for PrPs on the cell surface (Gauczynski *et al*., 2006). Here, we analysed the interaction between the non-integrin laminin receptor and cellular PrP by screening for the binding of all LR isoforms with PrP^C by co-immunoprecipitation assays, in both neuronal and non-neuronal cell systems. Despite previous and controversial findings of interaction between 37kDa LRP and FLAG-PrP in transiently co-transfected COS-7 cells (Rieger *et al*., 1997), the localization of this interaction and its physiopathological role are still

debated, therefore our attempt to investigate the interaction between the two proteins under physiological conditions in neuronal cells is novel. In particular, we asked whether the two proteins interacted in neuronal cells, as well as in non-neuronal cells, and which of the laminin receptor isoforms specifically interacted with PrP^C.

Since PrP^C is localized on the surface of neuronal cells (Stahl *et al*., 1993; Harris *et al*., 1999) and 37/67kDa LR is also present in neuronal cells (Douville *et al*., 1988), we hypothesized that the interaction between the two proteins could occur on the surface of the cells. By double immunofluorescence assay in non permeabilized cells and a cell-surface immunoprecipitation of PrP^C followed by detection of laminin receptor by immunoblotting, we could show that the two proteins colocalized on the plasma membrane and that PrP^C preferentially co-immunoprepitated with the mature 67kDa LR.

Interestingly, we detected the presence of Calnexin and Calreticulin, which are typical molecular chaperones resident in the ER, in the surface immunoprecipitate. This finding was (Figure 4) unpredicted regarding the co-immunoprecipitation with PrP^C, but was in agreement with other results in which it has been demonstrated that typical ER proteins, like Calreticulin, could be located on the cell surface also (Johnson *et al*., 2001; Itakura *et al*., 2013). The marked co-immunoprecipitation of PrP^C with Calnexin and Calreticulin on the plasma membrane is particularly interesting considering that catalysis of protein folding is controlled by the interaction with these two chaperones (Zapun *et al*., 1998) and that PrP^C to PrP^{Sc} conversion is underlined by unfolding process (Sarnataro *et al*., 2004). Moreover, the presence of ER chaperones CNX and CLR (which retains a KDEL signal), in the surface Co-IP materials, was specifically confirmed by the absence of Golgi resident proteins (as Golgin), as well as the absence of other ER-resident proteins, such as ERp57 (which often associates with CNX in the ER), and other KDEL proteins. Accordingly, to previous results in neuronal cells (Itakura *et al.*, 2013), where a

significant fraction of CNX was found on the cell surface of neurons and that ERp57, in contrast to CNX, was highly enriched in the non-synaptic membrane fractions, our findings indicate that CNX and ERp57 not necessarily follow the same fate into the cells.

Moreover, although CLR is a KDEL protein, we found only a negligible KDEL band in the Co-IP material. The most likely explanation for this is that the complex of CLR with cell surface PrP^C could somehow mask the KDEL signal, rendering CLR "not well recognizable" by the anti-KDEL antibody; the chaperons proteins might be expressed in different isoforms that do not contain the ER-retrieval sequence (KDEL) (Johnson et al., 2001). Another possibility is that CLR might be proteolytically processed by ER-luminal proteases to a form missing the KDEL, given that, under ER-luminal Ca^2 concentrations, the C-domain of the protein containing the KDEL amino acid sequence is susceptible to proteolysis (Corbett *et al*., 2000).

Therefore, Co-IP assays from the cell surface give rise to a series of questions, among these, whether PrP^C on the cell surface of GT1 cells is properly folded or not. However, this phenomenon deserves further investigation.

Although the interaction between 37/67kDa LR and PrP^C has been previously proposed, our results provide the first clear evidence that this interaction occurs on the plasma membrane, suggesting that the 67kDa LR may act as a PrP^C cell surface receptor in neuronal mammalian cells.

To analyze the nature of 37/67kDa LR-PrP^C interaction, we decided to study whether the laminin recepotor inhibitor NSC47924, targeting the peptide G sequence of 37/67kDa LR (residues 161-180) able to directly bind both laminin-1 (Castronovo *et al*., 1991) and PrP^C (Hundt *et al*.,2001), influenced the interaction between 37/67kDa LR and PrP^C and eventually their intracellular trafficking. NSC47924 specifically inhibited 37/67kDa LR direct binding to PrP^C in ELISA assays and perturbed the interaction between the two proteins in live cells also. We speculate that is most likely because NSC47924 is able to antagonize both

the direct, peptide G-mediated, 37/67kDa LR binding to PrP^C and the HPSGs-mediated indirect one, which occurs in live cells (Hundt *et al*., 2001).

The drug treatment induces cell surface disappearance of 37/67kDa LR and accumulation in early and late endosomes/lysosomes, stabilizing cell surface distribution of PrP^C, suggesting that the inhibitor impairs 37/67kDa LR trafficking and definitively interaction with PrP^C.

We envisage the following hypothesis to explain our findings: the inhibitor NSC47924 could exploit its effect on the cell surface 37/67kDa LR by perturbing receptor anchorage to both laminin-1 and PrP^C, thus rendering the 37/67kDa LR more prone to be internalized. It is likely that this compound could exert its effect on both bound and free 37/67kDa LR on the cell surface, inducing its internalization and degradation. However, once internalized the 37/67kDa LR partially accumulates in EEA1 enriched-endosomes and, ultimately, into endo-lysosomal vesicles. This effect dramatically decreases cell binding to the laminin of extracellular matrix (Pesapane *et al*., 2005), for which peptide G is crucial (Castronovo *et al*., 1991). Thus, the fact that the presence of 37/67kDa LR decreased along with increasing times of treatment, resulting in its partial early endosomes accumulation and progressive late endo-lysosomal localization after inhibitor incubation, suggests that the intracellular trafficking and presumably the normal endocytic pathway of 37/67kDa LR is altered by NSC47924. This compound, inducing 37/67kDa LR internalization, is able to subtract laminin receptor from binding to PrP^C, which in presence of the inhibitor, is no longer able to be internalized.

These findings, on one hand, are very crucial if we consider that the main function of 37/67kDa LR is to enhance tumor cell adhesion to the laminin of basement membranes and cell migration, two key events in the metastasis cascade (Montuori and Sobel, 1996). Thus, inhibiting 37/67kDa LR binding to laminin (Zuber *et al*., 2008; Chetty *et al*., 2014), as well as modulating its expression on the cell surface and

degradation could be a feasible approach to block tumor invasion. On the other hand, the effect that the 37/67kDa LR inhibitor exerts on PrP^{C}, stabilizing its cell surface localization, provides good hopes to test it against prion conversion, which has been demonstrated to occur on the plasma membrane (Goold *et al*., 2011) and/or intracellular compartments (Marijonovic *et al*., 2009). However, whether the effects we observed, due to the inhibitor, could result in a stimulus or a stumbling block to determine PrP^{C} to PrP^{Sc} conformational transition has to be established with further investigations.

Moreover, the finding that 37/67kDa LR may play a role in Alzheimer's disease (AD) (Jovanovic *et al*., 2015; Da Costa Dias *et al*., 2014) and that modulation of 37/67kDa LR could affect A*β* cytotoxicity (Da Costa Dias *et al*., 2013; Pinnock *et al*., 2015) and its release from cells (Jovanovic *et al*., 2013), highlights the importance of NSC47924 inhibitor to modulate 37/67kDa LR trafficking and degradation, and the consequences that this inhibitor could have on other neurodegenerative disorders.

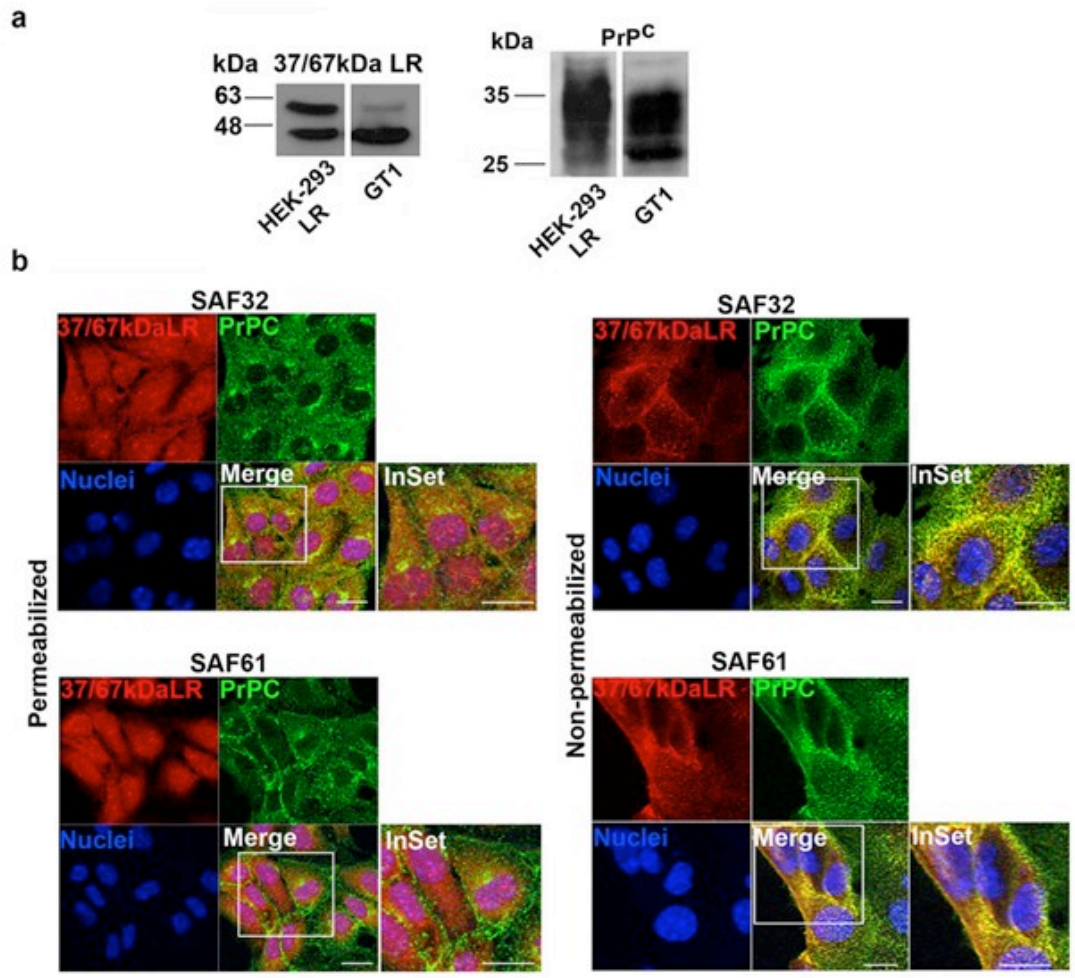

Figure 1. Expression levels and localization of 37/67kDa LR and PrP^C in GT1 and HEK-293 cells. (a) GT1 and HEK-293 LR cells grown in DMEM supplemented with 10% foetal bovine serum, were scraped in lysis buffer and 80µg of total proteins were subjected to SDS-PAGE. 37/67kDa LR and PrP^C were revealed by Western blotting on PVDF and hybridization with a 4290 pAb and SAF32 mAb, respectively. Molecular weights corresponding to the different bands revealed by ECL are indicated and expressed in kDa. (b) GT1 cells grown on coverslips and fixed in 4% paraformaldehyde, after 0.1% TX-100 permeabilization (left panel) or under non-permeabilized conditions (right panel), were double labelled with anti-PrP SAF32 (top panel) or SAF61 (bottom panel) antibody and 5004 anti-LR antibody; secondary Ab anti-mouse Alexa-488- (green) and anti-rabbit Alexa-546- (red) conjugated were used to reveal PrP^C and 37/67kDa LR, respectively. Samples were observed using a laser scanning confocal microscope LSM 510 META Zeiss. InSet shows 2x zoom of images acquired with a 63x objective lens. Scale bar, 10 µm.

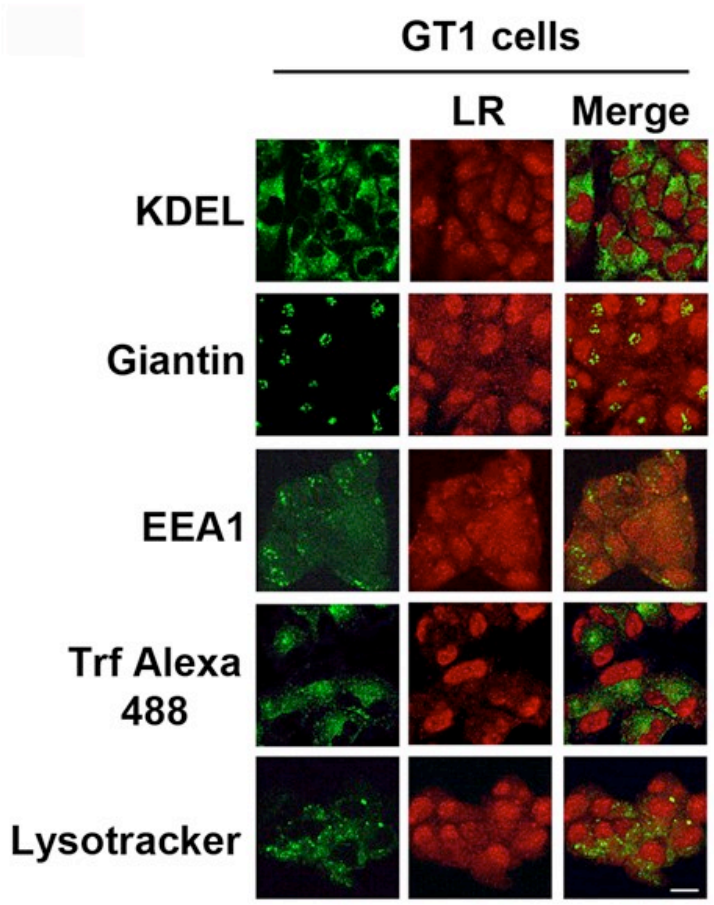

Figure 2. 37/67kDa LR does not localize in intracellular compartments.
GT1 cells grown on coverslips were fixed, permeabilized with TX-100 0.1% for 10 min and incubated with anti-37/67kDa LR 5004 pAb and with primary antibodies against different markers of intracellular compartments (KDEL, Golgin, EEA1 early endosomes antigen 1). The cells were then stained with anti-mouse and anti-rabbit secondary antibody conjugated with Alexa-488 and Alexa-546.
Lysotracker red was used to label lysosomes for 1 hour at 37°C and TfrAlexa-488 to label recycling endosomes for 45 min in vivo before fixation and confocal imaging. Scale bar, 10 μm.

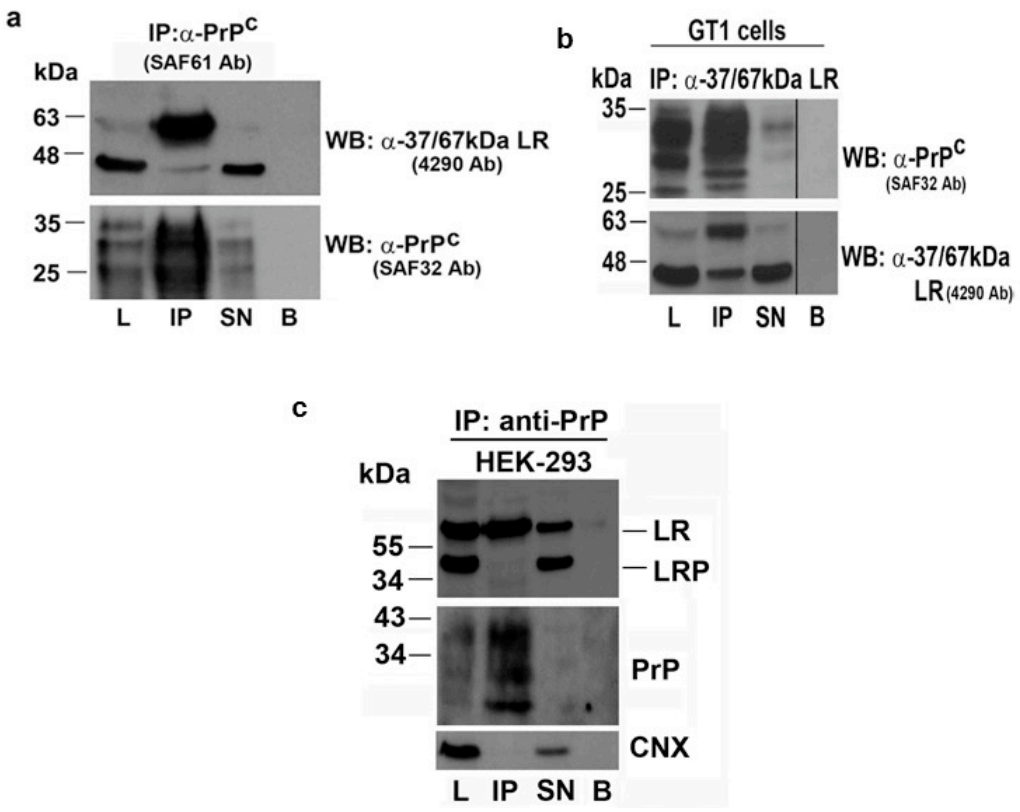

Figure 3. 37/67kDa LR and PrP^C co-immunoprecipitate in GT1 and HEK-293 cells. (a) GT1 cells were grown on 150 mm dishes, lysed and PrP^C was immunoprecipitated using SAF61 mAb. 37/67kDa LR was revealed using 4290 pAb. The membrane was stripped and blotted with SAF32 mAb to confirm the occurrence of the immunoprecipitation. L: input, IP: immunoprecipitated, SN: supernatant, B: protein-A beads alone. (b) GT1 cells were grown on 150 mm dishes, lysed and 37/67kDa LR was immunoprecipitated using anti-37/67kDa LR 4290 pAb. PrPC was revealed in the immunoprecipitate by western blotting by anti-PrP SAF32 antibody. The membrane was stripped and blotted with 4290 pAb to confirm the occurrence of the immunoprecipitation. L: input, IP: immunoprecipitated, SN: 1/10 supernatant of immunoprecipitated proteins, B: protein-A beads alone. (c). HEK-293 cells were grown and treated as before (fig. 3.a)

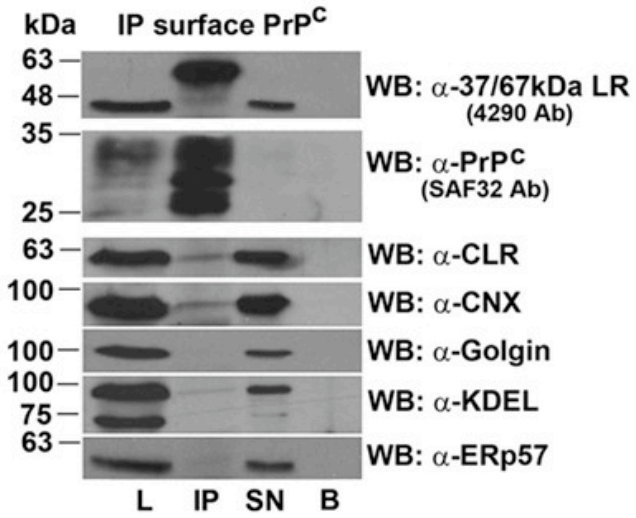

Figure 4 37/67kDa LR and PrP^C co-immunoprecipitate on the surface of GT1 cells. GT1 cells grown on 150 mm dishes were first incubated with SAF61 mAb 1 hr at 4°C, then washed and lysed in lysis buffer. PrP^C was immunoprecipitated with protein-A beads which were loaded on gels and transferred to nitrocellulose. Western blotting was performed by incubation with anti-37/67kDa LR 4290 pAb. To confirm immunoprecipitation the membrane was stripped and probed with anti-PrP SAF32 mAb. Calnexin, Calreticulin, Golgin, KDEL and ERp57, were revealed by Western blotting with the specific antibodies on the same membranes after stripping. Note the presence of CLR and CNX, as well as the absence of Golgin, KDEL and ERp57 in the IP lane. L: input, IP: immunoprecipitated, SN: supernatant, B: protein-A beads alone. Anti-KDEL antibody detects two bands of ~94kDa and ~78kDa.

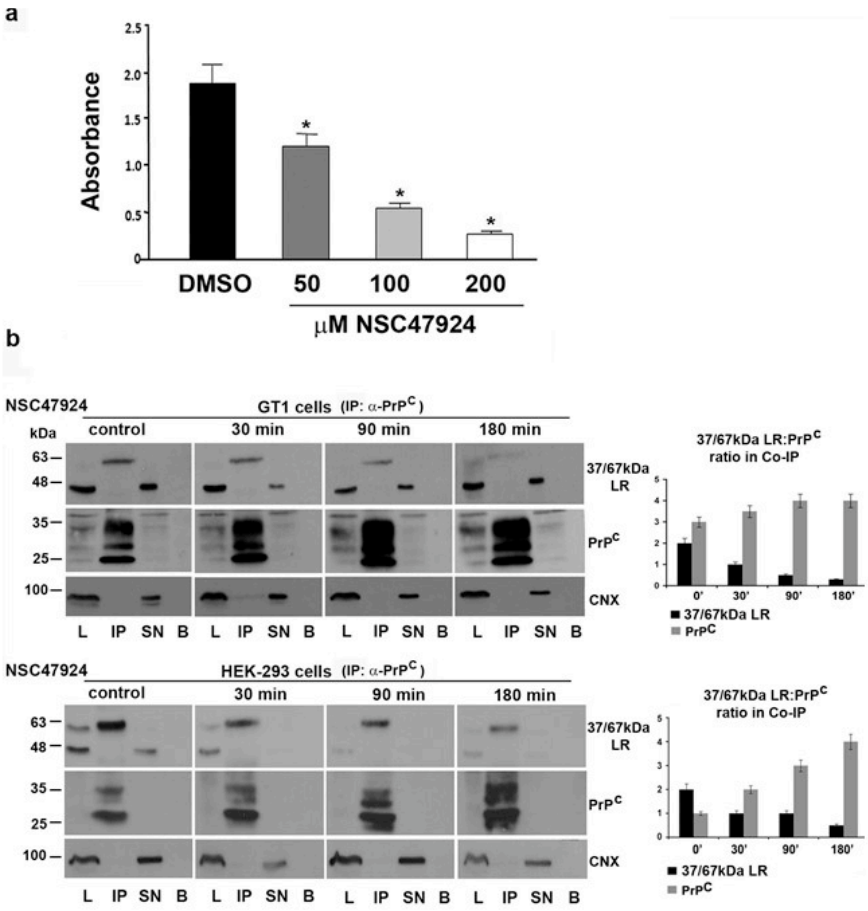

Figure 5. 37/67kDa LR inhibitor NSC47924 impairs recombinant PrP-r37LRP binding *in vitro* and perturbs co-immunoprecipitation of 37/67kDa LR and PrP^C in live cells. (a) Purified human His-tagged recombinant 37LRP (r37LRP) was placed for 1 hour at 37°C on wells coated with 125 ng of human recombinant PrP, in the presence of 50, 100 and 200 μM NSC47924, or DMSO as a vehicle control. Bound r37LRP was revealed by anti-His-HRP and OPD staining; the absorbance at 490 nm was measured. r37LRP binding to BSA-coated wells was subtracted to obtain specific binding. Values represent the mean±SEM of three experiments carried out in triplicate; (*, $P< 0.05$). (b) Co-IP in GT1 and HEK-293-LR cells was carried out after inhibitor treatment in kinetic assays, for indicated times, using anti-PrP SAF32 mAb to immunoprecipiate PrP^C and anti-37/67kDa LR 4290 pAb to reveal 37/67kDa LR in the IP. Immunoblotting with SAF32 mAb was performed to ascertain the occurrence of IP. Calnexin was revealed by stripping the same membranes used above, immunoblotted with anti-CNX antibody and revealed with ECL. For comparison, signals of CNX are shown to exclude both aspecifics and defect in loading samples on gels. 37/67kDa LR/PrP^C ratio in the immunocomplex was determined by imposing as 100% the sum of 37/67kDa LR and PrP^C signals in the IP. To calculate ratio, densitometric analysis was performed with ImageJ software and values from the mean±SEM of three experiments, were considered ($P< 0.05$). All data were statistically significant

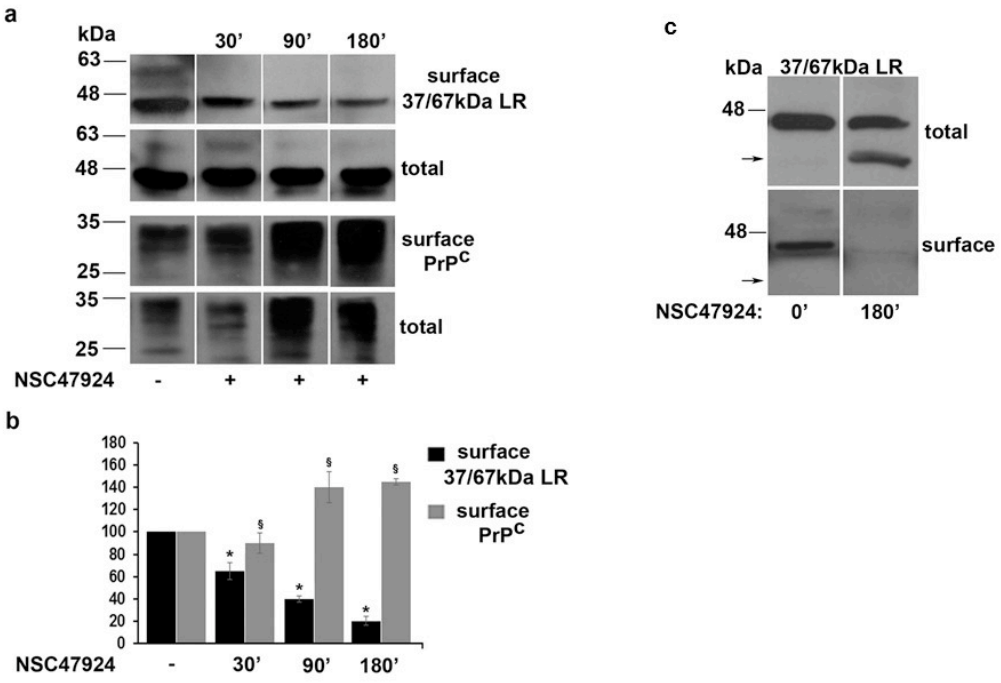

Figure 6. The inhibitor NSC47924 interferes with plasma membrane localization of 37/67kDa LR. (a) GT1 cell surface proteins were biotinylated at 4°C in control conditions (without inhibitor, -) or after 30 min, 90 min and 180 min of treatment with NSC47924 at 37°C, and were recovered from cell lysates by immunoprecipitation with streptavidin-beads. Total (80 µg of total cell lysates) and cell surface proteins (IP from streptavidin beads), were loaded on gel and processed for SDS-PAGE and ECL. 37/67kDa LR and PrP^C were immunodetected by blotting with 4290 pAb and SAF32 mAb, respectively.
(b) The plot shows the relative percentage of 37/67kDa LR and PrP^C on the surface of the cells after indicated times of NSC47924 treatment, using as 100% the maximal expression value at cell surface in control conditions (- NSC47924). Data are expressed as the means±SEM of three independent experiments (*,§, $P<0.05$). (c) GT1 cell surface proteins were biotinylated at 4°C in control conditions (without inhibitor,-) or after 180 min of treatment with NSC47924 at 37°C, cell lysates and blot were processed as (a). Note the presence 37/67kDa LR fragment in the total cell lysates and its absence on the cell surface (arrow).

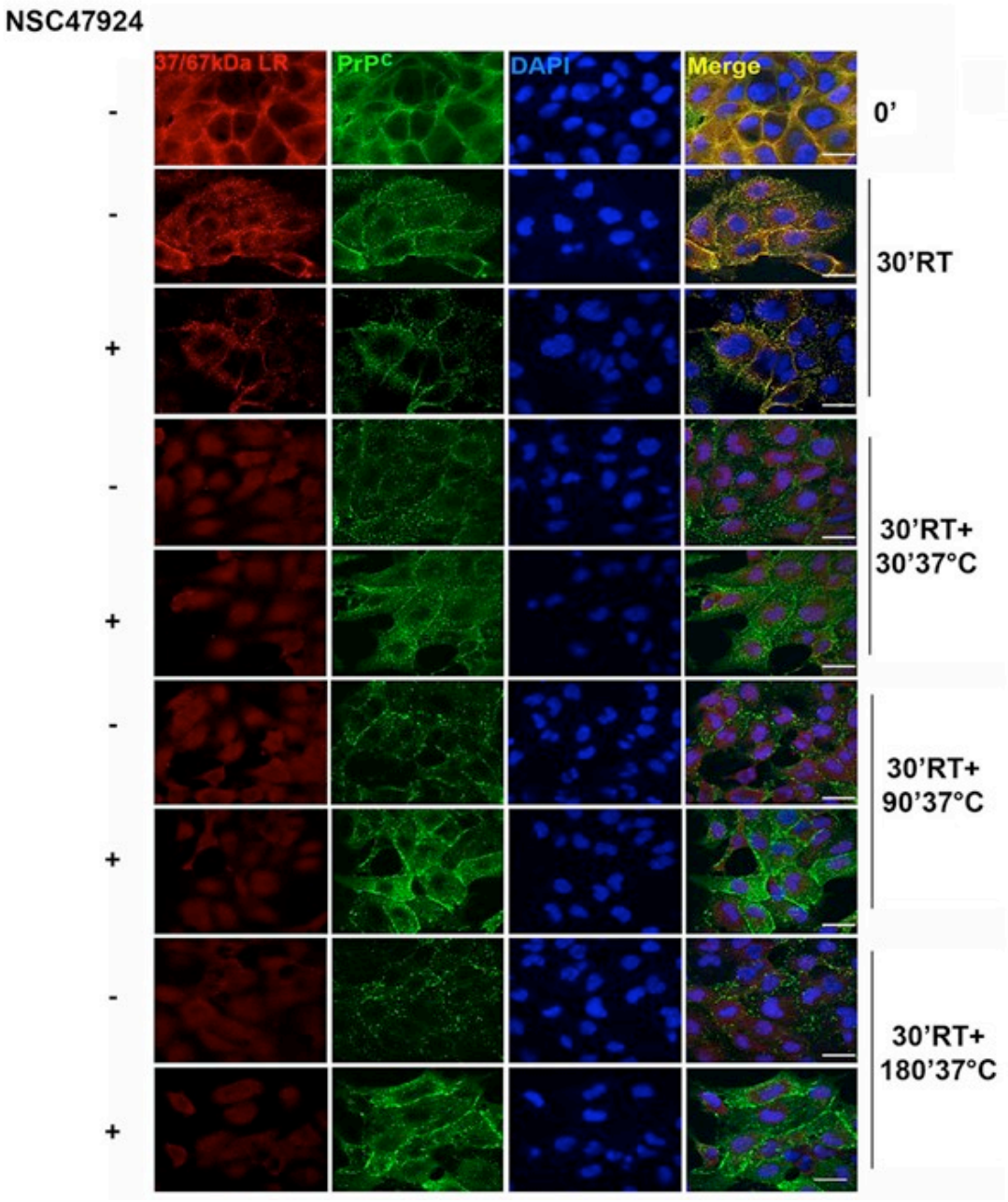

Figure 7. NSC47924 affects the intracellular fate of 37/67kDa LR and PrP^C. GT1 cells were grown on coverslips, cooled at 4°C on ice, and stained with SAF32 mAb (1:100) and 5004 pAb (1:50) to label cell surface PrP^C and 37/67kDa LR, respectively. To allow membrane trafficking and internalization, GT1 cells were warmed at 37 °C in the in culture medium with or without NSC47924 for indicated times. After that, the cells were washed, fixed in PFA 4% and permeabilized in 0.1% TX-100 for 10 min. To detect internalized proteins the cells were labelled with secondary antibodies (PrP^C, green; 37/67kDa LR, red) and their colocalization was measured. RT: Room Temperature; Scale bars, 10 μm.

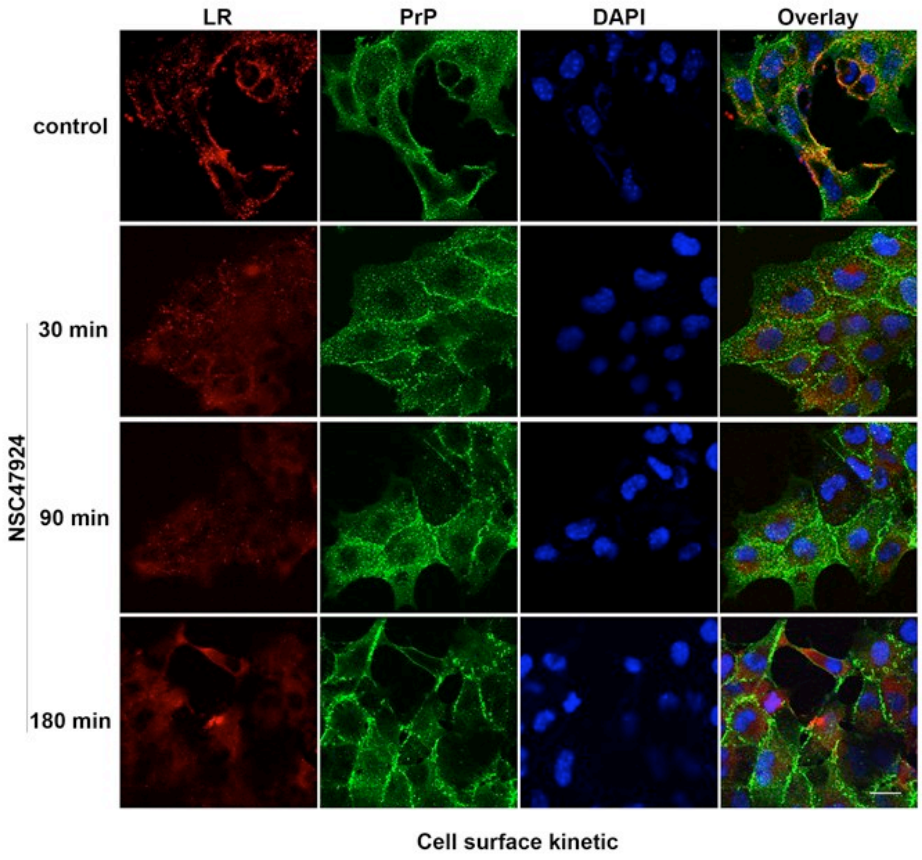

Figure 8. The inhibitor NSC47924 interferes with cell surface localization of 37/67kDa LR. GT1 cells were grown on coverslips and, after treatment with NSC47924 (or not, control-), were fixed and processed under non-permeabilized conditions for indirect immunofluorescence by labelling 37/67kDa LR (red) and PrP^C (green) with respective primary and secondary fluorescent antibodies. Nuclei were stained with DAPI. Scale bar, 10 μm.

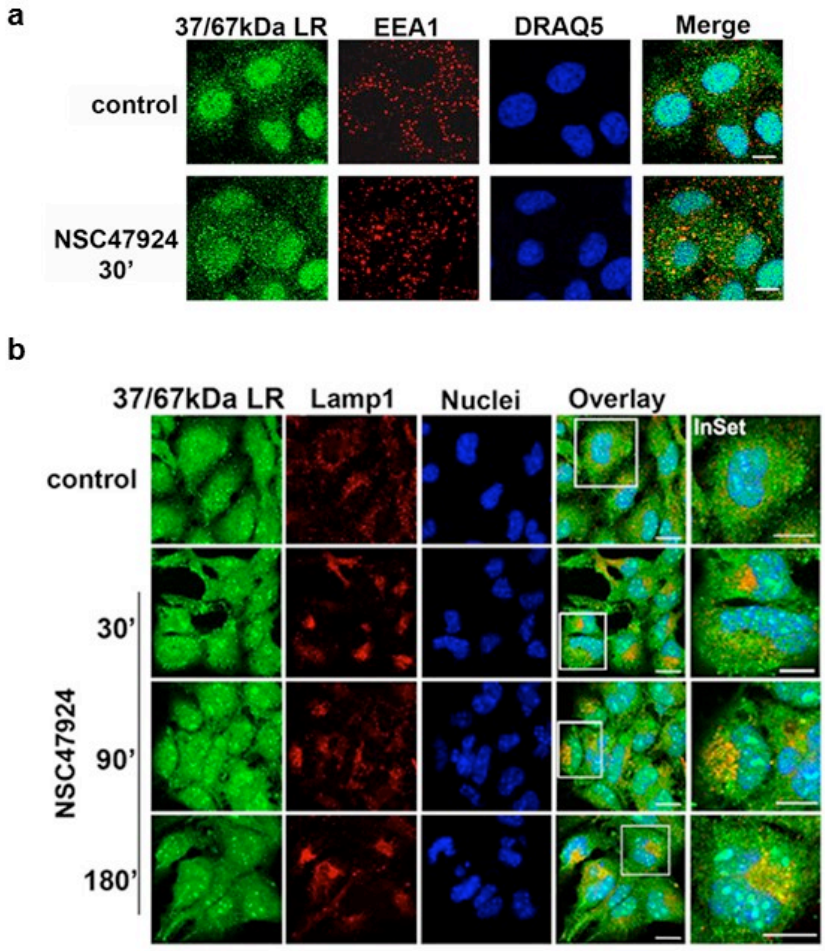

Figure 9. The inhibitor NSC47924 induces 37/67kDa LR and its lysosomal mediated degradation. (a) GT1 cells grown on coverslips in both control (without inhibitor) and treated conditions (30 min NSC47924) were fixed, permeabilized with TX-100 and probed with 5004 pAb and anti-EEA1 mAb to label 37/67kDa LR and early endosomes, respectively. Secondary antibodies Alexa-488- and Alexa-546-conjugated were used to visualize 37/67kDa LR and EEA1. Nuclei were stained with DRAQ5 dye (blue). Distribution of 37/67kDa LR and EEA1 were analyzed by confocal microscopy. Scale bar, 10 µm. (b) GT1 cells grown as before (a) were treated with NSC47924 for indicated times and immunostained with anti-37/67kDa LR 5004 antibody (green) and anti-Lamp1 (marker of endo-lysosomes, red). Distribution of 37/67kDa LR and Lamp1 were analyzed by confocal microscopy. Scale bar, 10 µm.

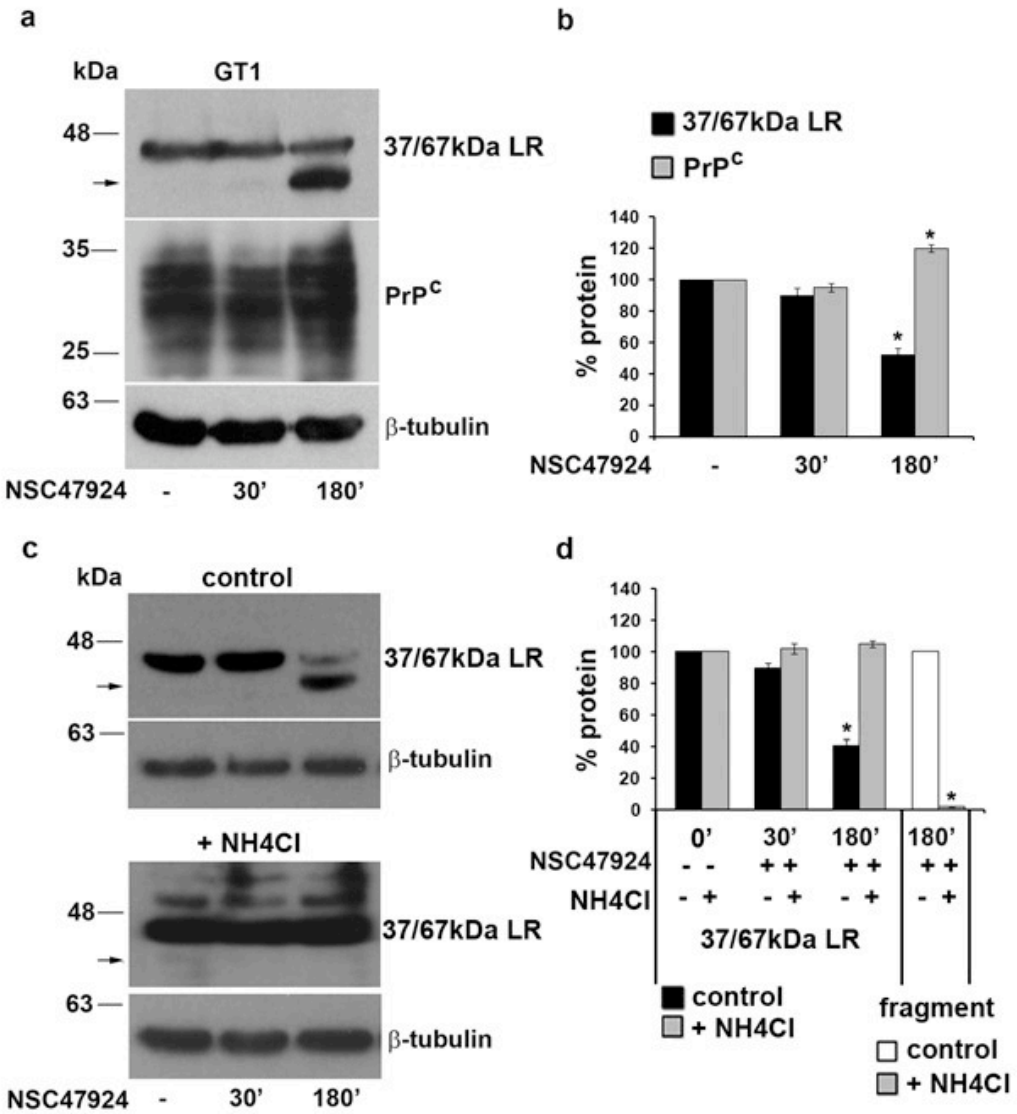

Figure 10. NSC47924 induces accumulation of PrP^C and lysosome degradation of 37/67kDa LR in live cells. (a) GT1 cells grown in 60 mm dishes were treated (30 min, 180 min) or not (-) with NSC47924. They were then scraped in lysis buffer and 80µg of total proteins were subjected to SDS-PAGE. 37/67kDa LR and PrP^C were revealed by Western blotting on PVDF and hybridization with a 4290 pAb and SAF32 mAb, respectively. β-tubulin was carried out as loading control. Arrow likely points to 37/67kDa LR degradation fragment. (b) Bands corresponding to 37/67kDa LR and PrP^C were quantified imposing as 100% the amount of both proteins in control conditions, without NSC47924 (-) (N=3, **P*<0.05). (c) GT1 cells were treated as in (a) with the exception that here NH_4Cl (20 mM, 2 days) was added (+) or not (control) to the culture medium. 37/67kDa LR was revealed by Western blotting on PVDF and hybridization with a 4290 pAb. Note the absence of 37/67kDa LR fragment in NH4Cl panel (arrow). (d) 37/67kDa LR before (-) and after (+) 2 days NH_4Cl treatment, was quantified imposing as 100% the amount of 37/67kDa LR without NSC47924 (-) (N=3, **P*<0.05). Since the 37/67kDa LR fragment generates only after 180 min of NSC47924 treatment, it was quantified, separately from 37/67kDa LR, imposing as 100% the amount of fragment under 180' NSC47924 (control) but without (-) NH_4Cl.

RESULTS AND DISCUSSION

PROJECT-2

Results

2.1) Endogenous Shadoo and PrP^C expression and localization in neuronal cells

The endogenous Shadoo, from mouse neuronal GT1 cell lysates, migrated on SDS-PAGE as different bands corresponding, respectively, to the glycosylated (~22kDa) and unglycosylated (~16kDa) form, as shown before (Watts et al., 2007) (Figure 2.1a). Furthermore, by Western blot analysis with the anti-Shadoo SPRN-R-12 antibody, another band around 12kDa appeared on SDS-PAGE 14% polyacrylamide gel. Based on the description by Premzl et al., 2003, by which Shadoo is predicted to have both a signal peptide (ER-SP) at aa 25 and a GPI-AS (attachment signal) at the aa 125 (human sequence), we reported the 12kDa isoform as the Shadoo form lacking both the ER-SP and the GPI-AS

PrP^C was typically glycosylated, showing different bands ranging from ~27 to ~37 kDa; the unglycosylated form which migrates at ~27 kDa, the intermediate monoglycosylated form, which migrates at 28–30 kDa; and the highly glycosylated forms which migrate as bands spanning 33–37 kDa.

Next, to characterize the subcellular distribution of both Shadoo and PrP^C in GT1 cells, we analyzed their localization performing double indirect immunofluorescence analysis using their respective primary antibodies (polyclonal SPRN-R12 and monoclonal SAF32 Abs) followed by fluorescently labeled secondary antibodies (Figure 2.1b). As shown, Shadoo was localized both intracellularly, and on the plasma membrane with PrP^C. In order to quantify the amount of plasma membrane localized Shadoo, we employed biotinylation assays which confirmed its cell surface localization (Figure 2.1c). Interestingly, all Shadoo isoforms, as well as for PrP^C, were present on the

plasma membrane of GT1 cells (see the IP lane of Figure 2.2c, left panel).

2.2) Mitochondrial localization of Shadoo and TRAP1 chaperoning

Based on previous report showing that the ER signal peptide of Shadoo can mediate targeting to mitochondria (Pfeiffer et al., 2013), we decided to further explore the subcellular localization of endogenous Shadoo, using indirect immunofluorescence microscopy followed by confocal analyses. We found that Shadoo colocalized both with the ER (PCC = 0.62) and mitochondria (PCC =0.88, N=80) (Figure 2.2), and by western blot analysis of purified mitochondrial fraction (Figure 2.3), we found that specifically an isoform of Shadoo with an electrophoretic motility around 18kDa co-purified with mitochondria. Reasonably, this latter form could likely correspond to the non-translocated Shadoo, which should retain the N-terminal ER-signal peptide (ER-SP).
Furthermore, analyzing the fractionation assay (Figure 3), we obtained the following informations: three isoforms of Shadoo enriched the ER, the fully glycosylated (22kDa), the unglycosylated translocated Shadoo (16kDa, without the ER-SP) and the 12kDa isoform (lacking both the ER-SP and the GPI-AS).
It has been described the presence of the mitochondrial chaperone TRAP1 (Heat shock protein 75 kDa) on the outer side of the ER and has a role in the quality control of proteins destined to the mitochondria (Amoroso et al., 2012), for this reason, we decided to investigate the relationship between TRAP1 and Shadoo.
In order to understand whether Shadoo and TRAP1 entertained physical interaction in SHSY5Y cells, we first subjected them to double immunofluorescence analysis with anti-Shadoo SPRN-R12 Ab and with the mitochondrial marker Mitotracker green or with anti-TRAP1 Ab (Figure 2.4 a,b); in parallel, total lysates of SHSY5Y cells were processed for co-immunoprecipitation (Co-IP) assays (Figure 2.4c). Specifically, as well as for GT1 cells, we were able to show

that Shadoo localized in the mitochondria also in SHSY5Y cells and, by immunoprecipitation analysis we first immunoprecipitated TRAP1 from lysates and then immuno-identified Shadoo in the precipitate by Western blotting with SPRN-R12 antibody. Importantly, to confirm the occurrence of the co-immunoprecipitation, as control we used non-specific immunoglobulins (IgM) in the precipitation step or protein-A beads alone (Figure 2.4c). As deduced by molecular weight analysis from electrophoresis and as shown in the Figure 2.4c, exclusively the non-translocated isoform retaining the ER-signal peptide of Shadoo (~18kDa, asterisk) could be immunoprecipitated along with TRAP1, whereas the other isoforms remained in the supernatant (SN) of the immunoprecipitate.

2.3) Shadoo DRM-association

We have previously demonstrated that PrP^C was localized on the plasma membrane of epithelial cells and that it was associated with lipid rafts, whose perturbation did not affect its surface distribution, but rather affected its folding (Sarnataro et al., 2004; Campana et al., 2005), rendering PrP^C partially resistant to PK digestion. On the basis of these findings, we asked whether Shadoo was associated with lipid rafts and they had any role in its metabolism. To this aim, we first performed an insolubility TX-100 extraction assay, finding Shadoo in the insoluble (I) material as expected for a DRM-associated protein (Figure 2.5a). Interestingly, all Shadoo isoforms were present in the insoluble material. Furthermore, to confirm its association with lipid rafts, we employed floatation-based sucrose density gradients in which Shadoo was purified by centrifugation to equilibrium, as well as Flotillin-2 (Flot 2) and PrP^C, which were used as markers of both DRMs and control of the procedure (Caputo et al., 2009). We found that glycosylated Shadoo and 12 kDa its isoform floated to the lighter fractions of the gradients (fractions 4-7) where normally DRM-associated proteins reside. Notably, both the mature glycosylated and the ER-translocated isoform of Shadoo (~12kDa) associated with DRMs (Figure 2.5b).

2.4) Acquisition of "scrapie-like" properties of Shadoo

Our previous data showing the "protective role" of DRM-association in the correct folding of PrP^C (Sarnataro *et al.,* 2004), together with our finding that Shadoo partitioned in the DRM fractions of the sucrose density gradients, prompted us to investigate the folding of Shadoo in both GT1 and SHSY5Y cells, as well as its "scrapie-like" properties (Lehmann and Harris, 1997; Priola and Chesebro 1998; Sarnataro et al., 2004). We reasoned that if Shadoo possesses a natural tendency to convert to amyloid-like forms *in vitro* (Daude et al., 2010), it should be able to acquire "scrapie-like" properties also in live cells. To test this hypothesis, we first analyzed Shadoo sensitivity to PK digestion under normal conditions, by using PK enzyme on cell lysates. As expected by our hypothesis, we found that Shadoo was partially resistant to PK digestion both at 3.3 μg/ml and 20 μg/ml (concentrations at which PrP^C was completely sensitive after 2 and 10 min treatment) (Sarnataro *et al.,* 2004) Figure 2.6a,b. We also analyzed Shadoo scrapie-like properties evaluating the detergent insolubility of the protein by centrifuging Triton/DOC lysates at 265,000 g for 40 minute. Furthermore, glycosylated, unglycosylated and 12 kDa forms of Shadoo were recovered in the pellet after ultracentrifugation of Triton/Doc lysates of GT1 cells (Figure 2.6b), indicating that they were aggregated. These two assays have been used to identify the "scrapie-like" characteristics of prion protein and its mutants, because they reveal an abnormal folding of the protein (Campana et al., 2005). The presence of the bands at ~22kDa (glycosylated Shadoo), as well as at ~16kDa and at ~12kDa in the pellet of Triton/Doc assay, indicates that Shadoo shows a tendency to form aggregates into the cells. Overall, these data are consistent with a proteinase K signature acquisition of Shadoo under native conditions (Daude et al., 2010).

2.5) Role of DRM association in Shadoo folding

To understand in which measure association of Shadoo with DRMs could be involved in determining the folding of the protein, we performed a PK assay after cholesterol depletion. According to our previous findings in epithelial cells (Sarnataro et al., 2004), while PrP^C was found partially PK-resistant only after 2 min of PK digestion after DRM perturbation by cholesterol depletion, Shadoo was partially PK-resistant already under normal growth conditions in neuronal cell lines and its resistance to PK digestion increase of about 30% after cholesterol depletion by βCD (10' at 3.3 μg/ml PK), respect to control (Figure 2.6. right panel). Moreover, in this condition we have observed an accumulation of 12 kDa isoform of Shadoo. Then, we sought to check whether in control conditions and after perturbation of lipid rafts, the protein remained associated with the ER chaperones. To test whether Shadoo interacted with ER chaperones, we performed Co-immunoprecipitation (Co-IP) assays by immunoprecipitating CLR or BiP (not shown), with its own antibody and revealing Shadoo by Western blotting (WB) with SPRN-R12 antibody (Figure 2.6c). To confirm the occurrence of the immunoprecipitation, CLR was revealed by anti-CLR antibody. Interestingly, accordingly with its partial resistance to PK digestion under normal growth conditions, we found that mature glycosylated Shadoo Co-IPed with CLR, which might be indicative of incorrect folding. Furthermore, after DRM perturbation by cholesterol depletion, the amount of mature Shadoo increased in the immunocomplex with CLR (about 3-fold respect to control) and together with the non-translocated (18kDa) and ER-translocated isoforms (12kDa), appeared in the immunocomplex. Moreover, this isoform was accumulated and pk-resistant suggesting that suggesting it was aggregated. Thus, lipid rafts could be involved in the processing of Shadoo.

However, as we found that in cholesterol-depleted cells a major portion of the protein was misfolded,

our hypothesis was that Shadoo possesses a naturally tendency to misfold and that the integrity of lipid rafts, as well as for PrP^C, plays a role in its folding and processing.

The fully glycosylated isoforms, as well as the other two Shadoo isoforms, interacted in a stronger manner with the ER chaperones, after DRM perturbation, indicating that, as proposed for other polypepdides by Brundin et al., 2010, they could represent unfolded isoforms of "naturally unstructured" Shadoo protein which increased after perturbation.

2.6) The proteasomal pathway in "scrapie-like" properties acquisition of Shadoo

Shadoo was partially localized in the ER (Figs. 2 and 3) and it has been proposed that ER retention of misfolded proteins might lead to degradation through the endoplasmic reticulum-associated degradation (ERAD) pathway, as in the case of some pathological PrP mutants (Zanusso et al., 1999; Jin et al., 2000; Campana et al., 2006). Thus, we checked for the role of this pathway in the "scrapie-like" properties acquisition of Shadoo.

GT1 cells were treated with the proteasome inhibitor ALLN (150 μM for 7h) and subjected to PK-assay. We found that the band at ~12kDa accumulated into the cells (Figure 6d, PK-), suggesting that under proteasomal block the unglycosylated isoform of Shadoo (likely lacking its GPI-AS) was not degraded, as it should be. Second, by comparing the bands of PK digestion under proteasomal block (ALLN) to control conditions, both mature and translocated Shadoo lacking its GPI-AS, resulted almost completely resistant to PK treatment, both after 2' and 10' at 3.3 μg/ml (Figure 6d ALLN and compare with control 6a, upper panel). While in control conditions after 2' at 20 μg/ml of PK, Shadoo resulted almost completely digested, we calculated that under ALLN about 40% of fully glycosylated Shadoo resulted resistant to PK treatment and that the 12 kDa isoform lacking GPI-AS (+/- GPI anchor) accumulated (see black and white arrowheads in Fig. 6d) and were partially PK resistant. To

demonstrate that 12kDa isoform was specifically degraded by proteasome, to exclude the involvement of lysosomal-pathway, we performed a block of the latter point by NH_4Cl (2 days, 20mM) under control and cholesterol depletion conditions (Figure 7). In control cells, we found that NH_4Cl treatment did not result in the accumulation of 12 kDa isoform, implying that this isoform is degraded by proteasome and is not generated by a lysosomal degradation.

Discussion

A depletion in Shadoo, a neuronal paralog of PrP^C has been demonstrated in several experimental scrapie-infected rodents and in naturally infected scrapie sheep (Watts et al., 2011, Westaway et al., 2011; Sakthivelu et al., 2011). The similarity between N-terminals of Shadoo and PrP^C, together with demonstration of their interaction by surface plasmon resonance and yeast two-hybrid analysis (Jiayu et al., 2010), suggests that the two proteins share biological functions. Thus, a functional link between mammalian PrP and Shadoo and a possible involvement of Shadoo in conformational transition of PrP^C to its misfolded scrapie isoform PrP^{Sc} has been postulated.

In line with a previous report (Mays et al., 2014), we found that Shadoo was expressed as two major bands likely corresponding to the unglycosylated and glycosylated isoforms (Figure 2.1a) and that it was partially localized in the ER and mitochondria of both GT1 and SHSY5Y cells (Figures 2.2 and 2.4). Based on previous evidences that the pathogenic effects of PrP^{Sc} could be related to the presence of misfolded forms in the ER (Beranger 2002 et al.; Campana et al., 2006) and that the ER localization and DRM association of PrP^C in the early secretory pathway was crucial for its correct folding (Sarnataro et al., 2004), our immunofluorescence and biochemical assays (ER/mitochondria fractionation assay) confirmed a partial ER localization of Shadoo, except for its non-translocated isoform which was targeted to mitochondria and specifically interacted with the molecular chaperone TRAP1. Whether TRAP1 could function to assist and/or mediate Shadoo mitochondrial localization has to be established with further experimentations.

However, mitochondrial localization of Shadoo was in agreement with a recent description that the ER signal

peptide of Shadoo, as well as of amyloid precursor protein (APP), has the property to mediate alternative targeting to mitochondria (Pfeiffer et al., 2013). The dual targeting to either the ER or mitochondria is mediated by structural features (α-helical domains and/or GPI signal sequence) within the nascent chain. As suggested by Pfeiffer et al., 2013, if the protein cannot be productively imported because it lacks structured domains, then the non-translocated polypeptide is released into the cytosol where the uncleaved signal peptide can mediate targeting to mitochondria. Furthermore, as previously proposed also for APP protein (Pfeiffer et al., 2013), the mistargeting of secretory proteins to cytosol or mitochondria may challenge protein homeostasis and cause toxicity, contributing to pathomechanisms. Interestingly, we found the untranslocated Shadoo isoform associated to Calreticulin under cholesterol depletion, indicating its misfolding.

Anyway, the question arises as for why Shadoo becomes misfolded in normal growth conditions.

It has been proposed that the folding of newly synthesized polypeptide chains into their native conformations, and the unfolding of proteins from their native states, proceeds through distinct intermediates from which derive non-native oligomeric species of different sizes and structures which are able to self-associate (Brundin et al., 2010). As the polypeptides involved in Prion, Parkinson's, Alzheimer's and Huntington's diseases populate a wide variety of folding intermediates, they have a higher propensity to form such oligomeric species (Victoria et al., 2015). Thus, analyzing our results, we propose that Shadoo could be a new member of this protein family.

Because the role of lipid rafts has never been tested before for Shadoo metabolism/processing, we sought to check for the association of Shadoo with DRMs and their role in its folding.

As expected for a GPI-anchored protein, we found Shadoo in the insoluble fraction of TX-100 extraction assay, as well as in the lighter fractions of the sucrose

density gradients where normally lipid raft-associated proteins float. Indeed, to investigate whether Shadoo acquired scrapie-like characteristics (which implies protein misfolding), we analysed its PK sensitivity under conditions where PrP^C was found to be completely digested or resistant (Sarnataro et al., 2004). Strikingly, as clearly shown in Figure 2.6 a, Shadoo was found partially resistant to PK digestion under control conditions and its resistance was reinforced by lipid rafts perturbation by cholesterol depletion. These results are in contrast with the behavior of PrP^C, which in control conditions is completely digested by PK, while they are in agreement with the fact that PrP^C becomes partially misfolded and PK-resistant after DRMs perturbation.

However, our findings are in line with recent data showing that recombinant mouse or sheep Shadoo converted to an aggregated/amyloid form without recourse to chemical modification (denaturation or acidification, etc.), thus defining a proteinase-K signature for Shadoo under native conditions (Daude et al., 2010). In addition, it was interesting to note that under cholesterol depletion, respect to control conditions, the ER-translocated Shadoo of 12kDa accumulated. However, it is known that proteins which do not pass the quality control system, are retained in the ER and retrotranslocated into the cytosol to be then degraded by the proteasome (Hampton 2002). Interestingly, the ERAD pathway was described to be related to the cytotoxicity of PrP (Ma and Lindquist, 2001) and to some PrP pathological mutants (Zanusso et al., 2001). Moreover, in agreement with very recent findings which describe, in both cultured cells and in scrapie-infected rodents, disruption of glycosylation and enhancement of Shadoo proteasomal degradation (Zhang et al., 2014), we found that the proteasomal inhibitor ALLN led to the accumulation of 12 kDa band corresponding to the Shadoo isoform which expresses as a doublet band (see Figure 2.6d, black and white arrowheads, respectively). This doublet could be ascribed to the ubiquitination of this Shadoo isoform.

While confirming the involvement of proteasomal pathway in the degradation of translocated Shadoo isoform, we asked why proteasomal block induced a PK-resistance of Shadoo.

One explanation comes from analysis Co-IP assays between Shadoo and ER chaperones (Figure 2.6c) showing that, in normal condition, fully glycosylated Shadoo was present in the immunocomplex with the ER chaperone Calreticulin, strongly indicating that Shadoo was tendentially unfolded. Furthermore, our finding that under cholesterol depletion not only translocated Shadoo intermediate forms Co-IPed with CLR, but also the untranslocated one (Figure 2.6c), could be explained by the existence of cytosolic CLR which can generate by an inefficient ER import (Shaffer et al., 2005).

However, the fact that under cholesterol depletion the presence of mature Shadoo increased in the immunocomplex together with its non-translocated 18kDa isoform and translocated 12kDa one, suggests that integrity of lipid rafts has a role in the maturation/processing of Shadoo and that Shadoo proceeded through unfolded aggregated non-native isoforms (Brundin et al., 2010). Indeed, these isoforms of Sho appeared in the pellet of the Triton/Doc assay, reinforcing the idea that they were aggregated.

We can conclude that Sho is associated to DRMs and acquires "scrapie-like" properties in neuronal cells. These features fit well to protein that belongs to the family of intrinsically disordered secretory proteins. Moreover, cholesterol depletion leads to accumulation of its intermediate forms and while ER-translocated Shadoo lacking the GPI-AS was degraded via the proteasome, block of the latter accounts for the accumulation of this form into the cells and to the increase of Sho misfolding confirmed by the increase of its PK-resistance.

In the light of a very recent finding (Ciric et al., 2015) describing a key role for Shadoo in the folding pathway of PrP, it remains to be further investigated which is the action of misfolded Shadoo in the metabolism of PrP^{C} and/or its pathological mutants.

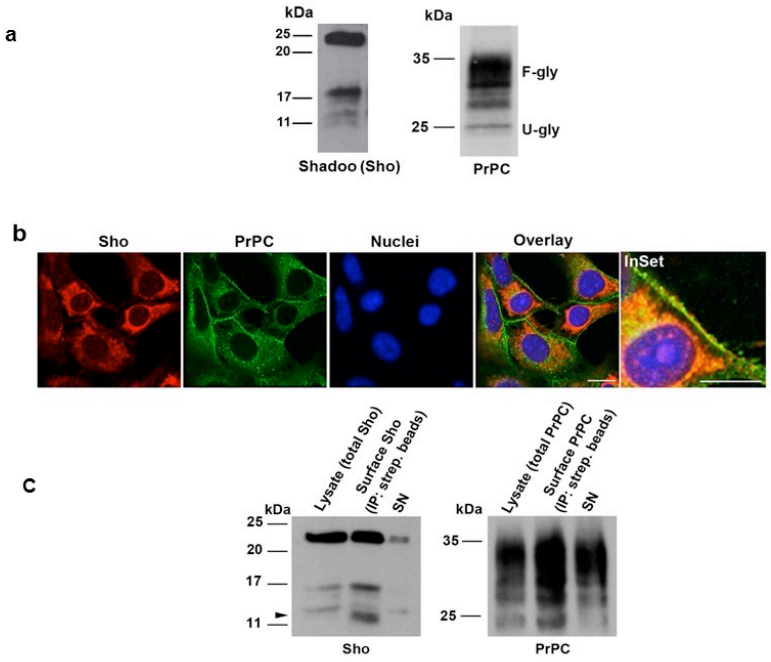

Figure 2.1. Shadoo is localized intracellularly and on the plasma membrane of GT1 cells. (a) GT1 cells were grown on 60-mm dishes and 80 µg of total cell lysates were loaded on gel, subjected to SDS-PAGE (14% polyacrylamide gel) and immunoblotted with the SRNP-R-12 antibody and SAF32 to reveal Sho and PrP^C, respectively with ECL. (b) GT1 cells were grown on coverslips, fixed and incubated with R-12 and SAF32 primary antibodies followed by secondary antibodies conjugated to Alexa-fluor546 and Alexa-fluor488 to localize Sho and PrP^C. Nuclei were stained by DRAQ5 dye (blue channel). Scale bars: 10 µm. (c) GT1 cells were grown for 3 days on dishes and surface expressed Sho and PrP^C were biotinylated. The cell lysates were collected and immunoprecipitated (IP) with streptavidin beads. Total cell lysates (80 µg of total proteins), the IP (cell surface biotinylated proteins) and supernatant (1/10 of the SN) were loaded on gel and transferred to PVDF for Western blotting with R-12 or SAF32 Abs to reveal Sho and PrP^C, respectively.

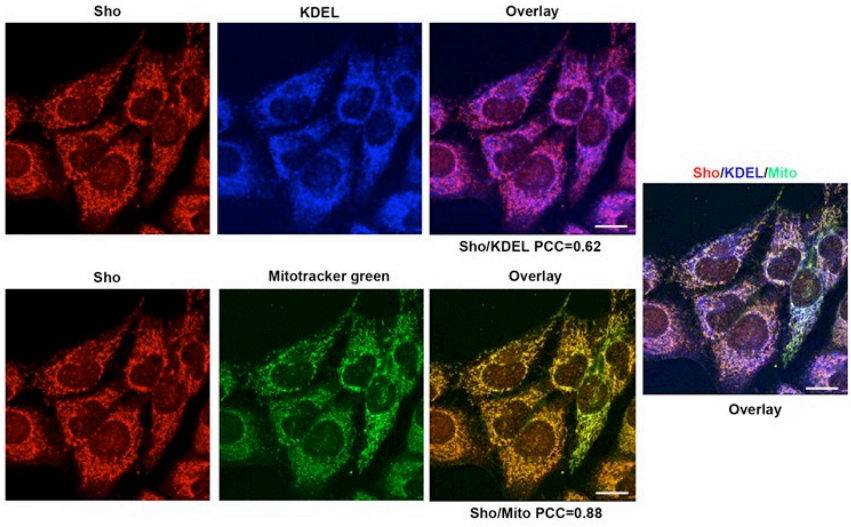

Figure 2.2. Sho localizes in the ER and mitochondria of GT1 cells. GT1 cells grown on coverslips were fixed and probed with anti-Sho R-12 and anti-KDEL primary antibodies followed by secondary antibodies conjugated to Alexa-fluor546 (red) and Cy5 (blu) to localize Sho and KDEL. To localize mitochondria, Mitotracker green was added to live cells into cell culture medium 15 minutes before fixation. PCC is an average value. Scale bars: 10 μm.

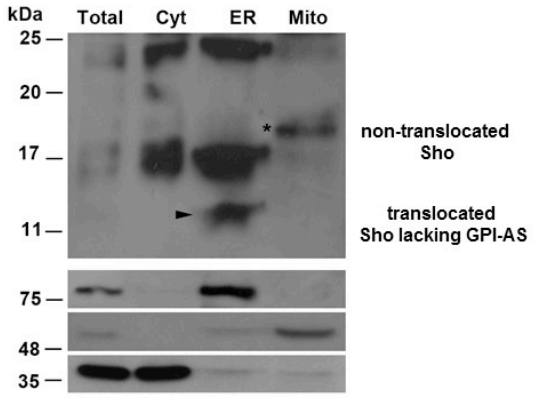

Figure 2.3. The non-translocated Sho isoform is targeted to mitochondria. SHSY5Y cells were processed for mitochondria fractionation assay by QproteomeTM Mitochondria Isolation kit from Qiagene. Total represents the InPut; Cyt: cytosol and membranes; ER: microsomal fraction; Mito: mitochondrial fraction. Western blotting with anti- BiP (ER marker), anti-F1ATPase (mitochondrial marker) and anti-GAPDH (cytosolic marker) antibodies were performed as control of the procedure. Asterisk indicates the 18kDa non-translocated Shadoo; arrowhead indicates the ER-translocated Shadoo lacking GPI-AS(12kDa)

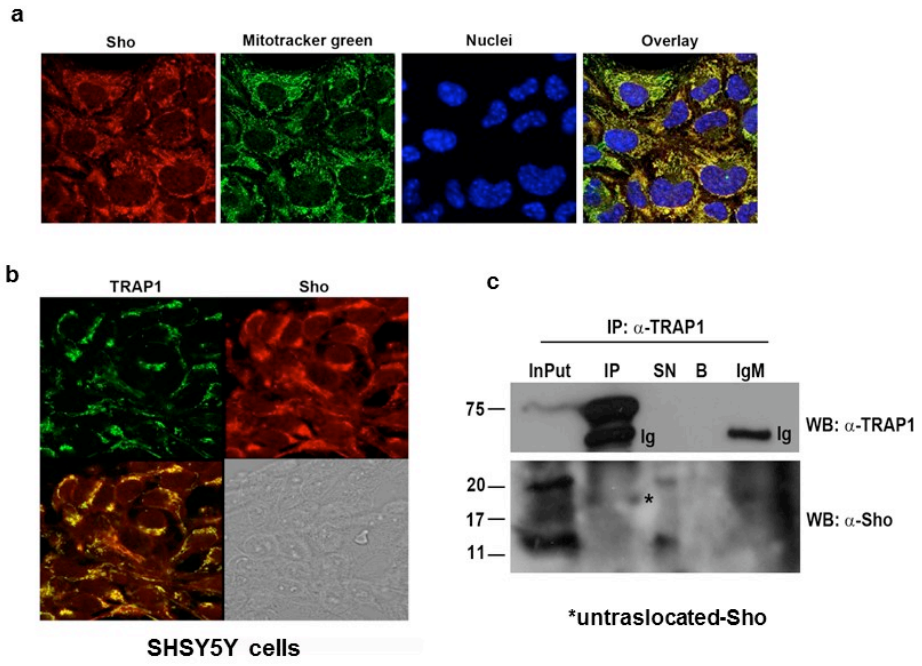

Figure 2.4. Shado localizes in mitochondria of SHSY5Y cells and its non-translocated isoform co-immunoprecipitates with TRAP1. (a) SHSY5Y cells were grown on coverslips and processed as in Figure 2 or (b) were subjected to double immunofluorescence analysis probing with anti-TRAP1 and anti-Sho R12 Abs followed by secondary Abs conjugated to Alexa-fluor488 and Alexa-fluor 546, to reveal TRAP1 (green) and Sho (red) respectively. Brightfield image shows the cells. Scale bars: 10 μm. (c) SHSY5Y cells were lysed in Buffer 1X and TRAP1 was immunoprecipitated (IP) using the monoclonal anti-TRAP1 Ab (SC-73604). The immunoprecipitate was then immunolabeled with the R-12 anti-Sho antibody. (Ig) indicates the immunoglobulins and (*) indicates non-translocated Sho (18kDa). To confirm the occurrence of the immunoprecipitation, the membranes were probed with the anti-TRAP1 antibody. InPut: loading control (50 μg of total lysate); IP: immunoprecipitate; SN: 1/10 of the supernatant; B: protein-A beads alone.

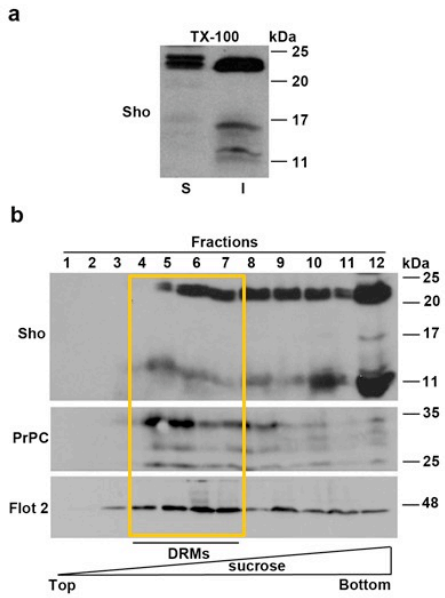

Figure 2.5. Shadoo is insoluble in non-ionic detergents and is associated to DRMs. (a) Cells from 60-mm dishes were washed twice with PBS and then lysed for 20 min on ice in 1ml of Extraction Buffer. After centrifugation of the lysates, the supernatants (S) represent the TX-100 soluble material. The pellets (I) were then solubilized in 100 µl of solubilization buffer (50 mM Tris pH 8.8, 5 mM EDTA, 1% SDS). Proteins were TCA precipitated from the soluble and insoluble materials and Sho was revealed by Western blotting. (b) GT1 cells were grown to confluence on 150-mm dishes, washed in PBS and lysed for 20 min in TNE/TX-100 1% (25mM Tris-HCl pH 7,5, 150mM NaCl, 5mM EDTA, 1%TX-100) on ice (Sarnataro et al., 2002; Broquet et al., 2003). A sucrose gradient (5-35% TNE, Top-Bottom) was layered on the top of the lysates and one-milliliter fractions (12 fractions in total) were harvested from the top of the gradient. Specifically, starting from the top of the gradient the fractions 4-7 (representing DRMs) and 8-12 (non-DRMs) were collected and loaded on gel. After transfer on PVDF by Western blot, Sho, PrP^C and Flotillin-2 (Flot2) were revealed by specific antibodies and ECL.

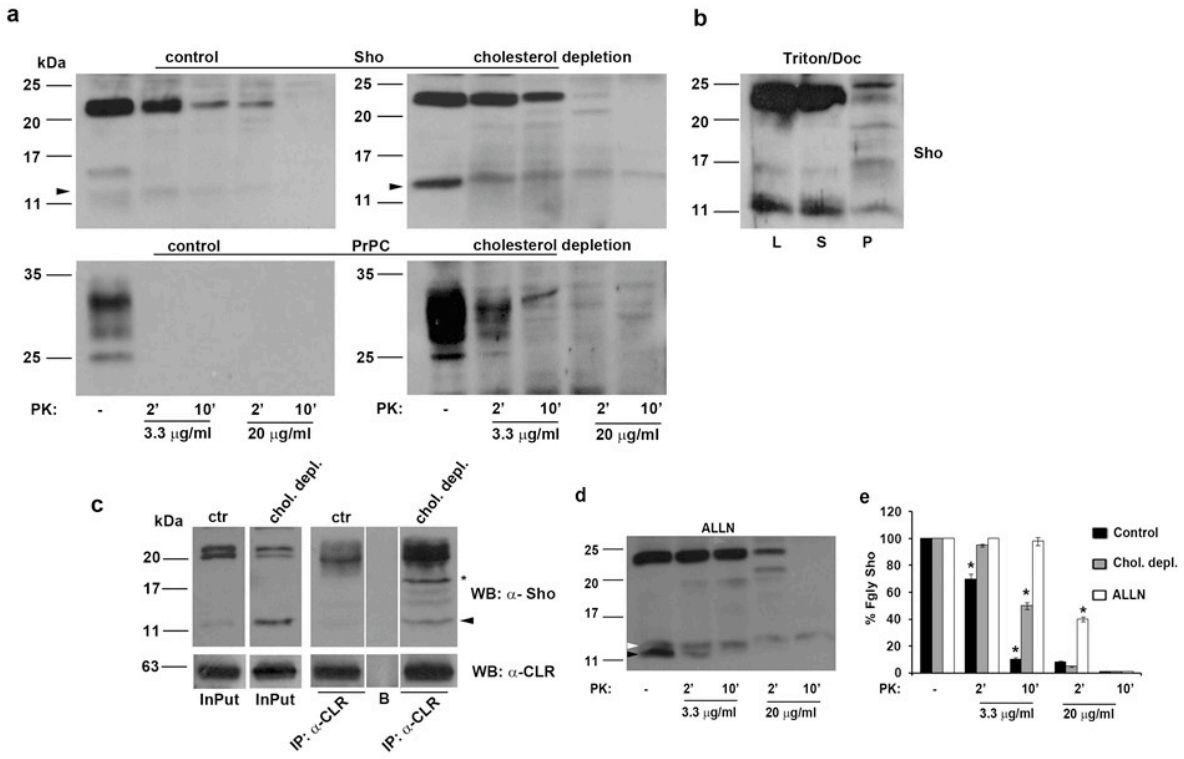

Figure 2.6. Lipid rafts perturbation and proteasomal block regulate Shadoo folding and its PK- resistance in neuronal cells. (a) Proteinase K (PK) digestion assay. GT1 cells were grown in 100-mm dishes in control (control) or cholesterol depletion conditions (chol. depletion). The cells were lysed in Triton/Doc buffer, in the absence of proteases inhibitors, and treated where indicated with PK (3.3 μg/ml, 20 μg/ml) at 37°C for 2-10 minutes. The proteins were separated by SDS-PAGE and immunoblotted. (b) Triton/DOC insolubility assay. After lysis in Triton/DOC buffer, lysates of GT1 cells were ultracentrifugated in a TLA 100.3 rotor at 265,000 *g* and separated into soluble (S) and insoluble (P) materials. In (a) and (b) Shadoo and PrP^C were revealed by Western blotting by using R12 or SAF32 Ab and ECL. The line L represents 80 μg of total cell lysate before centrifugation. (c) Analysis of Sho interaction with CLR chaperonine. GT1 cells were grown in 100-mm dishes in control, and cholesterol depletion (CD). The cells were then lysates in JS buffer and Calreticulin (CLR) was immunoprecipited in nondenaturing conditions. The immunoprecipites and 1/10 of the Supernatants (Sup) were loaded on the polyacrylamide gels. The gels were releved for the presence of Shadoo and Calreticulin by Western Blotting with the specific antibody by ECL. (*, 18kDa) indicates non-translocated Sho and (arrowheads, 12kDa) indicates the translocated Sho isoform lacking the GPI-AS. Note the presence of both isoforms in the Co-IP with CLR. B: protein-A beads alone indicates non-translocated Sho and (arrowheads, 12kDa) indicates the translocated. (d) The proteasomal pathway is involved in Shadoo metabolism and in the PK-sensitivity of Shadoo. GT1 cells were treated with ALLN (150 μM, 7 hours) and subjected to PK-assay as in (a). (e) The graph represents percentage of Sho quantified by densitometric analyses relative to PK-assays performed in control, chol. depl. or ALLN treated conditions. The amount of Sho in not-treated samples (PK -) was considered as 100 %. Results were quantified from three different independent experiments and represent the means +/− S.D. All data were statistically significant.

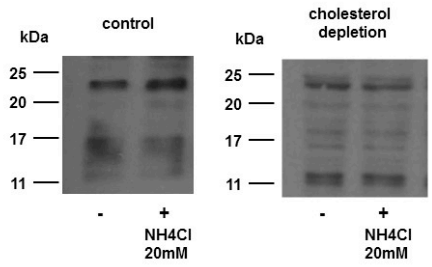

Figure 2.7. The 12kDa Shadoo isoform accumulates under cholesterol depletion but not under NH_4Cl treatment. GT1 cells were grown in 60-mm dishes and NH_4Cl was added (+) or not (-) to the culture medium. Then the cells were treated or not (control) with β-CD (cholesterol depletion). Cells were lysed with Triton/DOC and $80\mu g$ of total proteins were subject to SDS-PAGE. Shadoo was revealed by Western blotting on PVDF and hybridization with SPRN (R-12) antibody.

FUTURE PRESPECTIVE

FUTURE PRESPECTIVES

Proposed drugs against TSEs range from small organic compounds to antibodies; various therapeutic strategies have been proposed, including blocking the conversion of PrP^{C} to PrP^{Sc}, increasing PrP^{Sc} clearance, and/or stabilizing PrP^{C}. While several compounds have been effective in vitro and in animal models, none have been proven effective in clinical studies to date. Such lack of *in vivo* efficacy is attributable to high compound toxicity and the lack of permeability of the selected compounds across the blood-brain barrier. Interestingly, it has been shown that for pathological PrP^{Sc} propagation in scrapie-infected neuronal cells is required the 37/67kDa laminin receptor (LRP/LR), a non-integrin protein that binds both laminin-1 and PrP^{C} (Leucht el al., 2010; Sarnataro et al., 2016, under review in Sci. Rep.). Our data reveal NSC47924 as a useful tool to regulate PrP^{C} and 37/67kDa LR trafficking and degradation, representing a novel small molecule to be tested against prion diseases. The effect that the 37/67kDa LR inhibitor exerts on PrP^{C}, stabilizing its cell surface localization, provides good hopes to test it against prion conversion, which in a series of conflicting reports has been demonstrated to occur on the plasma membrane and/or intracellular compartments (Goold et al., 2011; Marijanovic et al., 2009). However, whether the inhibitor treatment could result in a stimulus or a stumbling block to determine PrP^{C} to PrP^{Sc} conformational transition has to be established with further investigations.

We will investigate the anti-prion activity of the organic compound NSC47924 and its analogs (NSC1 and NSC2), starting from initial *in vitro* screening of anti-amyloid formation, using purified recombinant prion protein, to *ex vivo* evaluation of scrapie conversion in prion infected *versus* non infected cell lines. We propose that a combination of *in vitro* and *ex vivo* approaches would be useful for the rapid identification of these novel small molecules as anti-prion drug candidates, with suitable features that would support their use as *in vivo* drugs.

Because of the great experience on prion diseases and the presence of all the biosafety level 3 facilities, practices and containment equipment for activities involving prion agents, the Chiara Zurzolo's "Membrane trafficking and

Pathogenesis lab" (Pasteur Paris, France) will be chosen for the development of this proposal. Our specific aims will be:

1) Our first objective is to assess whether NSC47924 can effectively inhibit the conversion of cellular prion protein (PrP^{C}) into the scrapie prion protein (PrP^{Sc}) by performing *in vitro* assays and using *ex-vivo* non infected models.
2) Another major objective is to study whether NSC47924 can prevent PrP^{Sc} propagation by using infected *ex-vivo* models: neuronal GT1 and N2a cells infected with scrapie prion protein.

Task 1. Amyloid formation. We will monitor whether NSC47924 can interfere with the amyloid formation. We will perform a Thioflavin-T (ThT)- binding assay, which is regularly used to quantify the formation and inhibition of amyloid fibrils in the presence of anti-amyloidogenic compounds. For this assay we will use recMoPrP(23-231) protein (Moda et al., 2015), which is able to convert to amyloid fibrils without any seeding factor but is altered by denaturant concentrations, pH and buffer composition . The reaction mixtures will be composed by recMoPrP(23-231) and an increasing range of NSC47924 concentrations. At regular time intervals, the assembly reaction will be monitored using a Thioflavin-T (ThT)- binding assay (McParland et al, 2000). The binding will be measured by averaging the emission fluorescence signal over 60s using a spectofluorometer.

1.1 PrP conversion: Recently we have found that NSC47924 affects the trafficking of PrP^{C} in cultured neuronal GT1 cells stabilizing it on the plasma membrane, while inducing internalization and subsequent degradation of 37/67kDa LR. Thus, we will investigate whether the prion protein that accumulated on the plasma membrane after inhibitor treatment, is correctly folded or not. To test PrP scrapie properties on the plasma membrane, we will biotinylate cell surface proteins and then will immunoprecipitate them with streptavidin beads. The immunoprecipitated materials will be subjected to the major biochemical assays to evaluate PrP folding: 1) PIPLC sensitivity, 2) Triton/Doc Insolubility and 3) Proteinase K (PK) resistance assays.

1.2 Prion infection. Moreover, by immunoblotting assays we will test whether non-infected GT1 and N2a cells are able to be infected by prions in the presence of the drugs.

Task 2. PrP^{Sc} spreading: It is known that dendritic cells (DCs) can mediate the PrP^{Sc} spreading from the intestine to the central nervous system (CNS). To examine whether cell-to-cell PrP^{Sc} spreading will be affected by NSC47924 treatment (and or its analogs), we will perform co-culture experiments between Dendritic Cells (DCs) loaded with prions and primary neurons in presence or absence of inhibitor. This procedure has been widely consolidated in the Zurzolo's lab at Pasteur Institute. To pursue this aim, we will use Alexafluor-labelled PrP^{Sc}. We will follow the movement of Alexa-PrP^{Sc} in live cells (+/- inhibitor) in real time using spinning disk confocal microscopy. We will examine scrapie production in neuron after inhibitor treatment.

2.2 PrP^{Sc} clearance: In order to understand whether NSC47924 induces PrP^{Sc} clearance in infected cells (ScGT1 and ScN2a cells), we will quantify the amount of PrP^{SC} present in control *versus* NSC47924 treated cells, using both fluorescence microscopy and biochemical approaches. In parallel, we will check also the effects of NSC47924 analogs.

ScGT1 and ScN2a will be cultured from 1 to 4 days in presence or absence (control) of NSC47924. We will perform quantitative immunofluorescence assays: after fixation, permeabilization and guanidine hydrochloride (GND) treatment, the samples will be immunostained for PrP (SAF-32 antibody). Due to the lack of PrP^{Sc} specific antibodies, a denaturation step of the samples with guanidine hydrochloride (Gnd) is required. Immunofluorescence will be acquired using a high-field microscope Marianas (intelligent imaging innovation) with a 63x oil. In parallel, we will perform also biochemical assays to evaluate clearance of PrP^{Sc} from prion infected cells treated with inhibitor. Also under this condition, ScGT1 and ScN2a will be cultured from 1 to 4 days in the presence or absence (control) of NSC47924. Then, the levels of PrP^{Sc} will be analysed immediately after the termination of inhibitor treatment by western blotting. To discriminate PrP^{Sc} from

PrP^C by western blotting, protein lysates will be treated with 20 μ/ml of Proteinase K (PK) for 30 min at 37°C and protein content will be pelleted by centrifugation at 14000 rpm for 1 hour. In contrast to PrP^C, which will be completely degraded by PK, only partial degradation of PrP^{Sc} occurs in this condition.

REFERENCE

References

1. Arancibia-Cárcamo, I. L., Fairfax, B.P., Moss, S.J., & Kittler, J.T. Studying the Localization, Surface Stability and Endocytosis of Neurotransmitter Receptors by Antibody Labeling and Biotinylation Approaches Frontiers in Neuroscience in *The Dynamic Synapse. Molecular Methods in Ionotropic Receptor Biology* (ed Kittler, J.T: and Moss, S.J.) (CRC Press, 2006).
2. Ardini, E. *et al*. The 67 kDa laminin receptor originated from a ribosomal protein that acquired a dual function during evolution. *Mol. Biol. Evol.* (1998); 15, 1017-1025
3. Arnold JE1, Tipler C, Laszlo L, Hope J, Landon M, Mayer RJ. The abnormal isoform of the prion protein accumulates in late-endosome-like organelles in scrapie-infected mouse brain. *J Pathol.* (1995);176:403-11,
4. Baloui, H. *et al*. Cellular prion protein/laminin receptor, distribution in adult central nervous system and characterization of an isoform associated with a subtype of cortical neurons. *Eur. J. Neurosci.* (2004);20, 2605-2616.
5. Bendheim, P. E., H. R. Brown, R. D. Rudelli, L. J. Scala, N. L. Goller, G. Y. Wen, R. J. Kascsak, N. R. Cashman, and D. C. Bolton. Nearly ubiquitous tissue distribution of the scrapie agent precursor protein. *Neurology* (1992);42:149–156.
6. Bernard, A. *et al*. Laminin receptor involvement in the anti-angiogenetic activity of pigment epithelium-derived factor. *J. Biol. Chem.* (2009);284, 10480-10490.
7. Berno V., Porrini D., Castiglioni F., et al. The 67nkDa laminin receptor increases tumor aggressiveness by remodeling laminin-1. *Endocr. Relat. Cancer* (2005);12, 393-406.
8. Berno, V. *et al*. The 67 kDa laminin receptor increases tumor aggressiveness by remodeling laminin-1. *Endocr. Relat. Cancer.* (2005);12, 393-406.
9. Bueler, H., Fischer, M., Lang, Y., Bluethmann, H., Lipp, H. P., DeArmond, S. J., Prusiner, S. B., Aguet, M., and Weissmann, C. Normal development and behaviour of mice lacking the neuronal cell-surface PrP protein. *Nature* (1992); 356(6370):577–582.
10. Bolte, S, & Cordelières, FP. A guided tour into subcellular colocalization analysis in light microscopy. *J. Microsc.* (2006); 224, 213–232.
11. Bounhar, Y., Zhang, Y., Goodyer, C. G., and LeBlanc, A. Prion protein protects human neurons against Bax-mediated apoptosis. *J. Biol. Chem*. (2001); 276(42):39145–39149.
12. Brown, D. R., Qin, K., Herms, J. W., Madlung, A., Manson, J., Strome, R., Fraser, P. E., Kruck, T., von Bohlen, A., Schulz-Schaeffer, W., Giese, A., Westaway, D., and Kretzschmar, H. The cellular prion protein binds copper in vivo. *Nature* (1997); 390(6661):684–687.
13. Brundin, P., Melki, R., and Kopito, R. Prion-like transmission of protein aggregates in neurodegenerative diseases. *Nat. Rev. Mol. Cell Biol.* (2010); 11, 301-307.
14. Bueler, H., Fischer, M., Lang, Y., Bluethmann, H., Lipp, H. P., DeArmond, S. J., Prusiner, S. B., Aguet, M., and Weissmann, C. Normal development and

behaviour of mice lacking the neuronal cell-surface PrP protein. *Nature* (1992); 356(6370):577–582
15. Bueler, H., Aguzzi, A., Sailer, A., Greiner, R. A., Autenried, P., Aguet, M., and Weissmann, C. Mice devoid of PrP are resistant to scrapie. *Cell* (1993);73(7):1339–1347.
16. Buto, S. *et al*. Formation of the 67-kDa laminin receptor by acylation of the precursor. *J. Cell Biochem*. (1998); 69, 244-251
17. Campana ,V., Sarnataro, D. and Zurzolo, C. The highways and byways of prion protein trafficking. *Trends Cell Biol.* (2005); 2,102-111.
18. Campana, V., Sarnataro, D., Fasano, C., Casanova, P., Paladino, S. and Zurzolo, C.. Detergent-resistant membrane domains but not the proteasome are involved in the misfolding of a PrP mutant retained in the endoplasmic reticulum. *J. Cell Sci.* (2006);119, 433-42.
19. Campana, V. *et al*. Characterization of the properties and trafficking of an anchorless form of the prion protein. *J. Biol. Chem.* (2007);282, 22747-56.
20. Caputo, A., Sarnataro, D., Campana, V., Costanzo, M., Negro, A., Sorgato, MC., Zurzolo, C. Doppel and PrPC co-immunoprecipitate in detergent-resistant membrane domains of epithelial FRT cells. *Biochem. J.* (2009); 425, 341-51.
21. Castronovo, V., Taraboletti, G., & Sobel, M.E. Functional domains of the 67-kDa laminin receptor precursor. *J. Biol. Chem.* (1991); 266, 20440-20446
22. Chetty, C. *et al*. Anti-LRP/LR specific antibody lgG1-iS18 impedes adhesion and invasion of liver cancer cells. *PLoS One* (2014);9, e96268.
23. Caughey, B., R. E. Race, and B. Chesebro. Detection of prion protein mRNA in normal and scrapie-infected tissues and cell lines. *J. Gen. Virol*. (1988);69:711–716.
24. Caughey B, Race R E, Ernst D, Buchmeier M J, Chesebro B. Prion protein biosynthesis in scrapie-infected and uninfected neuroblastoma cells. *J Virol*. (1989);175–181.
25. Ciric, D., Richard, C.A, Moudjou, M., Chapuis, J., Sibille, P., Daude, N., Westaway, D, Adrover Estelrich, M., Béringue, V., Martin, D. and Rezaei, H. Interaction between Shadoo and PrP affects the PrP folding pathway. *J. Virol.* (2015);03429-14.
26. Creutzfeldt, H. G.U¨ ber eine eigenartige Erkrankung des Zentralnervensystems. *Vorla¨ufige Mitteilung.Z. f. d. ges. Neurol. und Psych.*, (1920).
27. Da Costa Dias, B. *et al.* Anti-LRP/LR specific antibody IgG1-iS18 and knock-down of LRP/LR by shRNAs rescue cells from Abeta42 induced cytotoxicity. *Sci. Rep.* (2013); 3, 2702.
28. Da Costa Dias, B. *et al.* The 37kDa/67kDa Laminin Receptor acts as a receptor for Aβ42 internalization. *Sci. Rep.* (2014); 4, 5556.
29. Daude, N., Ng, V., Watts, J.C., Genovesi, S., Glaves, J.P., Wohlgemuth, S., Schmitt-Ulms, G., Young, H., McLaurin, J., Fraser, P.E. and Westaway, D. Wild-type Shadoo proteins convert to amyloid-like forms under native conditions. J. *Neurochem*. (2010); 1, 92-104.
30. Daude, N. and Westaway, D. Biological properties of the PrP-like Shadoo protein. Front. *Biosci*. (2011); 16, 1505–1516.
31. Demianova, M., Formosa, T.G., & Ellis, S.R. Yeast proteins related to the p40/laminin receptor precursor are essential components of the 40 S ribosomal subunit. *J. Biol. Chem.* (1996); 271, 11383-11391.

32. DiGiacomo, V., & Meruelo, D. Looking into laminin receptor: critical discussion regarding the non-integrin 37/67-kDa laminin receptor/RPSA protein. *Biol. Rev. Camb. Philos. Soc.* (2015); 12170
33. Diarra-Mehrpour, M., Arrabal, S., Jalil, A., Pinson, X., Gaudin, C., Pietu, G., Pitaval, A., Ripoche, H., Eloit, M., Dormont, D., and Chouaib, S. Prion protein prevents human breast carcinoma cell line from tumor necrosis factor alpha-induced cell death. *Cancer Res* (2004); 64(2):719–727.
34. Douville, P.J., Harvey, W.I., & Carbonetto, S. Isolation and partial characterization of high affinity laminin receptor in neuronal cells. *J. Biol. Chem.* (1988); 263, 14964-14969
35. Duffy, P., Wolf, J., Collins, G.,DeVoe,A.G., Streeten, B., and Cowen, D.. Letter: Possible personto-person transmission of Creutzfeldt–Jakob disease. *N. Engl. J. Med.* (1974); 290(12):692–693.
36. Dunn, K.W., Kamocka M.M., & McDonald, J.H. A practical guide to evaluating colocalization in biological microscopy. *Am. J. Physiol. Cell Physiol.* (2011); 300, C723–C742.
37. Ford, C.L., Randal-Whitism, L., & Ellis, S.R. Yeast proteins related to the p40/laminin receptor precursor are required for 20 S ribosomal RNA processing and the maturation of 40S ribosomal subunits. *Cancer Res.* (1999); 59, 704-710
38. Gauczynski, S. *et al*. The 37-kDa/67-kDa laminin receptor acts as the cell-surface receptor for the cellular prion protein. *EMBO J.* (2001); 20, 5863-5875
39. Gauczynski, S. *et al*. The 37-kDa/67-kDa laminin receptor acts as a receptor for infectious prions and is inhibited by polysulfated glycanes. *J. Infect. Dis.* (2006); 194, 702-709.
40. Goold, R., anian S., Sutton L., Andre R., Arora P., Moonga J., Clarke AR., Schiavo G., Jat P., Collinge J., Tabrizi SJ. Rapid cell-surface prion protein conversion revealed using a novel cell system. *Nat. Commun.* (2011); 2, 1282
41. Griffith, J. S. Self-replication and scrapie. *Nature* (1967); 215(105):1043–1044
42. Hampton, R. Y. ER-associated degradation in protein quality control and cellular regulation. *Curr. Opin. Cell Biol.*, (2002);14, 476-482
43. Harris, DA. Cellular biology of prion diseases. *Clin. Microbiol. Rev.* (1999);12, 429-444.
44. Hundt, C. *et al*. Identification of interaction domains of the prion protein with its 37-kDa/67-kDa laminin receptor. *EMBO J.* (2001); 20, 5876-5886.
45. Itakura, M., Tsujimura, J., Yamamori, S., Ohkido, T., & Takahashi, M. NMDA receptor-dependent recruitment of calnexin to the neuronal plasma membrane. *Neurosci. Letters* (2013); 550, 173-178.
46. Kaneko, K. *et al*. COOH-Terminal sequence of the cellular prion protein directs subcellular trafficking and controls conversion into the scrapie isoform. *Proc. Natl. Acad. Sci. USA*. (1997); 94, 2333-2338.
47. Khumalo, T. *et al*. Adhesion and invasion of breast and oesophageal cancer cells are impeded by anti-LRP/LR-specific antibody IgG1-iS18. *PLoS One* 8, e66297 (2013).
48. Khumalo, T., Ferreira, E., Jovanovic, K., Veale, R.B. & Weiss, S.F.T. Knockdown of LRP/LR induces apoptosis in breast and oesophageal cancer cells. *PLoS One* (2015); 10, e0139584.

49. Khusal, R. *et al*. In vitro Inhibition of Angiogenesis by antibodies directed against the 37kDa/67kDa Laminin Receptor. *PLoS One*(2013); 8, e58888.
50. Klamt, F., Dal-Pizzol, F., Conte da Frota, Ml Jr, Walz, R., Andrades, M. E., da Silva, E. G., Brentani, R. R., Izquierdo, I., and Fonseca Moreira, J. C. Imbalance of antioxidant defense in mice lacking cellular prion protein. *Free Radic. Biol. Med*. (2001); 30(10):1137–1144.
51. Kolodziejczak, D. *et al*. Prion interaction with the 37-kDa/67-kDa laminin receptor on enterocytes as a cellular model for intestinal uptake of prions. *J. Mol. Biol.* (2010); 402, 293-300.
52. Kretzschmar, H. A., Tings, T., Madlung, A., Giese, A., and Herms, J. Function of PrP(C) as a copper-binding protein at the synapse. *Arch. Virol. 16(Suppl.)* (2000); 239–249.
53. Jakob, A. U¨ ber eigenartige Erkrankungen des Zentralnervensystems mit bemerkenswerten anatomischen Befunden (spastische Pseudosklerose-Encephalomyelopathie mit dissemierten Degenerationsherden). *Vorl¨aufige Mitteilung. Z. Ges. Neurol. Psychiatr*(1921); 64:147–228
54. Jiayu, W., Zhu, H., Ming, X., Xiong, W., Songbo, W., Bocui, S., Wensen, L., Jiping, L., Keying, M., Zhongyi, L. and Hongwei, G. Mapping the interaction site of prion protein and Sho. *Mol. Biol. Rep.* (2010); 37, 2295-2300.
55. Jovanovic, K. *et al.* Anti-LRP/LR specific antibodies and shRNAs impede amyloid beta shedding in Alzheimer's Disease. (2013); *Sci. Rep.* 3, 2699.
56. Jovanovic, K. *et al.* Novel patented therapeutic approaches targeting the 37kDa/67 kDa laminin receptor for treatment of Cancer and Alzheimer's Disease. *Expert Opin. Therap. Pat.* (2015); 25, 567-582.
57. Jovanovic, K., Loos, B., Da Costa Dias, B., Penny, C. & Weiss, S.F.T. High resolution imaging study of interactions between the 37kDa/67kDa Laminin Receptor and APP, beta-secretase and gamma-secretase in Alzheimer's disease. *PLoS One* (2014); 9, e100373.
58. Johnson, S., Michalak, M., Opas, M., & Eggleton, P. The ins and outs of calreticulin, from the ER lumen to the extracellular space. *Trends Cell Biol.* (2001);11, 122-129.
59. Landowski, T.H., Dratz, E.A., & Starkey, J.R. Studies of the structure of the metastasis-associated 67 kDa laminin binding protein: fatty acid acylation and evidence supporting dimerization of the 32 kDa gene product to form the mature protein. *Biochem.* (1995); 34, 11276-11287.
60. Lesot, H., Kuhl, U. & Mark, K. Isolation of a laminin-binding protein from muscle cell membranes. *EMBO Journal* 2, (1983); 861–865.
61. Leucht, C. *et al*. The 37kDa/67 kDa laminin receptor is required for PrP^{Sc} propagation in scrapie-infected neuronal cells. *EMBO Rep.* (2003); 4, 290-295.
62. Ludewigs, H. *et al*. Therapeutic approaches for prion disorders. *Expert Rev. Anti-infect. Ther.* (2007); 5, 613-630.
63. Lugaresi, E., Medori, R., Montagna, P., Baruzzi, A., Cortelli, P., Lugaresi, A., Tinuper, P., Zucconi, M., and Gambetti, P.. Fatal familial insomnia and dysautonomia with selective degeneration of thalamic nuclei. *N. Engl. J. Med.* (1986); 315(16):997–1003.

64. Ma, J. and Lindquist, S. Wild-type PrP and a mutant associated with prion disease are subject to retrograde transport and proteasome degradation. *Proc. Natl. Acad. Sci.* (2001)*;* USA 98, 14955-14960.
65. Mays, C.E., Coomaraswamy, J., Watts, J.C., Yang, J., Ko, K.W., Strome, B., Mercer, R.C., Wohlgemuth, S.L., Schmitt-Ulms, G. and Westaway, D. Endoproteolytic processing of the mammalian prion glycoprotein family. *FEBS J.* (2014); 3, 862-76.
66. Malinoff, H. L. & Wicha, M. S. Isolation of a cell surface receptor protein for laminin from murine fibrosarcoma cells. *Journal of Cell Biology*(1983) 96;
67. Marijanovic, Z., Caputo, A., Campana, V., & Zurzolo, C. Identification of an intracellular site of prion conversion. *PLoS Pathog.* (2009); 5, e1000426.
68. Mastrianni, J. A., Nixon, R., Layzer, R., Telling, G. C., Han, D., DeArmond, S. J., and Prusiner, S.B.. Prion protein conformation in a patient with sporadic fatal insomnia. *N. Engl. J. Med.* (1999)*;* 340(21):1630–1638.
69. McKinley, M.P. *et al*. Scrapie prion rod formation in vitro requires both detergent extraction and limited proteolysis. *J. Virol.* (1991); 65, 1340-1351
70. Menard S., Tagliabue E., Colnaghi M.I. The 67 kDa laminin receptor as a prognostic factor in human cancer. *Breast Cancer Res. Treat.* (1998); 52, 137-145.
71. Mercurio, A. M. Laminin: multiple forms, multiple receptors. *Curr. Opin. Cell Biol.* (1990); 2, 845-849.
72. Montuori, N., & Sobel, M.E. The 67-kDa laminin receptor and tumor progression. *Curr. Top. Microbiol. Immunol.* (1996); 213, 205-214.
73. Montuori, N. *et al*. Laminin receptors in differentiated thyroid tumors: restricted expression of the 67-kilodalton laminin receptor in follicular carcinoma cells. *J. Clin. Endocrinol. Metab* (1999); 84, 2086-2092
74. Moodley, K. & Weiss, S.F.T. Downregulation of the non-integrin laminin receptor reduces cellular viability by inducing apoptosis in lung and cervical cancer cells. *PLoS One* (2013); 8, e57409.
75. Morel, E. *et al*. Bovine prion is endocytosed by human enterocytes via the 37 kDa/67 kDa laminin receptor. *Am. J. Pathol.* (2005);167, 1033-1042.
76. Naslavsky, N. et al. Characterization of detergent-insoluble complexes containing the cellular prion protein and its scrapie isoform. *J. Biol. Chem*. (1997); 272, 6324–6331.
77. Nikles, D. *et al*. Subcellular localization of prion proteins and the 37 kDa/67 kDa laminin receptor fused to fluorescent proteins. *Biochim. Biophys. Acta.* (2008);1782, 335-340.
78. Omar, A., Reusch, U., Knackmuss, S., Little, M. and Weiss, SFT. Anti-LRP/LR specific antibody lgG1-iS18 significantly reuduces adhesion and invasion on metastatic lung, cervix colon and prostate cancer cells. *J. Mol. Biol* (2012); 419, 102-109.
79. Pampeno, C., Derkatch, I.L., & Meruelo, D. Interaction of human laminin receptor with Sup35, the [PSI$^+$] prion-forming protein from S. cerevisiae, a yeast model for studies of LamR interactions with amyloidogenic proteins. *PLoS One.* (2014); 9, e86013.
80. Passet, B., Young, R., Makhzami,S., Vilotte, M., Jaffrezic, F., Halliez, S., Bouet, S., Marthey, S., Khalife, M., Kanellopoulos-Langevin, C., et al.. Prion protein and

shadoo are involved in overlapping embryonic pathways and trophoblastic development. *PLoS One*(2012) ;7, e41959;.
81. Pesapane, A. *et al*. Discovery of new small molecules inhibiting 67 kDa laminin receptor interaction with laminin and cancer cell invasion. *Oncotarget*(2015); 6, 18116-18133
82. Pimpinelli, F., Lehmann, S., & Maridonneau-Parini, I. The scrapie prion protein is present in flotillin-1 positive vesicles in central- but not peripheral derived neuronal cell lines. *Eur. J. Neurosci.* (2005); 21, 2063-2072.
83. Pinnock, E.C. *et al.* LRP/LR antibody mediated rescuing of Abeta induced cytotoxicity is dependent on PrPc in Alzheimer's Disease. *J. Alzheimers Dis.* (2015); 49, 645-657.
84. Pflanz, H. *et al*. Microinjection of lentiviral vectors directed against laminin receptor precursor mRNA prolongs the pre-clinical phase in scrapie-infected mice. *J. Gen. Virol*(2009); 90, 269-274
85. Pfeiffer N. V., Dirndorfer D., Lang S., Resenberger U. K., Restelli L. M., Hemion C, Miesbauer M., Frank S, Neutzner A., Zimmermann R,. Winklhofer K. F and Tatzelt J. Structural features within the nascent chain regulate alternative targeting of secretory proteins to mitochondria, *The EMBO Journal* (2013);32, 1036–1051.
86. Premzl M., Sangiorgio L., Strumbo B., Marshall Graves J.A., Simonic T., Gready J.E., Shadoo, a new protein highly conserved from fish to mammals and with similarity to prion protein, *Gene* (2003); 314 89–102.
87. Prusiner, S. B. Novel proteinaceous infectious particles cause scrapie. *Science* (1982); 216(4542):136–144;.
88. Prusiner, S B. Molecular biology of prion diseases. *Science* (1991); 252(5012):1515–1522;
89. Prusiner, S. B., Groth, D., Serban, A., Stahl, N., and Gabizon, R. Attempts to restore scrapie prion infectivity after exposure to protein denaturants. *Proc. Natl. Acad. Sci. U. S. A.* 90(7):2793–2797;(1993).
90. Prusiner, S. B. Molecular biology and genetics of prion diseases. *Philos. Trans. R. Soc. Lond. B.Biol. Sci.* 343(1306):447–463; (1994).
91. Prusiner, S.B. Prions. *Proc Natl. Acad. Sci. USA.* 95, 13363-13383. (1998).
92. Rao, N. C., Barsky, S. H., Terranova, V. P. & Liotta, L. A. Isolation of a tumor cell laminin receptor. *Biochemical and Biophysical Research Communications* 111, 804–808. Lesot, H., Kuhl, U. & Mark, K. Isolation of a laminin-binding proteinnfrom muscle cell membranes. *EMBO Journal* 2, 861–865;(1983).
93. Rao, N. C., Barsky, S. H., Terranova, V. P. & Liotta, L. A. Isolation of a tumor cell laminin receptor. *Biochemical and Biophysical Research Communication;* (1983).
94. Rao, C. N., Castronovo, V., Schmitt, M. C., Wewer, U. M., Claysmith, A.P., Liotta, L. A. & Sobel, M. E. Evidence for a precursor of the high-affinity metastasis-associated murine laminin receptor. *Biochemistry* 28,7476–7486;(1989).
95. Rieger, R., Edenhofer, F., Lasmezas, C.I., & Weiss, S. The human 37-kDa laminin receptor precursor interacts with the prion protein in eukaryotic cells. *Nat. Med.* 12, 1384-1388 (1997).
96. Rieger, R., Lasmezas, C.I., & Weiss, S. Role of the 37 kDa laminin receptor precursor in the life cycle of prions. *Transfus. Clin. Biol.* 6, 7-16 (1999).

97. Sarnataro, D., Paladino, S., Campana, V., Grassi, J., Nitsch, L. and Zurzolo, C.. PrP^C is sorted to the basolateral membrane of epithelial cells independently of its association with rafts. *Traffic* 11, 810-2; (2002).
98. Sarnataro, D., Campana, V., Paladino, S., Stornaiuolo, S., Nitsch, L. and Zurzolo,C.. PrP^C association with lipid rafts in the early secretory pathway stabilizes its cellular conformation. *Mol. Biol. Cell* 15, 4031– 4042; (2004).
99. Sarnataro, D. *et al*. Lipid rafts and clathrin cooperate in the internalization of PrP in epithelial FRT cells. *PLoS One* 4, e5829 (2009). Sanghera, N. and Pinheiro, T.J. Binding of prion protein to lipid membranes and implications for prion conversion. *J. Mol. Biol*. 315, 1241–1256 (2002)
100. Sarnataro D., Pepe A., Altamura G., De Simone I., Pesapane A., Nitsch L., Montuori N., Lavecchia A., Zurzolo C. The 37/67 kDa laminin receptor (LR) inhibitor, NSC47924, affects 37/67 kDa LR cell surface localization and interaction with the cellular prion protein. *Scientific Reports* (2016) 6:24457
101. Sanghera, N. and Pinheiro, T.J. Binding of prion protein to lipid membranes and implications for prion conversion. *J. Mol. Biol*. (2002); 315, 1241–1256
102. Selleri C., Ragno P., Ricci P., et al. The metastasis-associated 67-kDa laminin receptor is involved in G-CSF-induced hematopoietic stem cell mobilization. *Blood*. (2006); 108, 2476-2484,
103. Shyng, S.L., Huber, M.T., & Harris, DA. A prion protein cycles between the cell surface and an endocytic compartment in cultured neuroblastoma cells. *J. Biol. Chem.* (1993); 268, 15922-15928
104. Sunyach C., Jen A., Deng J., Fitzgerald K.T., Frobert Y., Grassi J., McCaffrey M. W., Morris R. The mechanism of internalization of glycosylphosphatidylinositol-anchored prion protein *EMBO J.* (2003); 3591–3601
105. Stahl, N., and Prusiner, S. B. Prions and prion proteins. *FASEB J.* (1991); 5(13):2799–2807;
106. Stahl, N. *et al*. Structural studies of the scrapie prion protein using mass spectrometry and amino acid sequencing. *Biochem.* (1993); 32, 1991-2002
107. Taraboulos A., Reaber, A.J., Borchelt, D.R., Serdon, D., and Prusiner, S.G.. Synthesis and trafficking of prion protein in cultured cells, *Mol. Biol., Cell*(1992); 3, 851-863.
108. Taraboulos et al., Cholesterol depletion and modification of COOH-terminal targeting sequence of the prion protein inhibit formation of the scrapie isoform *J Cell Biol*. 1995 121–132.
109. Vana, K., Zuber, C., Nikles, D., & Weiss, S. Novel aspects of prions, their receptor molecules, and innovative approaches for TSE therapy. *Cell. Mol. Neurobiol.* (2007); 27, 107-128
110. Vana, K. *et al*. LRP/LR as an alternative promising target in therapy of prion diseases, Alzheimer's disease and cancer. *Infect. Dis. Drug target.* (2009); 90, 69-80
111. Victoria, G.S. and Zurzolo, C. Trafficking and degradation pathways in pathogenic conversion of prions and prion-like proteins in neurodegenerative diseases. *Virus Res*(2015).. (in press)
112. Watts, J.C., Stohr, J., Bhardwaj, S., Wille, H., Oehler, A., Dearmond, S.J., Giles, K. and Prusiner, S.BProtease-resistant prions selectively decrease Shadoo protein. *PLoS Pathog.* . (2011). 7, e1002382.
113. Westaway, D., Genovesi, S., Daude, N., Brown, R., Lau, A., Lee, I., Mays, C.E., Coomaraswamy, J., Canine, B., Pitstick, R. et al.. Down-regulation of Shadoo in

prion infections traces a pre-clinical event inversely related to PrP(Sc) accumulation. *PLoS Pathog*(2011)*;* 7, e1002391.

114. Young, R., Passet, B., Vilotte, M., Cribiu, E.P., Beringue, V., Le Provost, F., Laude, H. and Vilotte, J.L. The prion or the related Shadoo protein is required for early mouse embryogenesis. *FEBS Lett.* (2009); 583, 3296–3300

115. Young, K., Piccardo, P., Dlouhy, S., Bugiani, O., Tagliavini, F. and Ghetti, B. The human genetic prion diseases. In *Prions: Molecular and Horizon Scientific* (1999); 139-175. Wymondham:;.

116. Zuber, C. *et al*. Anti- LRP/LR antibody W3 hampers peripheral PrP^{Sc} propagation in scrapie infected mice. *Prion.* (2007); 1, 207-212 .

117. Zuber, C. *et al.* Invasion of tumorigenic HT1080 cells is impeded by downregulating or blocking the 37kDa/67kDa laminin receptor. *J. Mol. Biol.* (2008); 378, 530-539

118. Zanusso, G. *et al*. Prion protein expression in different species: analysis with a panel of new mAbs. *Proc. Natl. Acad. Sci.* (1998); *U S A.* 95, 8812-6.

119. Zapun, A. *et al*. Enhanced catalysis of ribonuclease B folding by the interaction of calnexin or calreticulin with ERp57. *J. Biol. Chem.* (1998); 273, 6009-6012

120. Zurzolo, C., Le Bivic, A.L., & Rodriguez-Boulan, E. Cell surface biotinylation techniques, in *Cell Biology: A laboratory handbook* (1994); (ed. Celis, J.E) 185-192 (San Diego, CA, USA Academic Press)

APPENDIX

LIST OF PUBBLICATIONS

This dissertation is based upon the following publication:

"The 37/67kDa laminin receptor (LR) inhibitor, NSC47924, affects 37/67kDa LR cell surface localization and interaction with the cellular prion protein"

Daniela Sarnataro, Anna Pepe, Gennaro Altamura, Imma De Simone, Ada Pesapane, Lucio Nitsch, Nunzia Montuori, Antonio Lavecchia, and Chiara Zurzolo
In press Scientific Report 2016; 6:24457

"Lipid rafts perturbation and proteasomal block exacerbate "scrapie-like" properties of PrP-like protein Shadoo in cultured neuronal cells"

Anna Pepe, Rosario Avolio, Danilo Swann Matassa, Franca Esposito, Lucio Nitsch, Chiara Zurzolo, Simona Paladino and Daniela Sarnataro
In preparation